UNIVERSIDADE ESTADUAL PAULISTA
"JÚLIO DE MESQUITA FILHO"
Câmpus de Botucatu

Efeitos da melatonina nas células de carcinoma ovariano SKOV-3: análise do perfil proteômico global

Roberta Carvalho Cesário

Dissertação apresentada ao Instituto de Biociências, Campus de Botucatu, UNESP, para obtenção do título de Mestre no Programa de Pós-Graduação em Biologia Geral e Aplicada, Área de concentração *Biologia Estrutural e Funcional*

Orientador: Prof. Dr. Luiz Gustavo de Almeida Chuffa

BOTUCATU - SP

2022

Programa de Pós-graduação em Biologia Geral e Aplicada
Instituto de Biociências de Botucatu/ UNESP
Rua Professor Doutor Antonio Celso Wagner Zanin, 250 - CEP 18618-689 - Botucatu - SP - Brasil
Tel (14) 3880-0781 posgraduacao@ibb.unesp.br

UNIVERSIDADE ESTADUAL PAULISTA

"Julio de Mesquita Filho"

INSTITUTO DE BIOCIÊNCIAS DE BOTUCATU

Efeitos da melatonina nas células de carcinoma ovariano SKOV-3: análise do perfil proteômico global

ROBERTA CARVALHO CESÁRIO

PROF. DR. LUIZ GUSTAVO DE ALMEIDA CHUFFA

Dissertação apresentada ao Instituto de Biociências, Campus de Botucatu, UNESP, para obtenção do título de Mestre no Programa de Pós-Graduação em Biologia Geral e Aplicada, Área de concentração *Biologia Estrutural e Funcional*

Orientador: Prof. Dr. Luiz Gustavo de Almeida Chuffa

BOTUCATU - SP

2022

C421e

Cesário, Roberta Carvalho
Efeitos da melatonina nas células de carcinoma ovariano SKOV-3: análise do perfil proteômico global / Roberta Carvalho Cesário. -- Botucatu, 2022
68 f. : il., tabs., fotos, mapas

Dissertação (mestrado) - Universidade Estadual Paulista (Unesp), Instituto de Biociências, Botucatu
Orientador: Luiz Gustavo de Almeida Chuffa

1. Câncer de Ovário. 2. Melatonina. 3. Proteoma. 4. Mitocondria. 5. Células SKOV-3. I. Título.

Sistema de geração automática de fichas catalográficas da Unesp. Biblioteca do Instituto de Biociências, Botucatu. Dados fornecidos pelo autor(a).

Essa ficha não pode ser modificada.

DEDICATÓRIA

Dedico esse trabalho as pessoas mais importantes da minha vida, meus pais Edna e Roberto, minha irmã Natália e meus sobrinhos Mariana e Victor.

AGRADECIMENTOS

Agradeço ao meu orientador Prof. Dr. Luiz Gustavo de Almeida Chuffa não só pela orientação durante todo esse processo, mas também por ter acreditado em mim, ter me aceito como orientada e por todos os ensinamentos científicos e teóricos.

Aos meus colegas de grupo de pesquisa Maira e Henrique, pelo apoio, pela amizade, por todas as conversas e ajuda no desenvolvimento desse trabalho. Em especial a minha amiga Letícia Gaiotte que esteve comigo em cada momento dentro e fora da vida acadêmica e se tornou minha família em Botucatu.

A minha família, em especial a minha mãe Edna que sempre se sacrificou para tornar meus sonhos possíveis, sem seu apoio jamais teria chego até aqui. Ao meu pai Roberto, meus sobrinhos e minha irmã Natália que torceram por mim e me apoiaram em todas as decisões. A Maria Beatriz pelo companheirismo e por estar sempre ao meu lado em tudo.

A coordenação de Aperfeiçoamento de Pessoal de Nível Superior (CAPES) cujo auxílio financeiro foi essencial para manutenção dessa pesquisa.

SUMÁRIO

LISTA DE ABREVIATURAS.....X
LISTA DE FIGURAS.....XI
RESUMO.....XII
ABSTRACT.....XIII
CAPÍTULO 1.....XIV
1. INTRODUÇÃO.....15
1.1 Câncer de ovário: fatores de risco e variedades.....15
1.2 Melatonina e o CO.....18
1.3 Melatonina e CO: envolvimento com a análise proteômica.....21
2. JUSTIFICATIVA.....23
3. HIPÓTESE.....24
4. OBJETIVO GERAL.....25
4.1 Objetivos específicos.....25
5. REFERENCIAS.....26
CAPÍTULO 2.....30
Artigo…….....31
Supplementary material.....44

LISTA DE ABREVIATURAS

CO: câncer de ovário

ROS: espécies reativas de oxigênio

RNS: espécies reativas de nitrogênio

PDH: complexo piruvato desidrogenase

PDK: piruvato desidrogenase quinase

AANAT: Serotonin N-acetyltransferase

iTRAQ: isobaric tag for relative and absolute quantitation

DMBA: dimethylbenz(a)anthracene

HIF-1: fator induzível por hipóxia

MDR1: resistência a múltiplas drogas

ACETIL-COA: Acetilcoenzima A

ACTB: beta-actina

PD-1: proteína de morte celular programada

LISTA DE FIGURAS

Figura 1: Classificação do CO quanto a origem, subtipos histológicos e grau de malignidade do tumor.

Figura 2: Linhagem SKOV-3.

Figura 3: Efeitos da melatonina no metabolismo mitocondrial em células normais e tumorais.

Figura 4: Resumo dos efeitos inibitórios da melatonina em mecanismos moleculares envolvidos na progressão do CO.

Resumo

O câncer de ovário (CO) é a segunda malignidade mais letal do sistema genital feminino e apresenta uma expectativa de sobrevida menor que 50% após o quinto ano do diagnóstico. Dependendo do subtipo, o CO está associado com maior risco de desenvolvimento de quimioresistência e prognóstico ruim. A melatonina (Mel) é um neurohormônio secretado pela glândula pineal na fase de escuro e tem mostrado propriedades antitumorais em ensaios *in vitro* e *in vivo*. O objetivo do presente estudo foi avaliar a influência da terapia com melatonina, em diferentes doses, sobre o proteoma das células de carcinoma ovariano humano (linhagem SKOV-3). O estudo foi composto pelos seguintes grupos experimentais; 1) Grupo Controle: células SKOV-3 tratadas com veículo; 2) Grupo Mel 0.8 mM: células SKOV-3 tratadas com melatonina na concentração de 0.8 mM por 48h; 3) Grupo Mel 1.6 mM: células SKOV-3 tratadas com melatonina na concentração de 1.6 mM por 48h; 4) Grupo Mel 2.4 mM: células SKOV-3 tratadas com melatonina na concentração de 2.4 mM por 48h. Após 48h de tratamento com melatonina, foi realizada a extração e a quantificação das proteínas. O perfil proteômico foi analisado e identificou-se 636 proteínas totais no grupo controle. A partir desses dados, foram selecionadas proteínas diferencialmente reguladas para cada grupo, comparando as expressões das proteínas do grupo controle usando $p<0,05$ e *fold change* de +1.5 ou -1.5 para determinar as proteínas que foram reguladas de maneira positiva e negativa, respectivamente. Proteínas relacionadas com o sistema imune e o metabolismo do ácido tricarboxílico foram reguladas positivamente nos três grupos expostos a melatonina. Especificamente, a dose de 2.4 mM promoveu alterações importantes, regulando genes envolvidos na síntese de proteínas. Também identificamos 28 genes potenciais compartilhados entre o tecido normal e o tecido tumoral ovariano considerando todos os grupos experimentais, onde a melatonina mostrou alterações na predição de genes codificadores de proteínas ribossomais. Concluímos que a melatonina modula o proteoma das células SKOV-3, principalmente regulando proteínas envolvidas com o sistema imune e metabolismo mitocondrial. Além disso, o tratamento com a dose de 2.4 mM de melatonina promoveu maiores alterações na rede proteica, revelando uma estratégia terapêutica eficaz no combate ao CO.

Palavras-chave: Câncer de Ovário, melatonina, proteoma, mitocôndria, células SKOV-3.

Effect of melatonin on ovarian carcinoma SKOV-3 cells: analysis of the global proteomic profile

Abstract

Ovarian cancer (OC) is the second most lethal malignancy of the female genital system and has a survival expectation of less than 50% after the fifth year diagnosis. Depending on the subtype, OC is associated with an increased risk of chemoresistance and poor prognosis. Melatonin (5-methoxytriptamine) is a neurohormone secreted by the pineal gland in the dark phase and has shown antitumor properties in both in vitro and in vivo assays. The present study aimed to evaluate the influence of melatonin therapy, at different doses, on the proteome of human ovarian carcinoma cells (SKOV-3 cell line). The study consisted of the following experimental groups; 1) Control Group: SKOV-3 cells treated with vehicle; 2) 0.8 mM Mel Group: SKOV-3 cells treated with melatonin at a concentration of 0.8 mM for 48h; 3) Mel 1.6 mM Group: SKOV-3 cells treated with melatonin at a concentration of 1.6 mM for 48h; 4) Mel 2.4 mM group: SKOV-3 cells treated with melatonin at a concentration of 2.4 mM for 48h. After 48 h of treatment with melatonin, protein extraction and quantification were performed in these cells. The proteomic profile was analyzed, and a total of 636 proteins were identified in the control group. From these data, differentially regulated proteins were selected for each group, comparing the level of the proteins in the control group using $p<0.05$ and fold change of +1.5 or -1.5 to determine which proteins were positively and negatively regulated, respectively. Proteins related to the immune system and tricarboxylic acid metabolism were upregulated in the three groups exposed to melatonin. More specifically, the dose of 2.4 mM promoted significant changes, thereby regulating molecules involved in protein synthesis. We also identified 28 potential genes shared between normal tissue and ovarian tumor tissue considering all experimental groups, where melatonin showed alterations in predicting genes encoding ribosomal proteins. We conclude that melatonin modulates the proteome of SKOV-3 cells, mainly via regulating proteins involved with the immune system and mitochondrial metabolism. Furthermore, treatment with a dose of 2.4 mM of melatonin promoted more significant alterations in the protein network, thus revealing an effective therapeutic strategy against OC.

Keywords: Ovarian cancer, melatonin, proteome, immune system, mitochondria, SKOV-3 cells.

CAPÍTULO 1

1. INTRODUÇÃO

1.1 Câncer de Ovário: fatores de risco e variedades

O número de novos casos de câncer no mundo pode crescer cerca de 70% até 2030 e essa estimativa também inclui altas taxas de mortalidade devido ao câncer de ovário (CO), sendo a segunda neoplasia ginecológica que mais causa morte e o oitavo mais incidente entre as mulheres (WHO, 2018). Segundo o Instituto Nacional do Câncer (INCA), as pacientes diagnosticadas com CO apresentam uma expectativa de sobrevivência após o quinto ano menor que 50%. Isso está relacionado ao fato dos sintomas como: inchaço, saciedade precoce, dor e desconforto pélvico não serem específicos e, desse modo, são constantemente desprezados ou mesmo relacionados com outras doenças (BRETT; PERMUTH; THOMAS., 2017).

Os principais fatores de risco para o CO estão relacionados com idade precoce da menarca, menopausa tardia, números de gestações, tratamento com reposição hormonal e fatores genéticos. Já outros fatores, tais como a dieta, tabagismo, obesidade e consumo de álcool apresentam resultados menos significativos no desenvolvimento da doença, como apontado por Brett *et al*. (2017) e La Vecchia (2017).

O carcinoma ovariano primário pode ser classificado de acordo com a origem, podendo ser epitelial, mesenquimal, de célula germinativa ou da camada da granulosa. Cerca de 90% dos subtipos de CO originam-se a partir da superfície epitelial que recobre o órgão ou de derivações do epitélio *mulleriano* (CHUFFA *et al.*, 2017). O CO epitelial engloba todos os subtipos histológicos e, nesse sentido, são subclassificadas em serosos, mucinosos, endometrióide e célula clara (COOK; VANDERHYDEN, 2019).

Os tumores podem ser reconhecidos com base no seu crescimento e característica molecular, diferenciados em tipo I e tipo II. O tipo I inclui os serosos, de células claras, mucinosos e os tumores de Brenner, considerados de baixo grau, pois apresentam progressão gradual de forma comumente encontrada em outros canceres epiteliais, apresentando um melhor prognóstico. Já o tipo II, que abrange os serosos de alto grau, desenvolvem um comportamento mais agressivo e de rápida disseminação, sendo o subtipo com pior prognóstico e, consequentemente, é causador de 70 a 80% das mortes por CO (Figura 1) (LISIO *et al*., 2019)

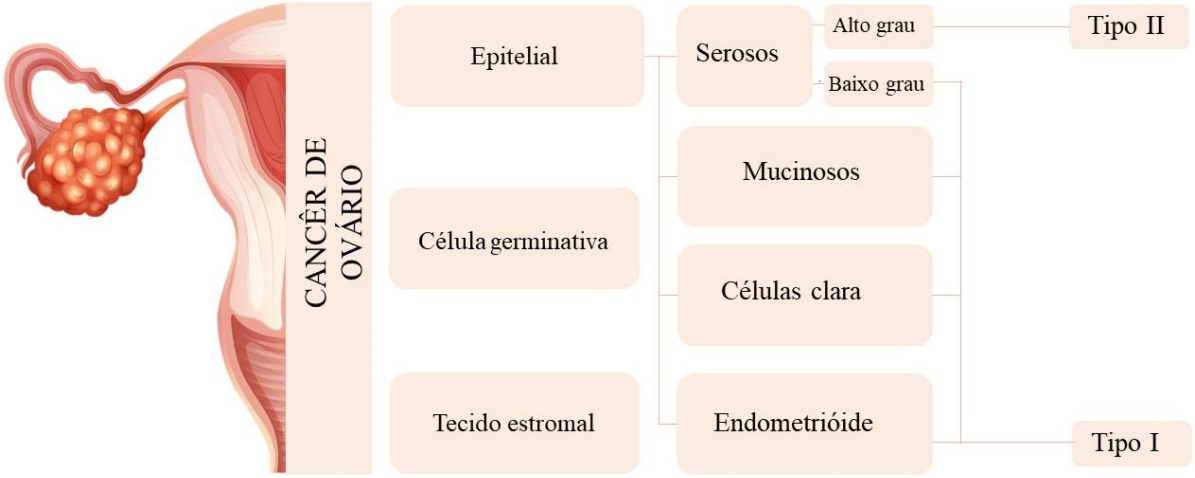

Figura 1: Classificação do CO quanto a origem, subtipos histológicos e grau de malignidade do tumor. Fonte: autor

Mais de 70% dos casos de CO são diagnosticados nos estágios avançados da doença (III ou IV). Por se tratar de um tumor sólido, diferentemente da maioria dos tumores, o CO apresenta metástase hematogênica rara (LENGYEL, 2010). O passo inicial para tal evento é a migração de células malignas para a cavidade peritoneal através da ação de proteases (ÖHLUND *et al*., 2013; SAWADA *et al*., 2008; SYMOWICZ *et al*., 2007).

As opções de tratamento de primeira linha inclui citoredução com associação a quimioterapia (JESSMON *et al.*, 2017), e a base da quimioterapia convencional constitui-se da combinação de derivados de platina e /ou taxol *(HSIEH et al.*, 2019). O diagnóstico tardio e a quimioresistência aos tratamentos convencionais tornam-se fatores limitantes ao tratamento, sendo frequente a reincidência da doença com maior agressividade (CHUFFA *et al.*, 2017). O câncer epitelial ovariano é considerado um tumor quimioresponsivo à terapia padrão com platina e/ou taxol, com aproximadamente 80% da taxa de resposta para o tipo seroso e endometrióide, e apenas 35% para o tipo mucinoso e de células claras (CLOVEN *et al*., 2004; HO *et al*., 2004). Porém, mesmo com a cirurgia e a quimioterapia, 70% dos pacientes apresentam recidivas nos três anos seguintes do tratamento (LEDERMANN *et al.*, 2013). A razão pela qual os tratamentos contra o CO apresentam recidivas ou baixa taxa de sucesso está relacionada com quimioresistência que essas células desenvolvem durante o processo de progressão tumoral (KIM *et al*., 2018). A heterogeneidade tumoral do CO é um obstáculo para a escolha do tratamento e, além disso, a variedade dos tipos de tumor pode ser um dos fatores responsáveis pela quimioresistência adquirida em muitos casos (ROJAS *et al*., 2016). Essa barreira influencia na sobrevivência de pacientes diagnosticados em estágio avançado de CO,

de modo que, em 90% dos casos, a quimioresistência leva a falhas nos tratamentos e ao aumento da mortalidade (LONGLEY; JOHNSTON, 2005). Os mecanismos de resistência utilizados pelas células tumorais são diversos, incluindo a capacidade celular de causar o efluxo de drogas, que está associado à superexpressão do gene MDR1, o qual codifica o transportador de membrana chamado glicoproteína-P (P-gp), diminuindo a concentração intracelular de medicamentos, como o paclitaxel (CORNELISON; LIANEZA; LANDEN, 2017). Outros fatores são correlacionados a quimioresistência adquirida pelas células de CO após a recorrência da doença, tal como a modificação de genes vinculados ao reparo de proteínas em vias de sobrevivência, ao mesmo tempo que reduzem a expressão de genes supressores tumorais (BRASSEUR; GÉVRY; ASSELIN, 2017). Nesse sentido, a linhagem de carcinoma ovariano SKOV-3 tem sido utilizada em diversos estudos, pois é resistente a diversos agentes quimioterápicos como a cisplatina e adriamicina (Figura 2). Dessa forma, a compreensão dos mecanismos celulares que levam a quimioresistência trará novas perspectivas que sejam mais eficazes no tratamento das pacientes.

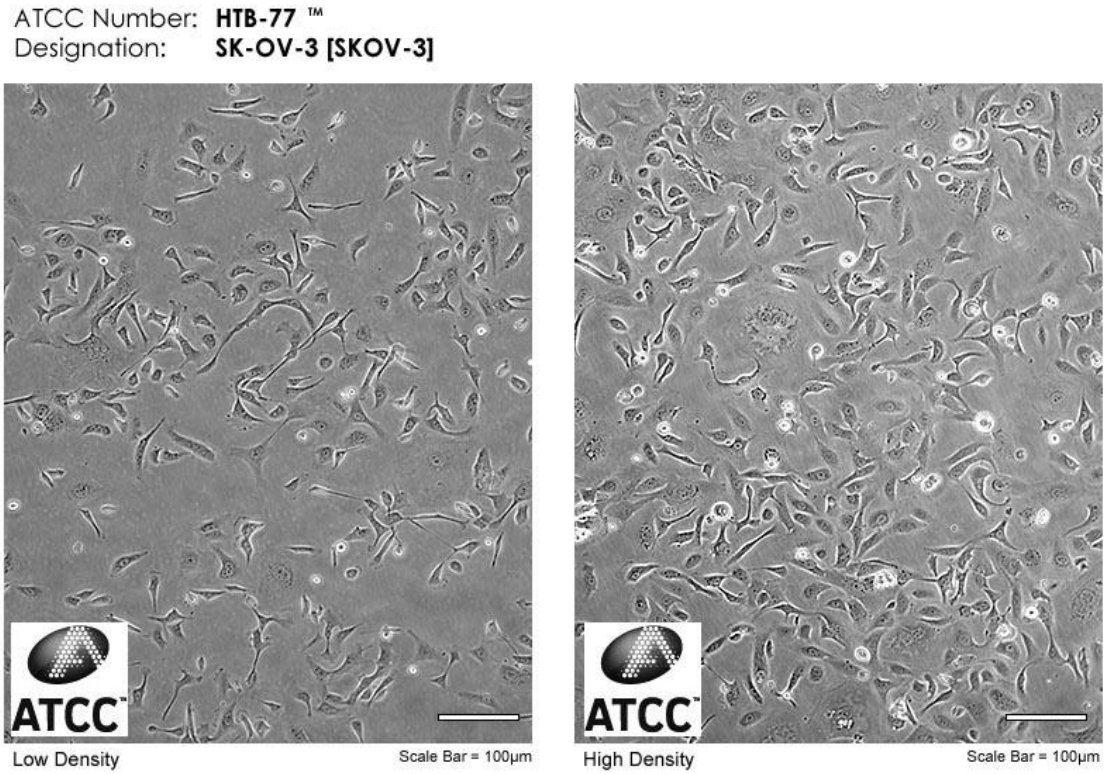

Figura 2: Linhagem SKOV-3. Fonte: ATCC.

1.2 Melatonina e o CO

A melatonina (N-acetil-5-metoxitriptamina), é uma pequena indolamina lipofílica secretada pela glândula pineal e em menor quantidade por outros tecidos, sendo principalmente responsável pela regulação do sono (GANDHI *et al*., 2015; TOSCHES *et al*., 2014). A melatonina apresenta função bem conhecida na célula normal atuando como um potente antioxidante, removendo espécies reativas de oxigênio (ROS) e nitrogênio (RNS) do organismo e aumentando a atividade de enzimas antioxidantes (HU *et al*., 2016); além disso, a melatonina previne indução de apoptose em células normais *(*REITER *et al.*, 2016). Entretanto, nas células tumorais, a melatonina tem sido descrita com propriedades antiproliferativas, anti-angiogênica, pró-apoptótica e imunomoduladora (CHUFFA *et al*. 2015; ZONTA *et al*. 2017). Um estudo que reuniu diversos trabalhos apresentou características da melatonina em tipos variados de câncer, como o de próstata, mama e ovário. Esse mesmo estudo indicou a melatonina como um adjuvante nas terapias, diminuindo os efeitos negativos dos tratamentos e aumentando a sensibilidade às drogas quimioterápicas (LI *et al.*, 2017). Os mecanismos moleculares envolvidos com essas propriedades estão relacionados com a síntese de estrogênio, que é regulada pela melatonina via modulação da expressão de receptores e estrogênio, além de atuar na indução de apoptose, e contra a proliferação celular e angiogênese (MENÉNDEZ-MENÉNDEZ; MARTÍNEZ-CAMPA, 2018).

A melatonina foi utilizada também como terapia neoadjuvante na linhagem tumoral cervical HeLa, e mostrou aumento na sensibilidade ao tratamento com cisplatina devido ao acúmulo de dano ao DNA e, consequentemente, aumento na taxa de apoptose (PARIENTE *et al*., 2016). A resistência aos tratamentos convencionais é um grande desafio no tratamento do câncer, particularmente nos carcinomas ovarianos. Em ovários normais, a melatonina é secretada pelas células da granulosa do folículo pré-ovulatório e o tratamento adicional com melatonina pode influenciar na produção de hormônios essenciais na ovulação, qualidade oocitária e atividade antioxidante (TAMURA *et al*., 2009). A melatonina promove a remoção de radicais livres e atividade de enzimas antioxidantes no ovário. Interessantemente, na tentativa de explicar a origem primária do CO, estudos revelaram que a geração de ROS, durante o processo ovulatório, pode transformar as células das fímbrias da tuba uterina através de alterações e perda da proteína p53; neste contexto, a melatonina pode interromper o efeito tumorigênico induzido por ROS e proteger o tecido original (HUANG *et al.*, 2015).

Reiter e colaboradores (2019) compilaram dados sobre o efeito oncostático da melatonina no câncer; nesse estudo foi mostrado que a melatonina está presente em maiores concentrações nas mitocôndrias de células normais comparadas as células tumorais e o tratamento com a melatonina teve um impacto na reversão do efeito Warburg, diminuindo a proliferação celular, invasão, migração e, consequentemente, a metástase tumoral. Células tumorais apresentam um diferencial em suas características metabólicas na via glicolítica, tendo como prioridade a oxidação da glicose e produção de lactato mesmo na presença de oxigênio; porém, essa característica é alterada a noite, onde a taxa de melatonina endógena se torna elevada, de modo que a célula volta a utilizar a fosforilação oxidativa para obter energia. Desse modo, um estudo observou que a melatonina atua revertendo o efeito inibitório da piruvato desidrogenase quinase (PDK) sobre o complexo piruvato desidrogenase (PDH), fazendo com que o piruvato, advindo da glicólise, seja oxidado e passe pelo ciclo de Krebs, chegando à fosforilação oxidativa, ao invés de ser metabolizado em lactato. Assim, o piruvato será metabolizado em acetil-CoA que também possui um papel importante na síntese de melatonina mitocondrial estimulando a enzima AANAT, limitante para síntese de melatonina (Figura 3) (REITER *et al*.; 2020).

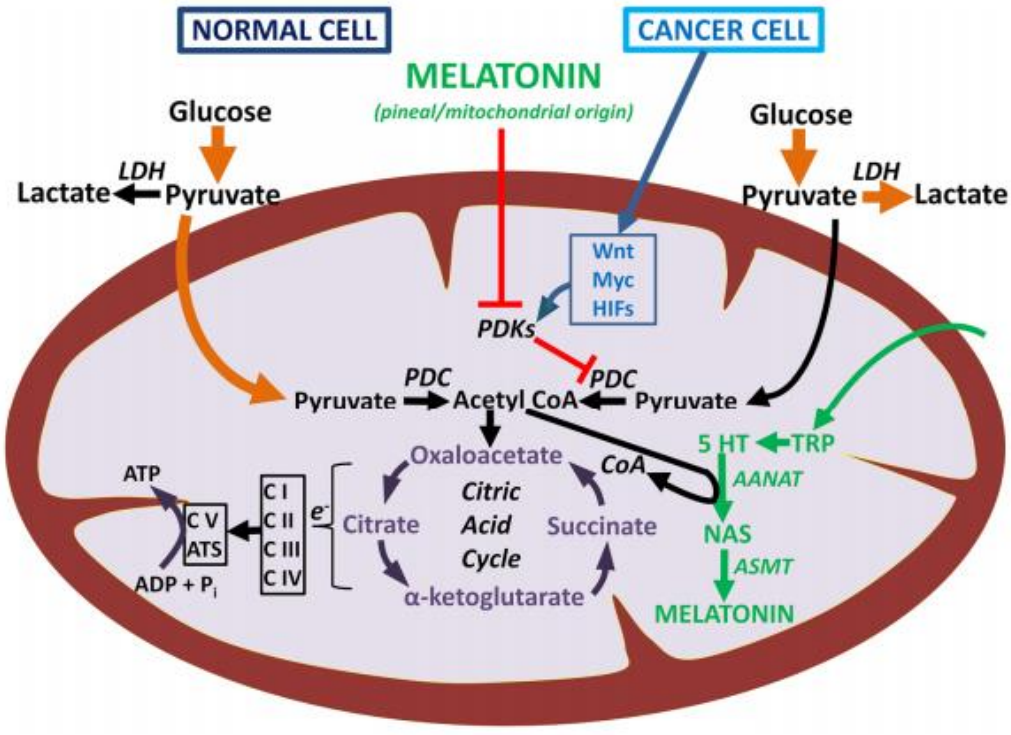

Figura 3: Efeitos da melatonina no metabolismo mitocondrial em células normais e tumorais. Fonte: adaptado de Reiter et al., 2020.

Adicionalmente, outro estudo confirmou que o tratamento com melatonina, nas concentrações de 400 a 600 µM, reduziu a taxa de sobrevivência e proliferação das linhagens de células tumorais ovarianas OVCAR-429 e PA-1, aumentando o número de células na fase G1 do ciclo celular e diminuindo o número de células na fase S do ciclo celular (SHEN *et al.*, 2016).

Em células tumorais SKOV-3, a melatonina tem apresentado efeitos inibitórios na sobrevivência celular, além de potencializar o tratamento em combinação com a cisplatina (ZEMLA, *et al*, 2017). Estudos *in vivo* reportaram os efeitos da terapia com melatonina a longo prazo estimulando as proteínas pro-apoptóticas (p53, BAX, caspase-3 total e clivada) e inibindo as proteínas anti-apoptóticas (Bcl-2 e survivina) em modelos animais de CO papilífero seroso. Interessantemente, a melatonina promoveu aumento na expressão de p53, BAX e caspase-3 ativa, além de induzir a fragmentação do DNA observada pelo teste do TUNEL (CHUFFA, *et al*., 2016a). O uso da melatonina no tratamento de CO tem demonstrado resultados promissores em estudos *in vitro* e *in vivo*, com um papel importante na apoptose das células tumorais e, em contrapartida, favorecendo a sobrevivência de células normais (Figura 4) (CHUFFA; REITER; LUPI, 2017).

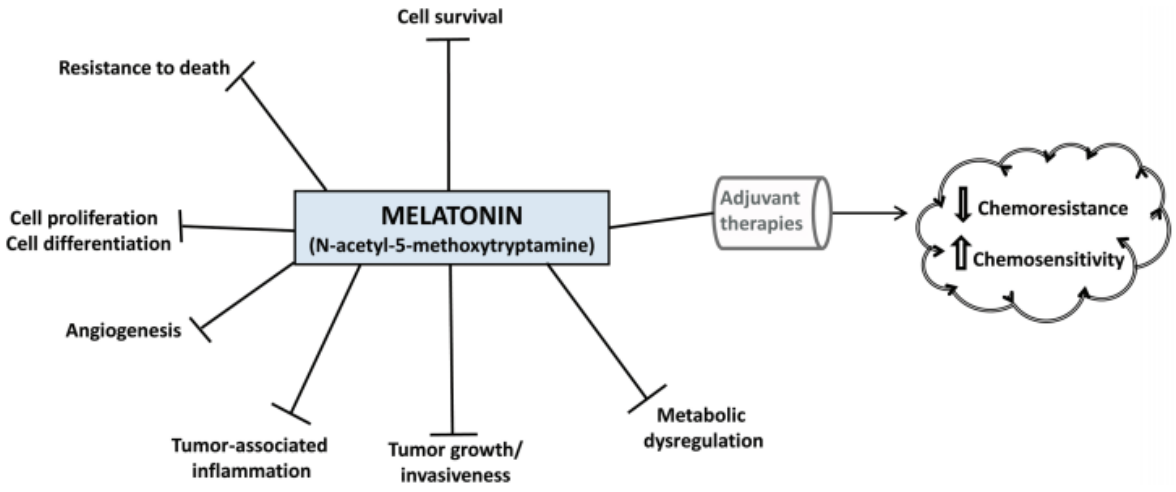

Figura 4: Resumo dos efeitos inibitórios da melatonina em mecanismos moleculares envolvidos na progressão do CO. Fonte: Chuffa et al., 2017.

Estudo prévio do nosso grupo de pesquisa já documentou a interação da melatonina com o metabolismo energético do CO em modelo experimental in vivo envolvendo a utilização da estratégia proteômica global. Embora nenhuma mudança histopatológica tenha sido evidenciada, a melatonina diminuiu a expressão de proteínas envolvidas em diversos processos

metabólicos, como na geração de metabólitos e energia celular, vias associadas ao estresse do retículo endoplasmático, proteínas de processamento e apresentação de antígeno, e ainda proteoglicanos relacionados ao CO. Outras proteínas importantes relacionadas aos processos mitocondriais (ex: desidrogenases) e enzimas associadas ao metabolismo energético também tiveram baixa expressão após a tratamento com melatonina. Essas alterações metabólicas podem afetar a glicólise aeróbica (efeito Warburg) resultando na diminuição da proliferação e potencial metastático das células tumorais *(*CHUFFA *et al.*, 2016b). Tendo a propósito que a melatonina regula muitas funções mitocondriais, existe a necessidade de se compreender qual tipo de relação é estabelecida na célula do CO humano e quais são as alterações moleculares apresentadas frente aos tratamentos com melatonina.

1.3 Melatonina e CO: envolvimento com a análise proteômica

Embora nos últimos anos ocorreram avanços nos métodos para diagnóstico de diversos tipos de câncer, o CO continua contabilizando altos índices de mortalidade devido à ausência de diagnóstico precoce (STENZEL; ABRAMS; MOYSICH, 2019). Nesse sentido, estudos estão sendo realizados para identificar formas de melhorar o prognóstico e, consequentemente, aumentar a expectativa de sobrevivência dos pacientes. Dessa forma, a análise proteômica se tornou uma alternativa promissora no estudo de alterações moleculares nas células tumorais (TOSS *et al.*, 2013; HUANG *et al.*, 2017;). Essa técnica gera informações que facilitam a identificação de alterações metabólicas e possíveis biomarcadores em células tumorais, importantes no aperfeiçoamento de prognósticos e no desenvolvimento de novas terapias (NA LI *et al*., 2018).

Recentemente, um perfil proteômico por espectrometria de massa em tecidos normais e tumorais de células de câncer ovariano, identificou 212 proteínas, das quais 6 foram observadas alteradas mostrando um papel importante na proliferação de células tumorais. A transgelin, queratina 14, ACTB, apoliproteína A1, peroxirredoxina-2 e a haptoglobina funcionam como ligantes em uma rede de sinalização que inclui resistência apoptótica, inflamação e motilidade celular, concluindo que mudanças na expressão dos genes dessas proteínas podem ser considerados biomarcadores para o diagnóstico dessa doença (ZADEH *et al.*, 2019).

Um estudo que utilizou células da linhagem SKOV-3 de câncer de ovário investigou mudanças proteicas em vias metabólicas mitocondriais. Após a análise, foi possível determinar proteínas modificadas em algumas vias importantes na progressão tumoral. Uma dessas vias, a

resistência a apoptose, é conhecida como um fator marcante em células tumorais e, nesse trabalho, foi observada uma disfunção na apresentação de antígenos relacionados aos receptores PD-1, importantes na morte celular programada. Alterações na via de sinalização GP6, relacionada a síntese plaquetária, no fator de tradução EIF2 e na função da glutationa sintase responsável por controlar a geração de ROS também foram identificadas nessas células tumorais (LI; ZHAN, 2019).

Fan e colaboradores (2015) utilizaram iTRAQ (isobaric tag for relative and absolute quantitation) para uma análise proteômica quantitativa, e observaram mudanças na expressão de proteínas entre 10 linhagens celulares de carcinoma ovariano e 2 linhagens celulares epiteliais normais. Alterações proteicas entre as linhagens foram identificadas e, desse modo, a comparação da expressão de proteínas entre as células de carcinoma e células normais demonstraram a importância da análise proteômica para a identificação de alvos moleculares que possam auxiliar no diagnóstico e tratamento da doença, apresentando melhor estratégia quando comparada apenas às mutações genômicas ou a transcrição de genes.

Nos últimos anos, os mecanismos moleculares da melatonina tem sido estudados em diversos tipos de câncer, incluindo o de ovário, apresentando efeitos pro-apoptóticos e parada do ciclo em células tumorais, sendo destacada como uma terapia adjuvante aos quimioterápicos já utilizados, melhorando sua eficácia e diminuindo os efeitos adversos (LI *et al.*, 2017). Nosso grupo de pesquisa analisou a perfil proteômico quantitativo em um modelo in vivo de câncer de ovário induzido com DMBA e, posteriormente, tratados com a melatonina. Dentre as proteínas reguladas negativamente por esse hormônio, estavam as pertencentes a diversas vias metabólicas que são essenciais para a sobrevivência da célula, como: sinalização via HIF-1, geração de energia, processamento e apresentação de antígenos e proteoglicanos relacionados aos câncer, apontando ação efetiva da melatonina na atenuação da proliferação celular e do metabolismo (CHUFFA *et al.*, 2016b). Para avaliar efetivamente a ação da melatonina na célula tumoral estudos adicionais são necessários para elucidar o metabolismo molecular da célula de carcinoma ovariano exposta a diferentes concentrações de melatonina e, então, traçar redes de eventos moleculares que possam auxiliar na compreensão dos seus efeitos terapêuticos.

2. JUSTIFICATIVA

Mecanismos moleculares envolvidos na proliferação, diferenciação celular, apoptose e resistência aos tratamentos estão associados com a progressão do CO, e já são conhecidos os efeitos benéficos da terapia funcional com a melatonina sobre essas vias de regulação no CO (CHUFFA *et al.*, 2018). O presente estudo investigará quais moléculas potenciais estão diferencialmente expressas nas células SKOV-3 frente ao tratamento com diferentes doses de melatonina. Sabendo que a melatonina é uma molécula que pode atuar por vários mecanismos, a compreensão desses efeitos poderá trazer novas oportunidades para o tratamento do CO.

3.HIPÓTESE

Considerando a importância do tratamento com melatonina nas células tumorais, a hipótese do estudo é de que o tratamento com melatonina altera a biossíntese de proteínas que estão relacionadas com o prognóstico ruim do CO, estimulando positivamente a apoptose e modificando o metabolismo das células SKOV-3.

4. OBJETIVO GERAL

Investigar o efeito da terapia com melatonina sobre as células de carcinoma ovariano humano (linhagem SKOV-3), utilizando a estratégia de análise proteômica global.

5. OBJETIVOS ESPECÍFICOS

- ✓ Avaliação da viabilidade celular e citotoxicidade através do ensaio do MTT;
- ✓ Análise proteômica global das células SKOV-3 por estratégia *shotgun*;
- ✓ Interpretação dos resultados junto ao software *PaternLab* e construção de redes de interação e heatmaps;
- ✓ Identificação de alterações na expressão de proteínas envolvidas em processos celulares importantes em células SKOV-3 posterior ao tratamento com melatonina;
- ✓ Correlação dos achados com dados de pacientes disponíveis em plataformas abertas.

6. REFERÊNCIAS

BRASSEUR, K.; GÉVRY, N.; ASSELIN, E. Chemoresistance and targeted therapies in ovarian and endometrial cancers. **Oncotarget**, Albany, v. 8, n. 3, p. 4008-4042, 2017.

BRETT, M.; PERMUTH, J. B.; THOMAS, A. S. Epidemiology of ovarian cancer: a review. **Cancer Biol. Med.**, Tianjin, v. 14, n. 1, p. 9-32, 2017.

CHUFFA, L. G. A. *et al*. Melatonin attenuates the TLR4-mediated inflammatory response through MyD88- and TRIF-dependent signaling pathways in an in vivo model of ovarian cancer. **BMC Cancer**, London, v. 15, p. 34, 2015.

CHUFFA, L. G. A. *et al*. Apoptosis is triggered by melatonin in an in vivo model of ovarian carcinoma. **Endocr. Relat. Cancer**, Woodlands, v. 23, n. 2, p. 65-76, 2016a.

CHUFFA, L. G. A. *et al*. Quantitative proteomic profiling reveals that diverse metabolic pathways are influenced by melatonin in an in vivo model of ovarian carcinoma. **J. Proteome Res.**, Washington, v. 15, n. 10, p. 3872-3882, 2016b.

CHUFFA, L. G. A. *et al*. The role of sex hormones and steroid receptors on female reproductive cancers. **Steroids**, New York, v. 118, p. 93-108, 2017.

CHUFFA, L. G. A.; REITER, R. J.; LUPI, L. A. Melatonin as a promising agent to treat ovarian cancer: molecular mechanisms. **Carcinogenesis**, Oxford, v. 38, n. 10, p. 945-952, 2017.

CHUFFA, L. G. A. *et al*. Mitochondrial functions and melatonina: a tour of reproductive cancers. **Cell. Mol. Life Sci.**, Basel, v. 76, n. 5, p. 837-863, 2018.

CLOVEN, N. G. *et al*. In vitro chemoresistance and biomarker profiles are unique for histologic subtypes of epithelial ovarian cancer. **Gynecol. Oncol.**, New York, v. 92, n. 1, p. 160-166, 2004.

COOK, D. P.; VANDERHYDEN, B. C. Ovarian cancer and the evolution of subtype classifications using transcriptional profiling†. **Biol. Reprod.**, New York, v. 101, n. 3, p. 645-658, 2019.

CORNELISON, R.; LIANEZA, D.; LANDEN, C. N. Emerging therapeutics to overcome chemoresistance in epithelial ovarian cancer: a mini review. **Int. J. Mol. Sci.**, Basel, v. 18, n. 10, p. 2171, 2017.

FAN, G. *et al*. A quantitative proteomic -based signature of platinum sensitivity in ovarian câncer cell lines. **Biocherm. J.**, London, n. 465, v. 3, p. 433-442, 2015.

GAMARRA-LUQUES, C. D. *et al*. Resistance to cisplatin and paclitaxel does not affect the sensitivity of human ovarian cancer cells to antiprogestin-induced cytotoxicity. **J. Ovarian Res.**, London, v. 7, p. 45, 2014.

GANDHI, A. V. *et al*. Melatonin is required for the circadian regulation of sleep. **Neuron**,

Cambridge, v. 85, n. 6, p. 1193-1199, 2015.

GUO, F.-J. *et al*. Effects of cyclooxygenase-2 gene silencing on the biological behavior of SKOV3 ovarian cancer cells. **Mol. Med. Rep.**, Boston, v. 11, n. 1, p. 59-66, 2015.

HO, C.-M. *et al*. Pure-type clear cell carcinoma of the ovary as a distinct histological type and improved survival in patients treated with paclitaxel-platinum-based chemotherapy in pure-type advanced disease. **Gynecol. Oncol.**, New York, v. 94, n. 1, p. 197-203, 2004.

HSIEH, S. F. *et al*. Prognostic factors of early stage epithelial ovarian carcinoma. **Int. J. Environ. Res. Public Health**, Basel, v. 16, n. 4, p. 1-12, 2019.

HU, W. *et al*. Snapshot: implications for melatonin in endoplasmic reticulum homeostasis. **Br. J. Pharmacol.**, London, v. 173, n. 24, p. 3431-3442, 2016.

HUANG, H. S. *et al*. Mutagenic, surviving and tumorigenic effects of follicular fluid in the context of p53 loss: initiation of fimbria carcinogenesis. **Carcinogenesis**, Oxford, v. 36, n. 11, p. 1419-1428, 2015.

HUANG, Z. *et al*. Proteomic profiling of human plasma for cancer biomarker discovery. **Proteomics**, Weinheim, v. 17, n. 6, p. 1-13, 2017.

INSTITUTO NACIONAL DO CÂNCER - INCA. **Estatística de câncer 2019**. Brasília: Ministério da Saúde, 2019.

JESSMON, P. *et al*. Epidemiology and treatment patterns of epithelial ovarian cancer. **Expert Rev. Anticancer Ther.**, v. 17, n. 5, p. 427-437, 2017.

KIM, S. *et al*. Tumor evolution and chemoresistance in ovarian cancer. **NPJ Precis. Oncol.**, London, v. 2, n. 20, p. 1-9, 2018.

LA VECCHIA, C. Ovarian cancer: epidemiology and risk factors. **Eur. J. Cancer Prev.**, Oxford, v. 26, n. 1, p. 55-62, 2017.

LEDERMANN, J. A. *et al*. Newly diagnosed and relapsed epithelial ovarian carcinoma: ESMO clinical practice guidelines for diagnosis, treatment and follow-up. **Ann. Oncol.**, Boston, v. 24, p. vi24-vi32, 2013. Suppl. 6.

LENGYEL, E. Ovarian cancer development and metastasis. **Am. J. Pathol.**, New York, v. 177, n. 3, p. 1053-1064, 2010.

LI, Y. *et al*. Melatonin for the prevention and treatment of cancer. **Oncotarget**, Albany, v. 8, n. 24, p. 39896-39921, 2017.

LI, N.; ZHAN, X. Signaling pathway network alterations in human ovarian cancers identified with quantitative mitochondrial proteomics. **EPMA J.**, Cham, v. 10, n. 2, p. 153-172, 2019.

LISIO, M, A. *et al*. High-Grade serous ovarian cancer: basic sciences, clinical and therapeutic

standpoints. **Int. J. Mol. Sci.**, Basel, v. 20, n. 4, p. 1-33, 2019.

LONGLEY, D. B.; JOHNSTON, P. G. Molecular mechanisms of drugs resistance. **J. Pathol.**, Chichester, v. 205, n. 2, p. 275-292, 2005.

MENÉNDEZ-MENÉNDEZ, J.; MARTÍNEZ-CAMPA. Melatonin: an anti-tumor agent in hormone- dependent cancers. **Int. J. Endocrinol.**, Cairo, v. 2, n. 3, p. 3271948, 2018.

LI, N.; LI, H.; CAO, L.; ZHAN, X. Quantitative analysis of the mitochondrial proteome in human ovarian carcinomas. **Endocr. Relat. Cancer**, Woodlands, v. 3, n. 25, p. 1-66, 2018.

OHLUND, D. *et al*. Type IV collagem stimulates pancreatic caner cell proliferation, migration, and inhibits apoptosis through an autocrine loop. **BMC Cancer**, London, v. 13, n. 1, p. 2-11, 2013.

PARIENTE, R. *et al*. Melatonin sensitizes human cervical cancer HeLa cells to cisplatin-induced cytotoxicity and apoptosis: effects on oxidative stress and DNA fragmentation. **J. Pineal Res.**, New York, v. 60, n. 1, p. 55-64, 2016.

REITER, R. J. *et al*. Melatonin as an antioxidant: under promises but over delivers. **J. Pineal Res.**, New York, v. 61, n. 3, p. 253-278, 2016.

REITER, R. J. *et al*. Inhibition of mitochondrial pyruvate dehydrogenase kinase: a proposed mechanism by which melatonina causes câncer cells to overcome cytosolic glycolysis, reduce tumor biomass and reverse insensitivity to chemotherapy. **Melatonin Res.**, San Antonio, v. 2, n. 3, p. 105-119, 2019.

REITER, J. R. Melatonin inhibits Warburg-dependent cancer by redirecting glucose oxidation to the mitochondria: a mechanistic hypothesis. **Cell. Mol. Life Sci.**, Basel, v. 77, n. 13, p. 2527-2542, 2020.

ROJAS, V. *et al*. Molecular characterization of epithelial ovarian cancer: Implications for diagnosis and treatment. **In. J. Mol. Sci.**, Basel, v. 17, n. 12, p. 2113, 2016.

SAWADA, K. *et al*. Loss of E-cadherin promotes ovarian cancer metastasis via 5-integrin, which is a therapeutic target. **Cancer Res.**, Baltimore, v. 68, n. 7, p. 2329-2339, 2008.

SHEN, C. J. *et al*. Melatonin suppresses the growth of ovarian cancer cell lines (OVCAR-429 and PA-1) and potentiates the effect of G1 arrest by targeting CDKs. **Int. J. Mol. Sci.**, Basel, v. 17, n. 2, p. 176, 2016.

STENZEL, A. E.; ABRAMS, S. I.; MOYSICH, K. B. A call for epidemiological research on myeloid-derived suppressor cells in ovarian cancer: a review of the existing immunological evidence and suggestions for moving forward. **Front. Immunol.**, Lausanne, v. 10, p. 1608, 2019.

SYMOWICZ, J. *et al*. Engagement of collagen-binding integrins promotes matrix metalloproteinase-9-dependent E-cadherin ectodomain shedding in ovarian carcinoma cells.

Cancer Res., Baltimore, v. 67, n. 5, p. 2030-2039, 2007.

TAMURA, H. *et al*. Melatonin and the ovary: physiological and pathophysiological implications. **Fertil. Steril.**, New York, v. 92, n. 1, p. 328-343, 2009.

TOSCHES, M. A. *et al*. Melatonin Signaling Controls Circadian Swimming Behavior in Marine Zooplankton. **Cell**, Cambridge, v. 159, n. 1, p. 46-57, 2014.

TOSS, A. *et al*. Ovarian cancer: Can proteomics give new insights for therapy and diagnosis? **Int. J. Mol. Sci.**, Basel, v. 14, n. 4, p. 8271-8290, 2013.

WORLD HEALTH ORGANIZATION - WHO. **Global cancer observatory**. Geneva: WHO, 2018.

ZADEH, F. H. B. *et al*. Proteome profiling of low grade serous ovarian cancer. **J. Ovarian Res.**, London, v. 12, n. 1, p. 1-14, 2019.

ZEMŁA, A. *et al*. Melatonin synergizes the chemotherapeutic effect of cisplatin in ovarian cancer cells independently of MT1 melatonin receptors. **In Vivo**, Attiki, v. 31, n. 5, p. 801-809, 2017.

ZHOU, Y. *et al*. Calycosin induces apoptosis in human ovarian cancer SKOV3 cells by activating caspases and Bcl-2 family proteins. **Tumor Biol.**, Basel, v. 36, n. 7, p. 5333-5339, 2015.

ZONTA, Y. *et al*. Melatonin reduces angiogenesis in serous papillary ovarian carcinoma of ethanol-preferring rats. **Int. J. Mol. Sci.**, Basel, v. 18, n. 12, p. 763, 2017.

Life Sciences 294 (2022) 120352

Contents lists available at ScienceDirect

Life Sciences

journal homepage: www.elsevier.com/locate/lifescie

The proteomic landscape of ovarian cancer cells in response to melatonin

Roberta Carvalho Cesário [a], Leticia Barbosa Gaiotte [a], Maira Smaniotto Cucielo [a], Henrique Spaulonci Silveira [a], Lucilene Delazari dos Santos [b,f], Debora Aparecida Pires de Campos Zuccari [c], Fábio Rodrigues Ferreira Seiva [d], Russel J. Reiter [e], Luiz Gustavo de Almeida Chuffa [a,*]

[a] Department of Structural and Functional Biology, Institute of Biosciences, UNESP - Sao Paulo State University, Botucatu 18618-689, São Paulo, Brazil
[b] Biotechnology Institute (IBTEC), São Paulo State University (UNESP), Botucatu, São Paulo, Brazil
[c] Faculty of Medicine of São José do Rio Preto, São José do Rio Preto, São Paulo 15090-000, Brazil
[d] Department of Biology, Biological Science Center, Universidade Estadual do Norte do Paraná – UENP, Luiz Meneghel Campus, Bandeirantes 86360-000, Paraná, Brazil
[e] Departament of Cell Systems and Anatomy, UT Health, San Antonio, TX 782229, USA
[f] Graduate Program in Tropical Diseases, Botucatu Medical School (FMB), São Paulo State University (UNESP), Botucatu, São Paulo, Brazil

ARTICLE INFO

Keywords:
Ovarian cancer
Melatonin
Proteome
Immune response
Mitochondrial metabolism
SKOV-3 cells

ABSTRACT

Ovarian cancer (OC) is the most lethal gynecological malignancy with a highly negative prognosis. Melatonin is an indoleamine secreted by the pineal gland during darkness and has shown antitumor activity in both in vitro and in vivo experiments. Herein, we investigated the influence of melatonin on the proteome of human ovarian carcinoma cells (SKOV-3 cell line) using the Ultimate 3000 LC Liquid NanoChromatography equipment coupled to a Q-Exactive mass spectrometry. After 48 h of treatment, melatonin induced a significant cytotoxicity especially with the highest melatonin concentration. The proteomic profile revealed 639 proteins in the control group, and 98, 110, and 128 proteins were altered by melatonin at the doses of 0.8, 1.6, and 2.4 mM, respectively. Proteins associated with the immune system and tricarboxylic acid cycle were increased in the three melatonin-exposed groups of cells. Specifically, the dose of 2.4 mM led to a reduction in molecules associated with protein synthesis, especially those of the ribosomal protein family. We also identified 28 potential genes shared between normal ovarian tissue and OC in all experimental groups, and melatonin was predicted to alter genes encoding ribosomal proteins. Notably, the set of proteins changed by melatonin was linked to a better prognosis for OC patients. We conclude that melatonin significantly alters the proteome of SKOV-3 cells by changing proteins involved with the immune response and mitochondrial metabolism. The concentration of 2.4 mM of melatonin promoted the largest number of protein changes. The evidence suggests that melatonin may be an effective therapeutic strategy against OC.

1. Introduction

Ovarian cancer (OC) is the most lethal malignant disease affecting the female reproductive system with high incidence among women [1]. This is likely related to the fact that symptoms such as swelling, early satiety, pain, and pelvic discomfort are not specific and are routinely ignored [2]. The main risk factors for OC include early age at menarche, late menopause, number of pregnancies, hormone replacement therapy, and genetic factors [3].

The heterogeneity of OC represents an obstacle to the choice of treatment and may contribute to the development of chemoresistance in many cases [4]. The resistance mechanisms used by tumor cells are diverse, including the cellular capacity to cause the efflux of drugs, which is associated with the overexpression of the MDR1 gene; this gene encodes the membrane transporter called P-glycoprotein (P-gp), decreasing the intracellular concentration of drugs such as paclitaxel [5].

Melatonin (*N*-acetyl-5-methoxytryptamine) is a small lipophilic indoleamine secreted by the pineal gland and to a lesser extent or not at all by other tissues [6]. Melatonin has well-known functions in healthy cells, acting as a potent antioxidant, removing reactive oxygen species (ROS) and reactive nitrogen species (RNS), increasing the activity of

* Corresponding author at: Department of Structural and Functional Biology, Institute of Biosciences of Botucatu, UNESP - São Paulo State University, 510, P.O Box: 18618-689, Rubião Júnior, s/n, Botucatu, SP, Brazil.
E-mail address: luiz-gustavo.chuffa@unesp.br (L.G. de Almeida Chuffa).

https://doi.org/10.1016/j.lfs.2022.120352
Received 9 November 2021; Received in revised form 14 January 2022; Accepted 18 January 2022
Available online 22 January 2022

antioxidant enzymes and preventing apoptosis [7,8]. On the contrary, in tumor cells, melatonin has anti-proliferative, anti-angiogenic, pro-apoptotic, pro-oxidant, and immunomodulatory properties [9–12].

It has been theorized that melatonin is present in higher concentrations in the mitochondria of normal cells compared to tumor cells [13]. Furthermore, melatonin functions in reversing the Warburg-type metabolism which is characteristic of many cancers including ovarian cancer [14], thus changing the energy metabolism of tumors and converting the cells to a healthier phenotype [15–17]. It has also hypothesized that melatonin (secreted at night) is capable of redirecting the pyruvate, the end product of glycolysis, from the cytosol to the mitochondria [18], thereby allowing for the conversion of pyruvate to acetyl-coenzyme A (acetyl-CoA) in the mitochondria and favoring oxidative phosphorylation. During melatonin synthesis, acetyl-CoA is also a necessary co-substrate for the rate limiting enzyme arylalkylamine *N*-acetyltransferase (AANAT), which is present in mitochondria [19]. The AANAT is essential for mitochondrial synthesis of melatonin which likely does not occur in cells that exhibit Warburg-type metabolism [20] since they lack acetyl-CoA in these organelles.

Although ongoing researches using multi-level proteomics have been useful to detect prognostic factors associated with OC [21], its application to determine the protein profile after OC treatment is still scarce. In this context, identifying novel methods and alternative therapies to improve patient outcomes is needed. Proteomic analysis has become a promising tool to identify molecular signatures in tumor cells [22,23]. This technique generates valuable information that facilitates the identification of metabolic changes and possible biomarkers in tumor cells, which are important for the development of new therapies [24].

To effectively access the proteome landscape of OC cells in response to melatonin, we examined the ability of melatonin, used at pharmacological levels, on human ovarian carcinoma SKOV-3 cells. We further constructed protein-protein interaction networks to evaluate the functional significance of melatonin treatment and to correlate the vitro data with OC patients.

2. Materials and methods

2.1. Cell lineage

The human ovarian carcinoma cell (SKOV-3 line) was originated from a patient with malignant ascites [25,26]. This cell line is potentially derived from clear cell adenocarcinoma and its mutational landscape is coincident with the most commonly mutated genes (e.g., *TP53*, *PIK3CA*, and *ARID1A*) [27].

2.2. Cell culture and reagents

SKOV-3 cells (ATCC® HTB-77) were obtained from the American Type Culture Collection (ATCC, Manassas, VA, USA) packaged in our laboratory. Cells were grown in RPMI medium (Gibco, Paisley, UK), supplemented with 10% fetal bovine serum (FCS; Gibco) and penicillin at 100 IU/mL and 100 μg/mL streptomycin (Gibco) at 37 °C in an atmosphere humidified with 5% CO2. The cells were periodically expanded in 75 cm2 cell culture flasks (Costar, Cambridge, MA, USA), with the base culture medium being changed every two days. After reaching 90% of confluence, the cell culture supernatant was aspirated, and the cells were incubated with trypsin/EDTA (Gibco) to block their adherence to the culture flask. After centrifugation, cells were washed in a base culture medium, resuspended, and frozen for future reuse.

2.3. Treatments and experimental groups

To investigate the effects of melatonin, the study examined the cells of four experimental groups: 1) Control Group: SKOV-3 cells treated with standard RPMI medium supplemented with FCS, penicillin, and streptomycin; 2) 0.8 mM melatonin Group: SKOV-3 cells treated with melatonin at a concentration of 0.8 mM for 48 h; 3) 1.6 mM melatonin Group: SKOV-3 cells treated with melatonin at a concentration of 1.6 mM for 48 h. 4) 2.4 mM melatonin Group: SKOV-3 cells treated with melatonin at a concentration of 2.4 mM for 48 h. The exposure period has been previously confirmed, and melatonin concentrations have also shown to be effective in inhibiting cell proliferation while inducing apoptosis [28].

2.4. Cytotoxicity assay

SKOV-3 cells were seeded in 96-well plates, and after exposure to different concentrations of melatonin, cell survival was measured using a colorimetric method. After 48 h of treatment, the MTT solution (5 mg/mL) was added, and the presence of formazan crystals was evaluated using a microplate reader (Epoch) at 550 nm. The reading spectrum (650 nm) was used for the reference curve. Percentage of cytotoxicity was calculated relative to the control group.

2.5. Enzymatic digestion of proteins in solution

Initially, 50 μg of lyophilized proteins from the cells were diluted in 60 μL of 50 mM ammonium bicarbonate, and then 25 μL of Standard RapiGest SF surfactant (code 186001861, Waters) was added to the samples, which were incubated at 37 °C for 60 min. Then, the samples were submitted to reduction and alkylation steps, using 10 mM DTT and 45 mM iodoacetamide, respectively. The enzymatic digestion solution was carried out using the enzyme trypsin at a concentration of 1:100 (enzyme: sample) solubilized in 50 mM ammonium bicarbonate buffer, pH 7.8. The hydrolysis took place for 18 h and was stopped with the addition of 10 μL of 5% formic acid (v/v). The samples were incubated for 90 min at room temperature and later centrifuged at 14,000 ×*g* at 6 °C for 30 min. The supernatant was placed into a new tube. The tryptic digests in each sample were submitted to the Peptide Cleanup C18 Spin desalting columns (code 5188-2750 Agilent Technologies) according to the manufacturer's recommendations.

2.6. Peptide sequencing by mass spectrometry

Label free mass spectrometry analyses were performed using an Ultimate 3000 LC Liquid NanoChromatography device (Dionex, Germering, Germany) coupled with a Q-Exactive mass spectrometry device (Thermo Fisher Scientific, Bremen, Germany). The mobile phases were: A) 0.1% formic acid [v/v] in LCMS water and B, 0.1% formic acid [v/v] in 80% [v/v] acetonitrile. Peptides were loaded onto a C18 guard column, 30 μm × 5 mm (Code 164649, ThermoFisher Scientific), and desalted in an isocratic gradient of 4% B for 3 min at a flow rate of 300 nL/min. Then, the peptides were fractionated by an analytical column Reprosil-Pur C18-AQ, 3 μm, 120 Å, 105 mm (Code 1PCH7515-105H354-NV, PICOCHIP) using a linear gradient of 4–55% B for 30 min, 55% at 90% B for 1 min, held at 90% B for 5 min, and rebalanced at 4% B for 20 min at a flow rate of 300 nL/min. Ionization was achieved using a Nano spray ion source (PICOCHIP). The operation mode was positive ionization using the DDA method. MS spectra were acquired from *m/z* 200 to *m/z* 2000, 70,000 resolution, and 100 ms injection time. The fragmentation chamber was conditioned with collision energy between 29 and 35% with a resolution of 17,500, 50 ms injection time, 4.0 *m/z* isolation window, and dynamic exclusion of 10s. Spectrometry data were acquired using Thermo Xcalibur software (version 4.0.27.19, Thermo-Fisher Scientific Inc.).

2.7. Analysis of proteomics data

Raw data was subjected to PatternLab software (version 4.0.0.84) to obtain protein identification. The main parameters used in this tool were: Swiss-Prot database (Arthropod taxonomy); trypsin enzyme; permission of 2 lost cleavages; post-translational modification

carbamidomethylation of cysteine residues; post-translational modification variable oxidation of methionine residues; tolerance errors MS 40 ppm and MS/MS 0.0200 ppm. The maximum false discovery rate (FDR) considered was ≤1%.

2.8. Identification of functional enrichment of proteins in melatonin-treated OC cell

We analyzed the ontological terms and molecular pathways enriched by the differentially regulated proteins using the KOBAS 3.0 software (http://kobas.cbi.pku.edu.cn/) [29]. The enriched pathways were set to the adjusted p-value ≤ 0.05 and a cutoff of at least four proteins participating in the given biological process or pathway. The functional enrichment analysis was generated by Graph Pad Prism (GraphPad Software, version 9.2.0). Shared proteins regulated by melatonin relative to the control group were plotted as a Venn diagram using the VENNY 2.0 tool (https://bioinfogp.cnb.csic.es/tools/venny/) and Intervene UpSet plot for multiple molecules sets [30].

2.9. Protein-protein interaction and overall survival analysis

The interaction between positively and negatively-regulated proteins were analyzed using the online STRING tool (https://string-db.org) [31]. The highest confidence with a minimum interaction of 0.900 was used in the networks, and all unconnected nodes were excluded.

For the analysis of overall survival and risk assessment, we used data from the TCGA tumor datasets available at the CBioPortal for cancer genomics (v. 3.5.4) (https://www.cbioportal.org/) [32]. The overall survival (%) and gene mutation frequency (%) were determined using data from the patients with ovarian cancer. Kaplan-Meier analysis was applied according to the Logrank test (P value < 0.05). This tool facilitates the assessment of patients' prognosis through the use of genes secreted in the OC that are potentially changed by melatonin.

2.10. Identification of secreted proteins and shared targets between healthy ovarian tissue and OC

With the aid of The Human Protein Atlas database (https://www.proteinatlas.org/) [33] we evaluated the classification of proteins regulated by melatonin using data from the following categories: molecules secreted by MDSEC (n = 2943), combined transmembrane protein topology, and signal peptide predictor (Phobius) (n = 3338), Signal IP (n = 2525), predicted membrane proteins (SPOCTOPUS) (n = 3710), and citric acid cycle (n = 30). Purple circles indicate the presence of the protein, and beige indicates the absence of proteins in the databases, as mentioned earlier. To access the connectivity of important targets in OC signaling based on the TCGA, we initially selected 48 targets and then associated them with an interaction network using the PINA 3.0 tool (https://omics.bjcancer.org/pina/home.action). The targets with the highest specificity were selected and demonstrated on a comparative heat map. We identified the changes in proteins which were found to be present in the SKOV-3-derived exosomes available from [34] a total of 732 proteins were detected in SKOV-3 cells in 2 or more replicates. The exosomes secreted by SKOV-3 cells were isolated from EV-depleted medium following differential centrifugation.

The Genotype-Tissue Expression (GTEx) database [35,36], provides gene expression data from various tissues, including normal ovarian tissue. Based on the 100 most expressed genes in ovarian tissue, we correlated them with the genes found in the control group. Thus, 54 genes were shared between normal tissue and the control group (SKOV-3 cells). Based on these targets, we correlated all genes altered by melatonin at the three dosages. Thus, 28 genes were shared between normal tissue, control group, and melatonin-exposed groups. The selected genes were depicted in a heat map using the webtool Morpheus (https://software.broadinstitute.org/morpheus/). We used the fold-change ≥|1.5| ≤ |-1.5| to cluster these DEGs. Data were clustered using Euclidean distance.

2.11. Statistical analysis and data representation

Heatmaps and similarity matrix for clustering analyses were performed using the web tool Morpheus (https://software.broadinstitute.org/morpheus) [37]. PCA and bar plots were performed using Graph Pad Prism (v. 9.2.0). The data were subjected to ANOVA analysis of variance complemented with Tukey's multiple comparisons test. For non-parametric data, the Kruskal-Wallis test was used, complemented by the Dunn's test. The results were expressed as mean ± SEM and presented in tables and graphs, considering the 5% of significance level (P < 0.05).

3. Results

3.1. Identification of the proteomic profile in human ovarian cancer SKOV-3 cells after melatonin treatment

After 48 h of treatment with specific concentrations of melatonin, a statistically significant reduction in cell viability was evidenced in only the group treated with 2.4 mM melatonin (Fig. 1A). By recognizing the potential cellular metabolic alterations, we investigated the proteomic changes in OC cells following melatonin exposure. From the total proteomic profile, we identified 432, 431, and 210 proteins following the administration of melatonin at the doses of 0.8 mM, 1.6 mM and 2.4 mM, respectively. Based on the spectral counts of proteins, we identified a distinct clusterization pattern for the two highest doses of melatonin compared to the lower dose and control group (Fig. 1B–D). Among all identified proteins, 146 of them were shared by the four experimental groups, and nine different clusters were formed, revealing an increase in the spectral count for most abundant proteins.

After proteins were extracted and processed through mass spectrometry, we identified a total of 636 proteins in the control cells (Table S1). Differentially expressed proteins were selected for each group based on the comparison with the control group using a p value of <0.05. In addition, we applied a fold change of +1.5 or −1.5 to determine which proteins were increased or decreased, respectively (PatternLab 4.0.0.84). OC cells treated with melatonin at a concentration of 0.8 mM had 59 increased proteins (60.2%) and 39 decreased proteins (39.8%) (Table S2, Fig. 2A). The cells that received 1.6 mM melatonin showed 57 increased proteins (51%) and 54 decreased proteins (49%) (Table S3, Fig. 2A). OC cells exposed to 2.4 mM of melatonin had 33 increased (25.38%) and 97 decreased proteins (74.61%) (Table S4, Fig. 2A).

Next, we identified eight common proteins among the experimental groups (control, 0.8 mM, 1.6 mM, and 2.4 mM); these were 4F2, S10A6, DHRS2, LDHAL6A, CANX, RPL14, CKB, and HMGA1. Also, we detected 382 proteins that were exclusive in the control group, two in the 0.8 mM (SDB, NMEI1), and four in the 1.6 mM (NEED8, ERBB3, ERZ, TMOD2) and 2.4 mM (HBD, KRT6, TPMK3, H1-2) melatonin groups (Fig. 2B). The interplots showed the number of shared and exclusive proteins that varied with melatonin concentrations. We observed three shared proteins (HMGA1, CKB and DHRS2) that were increased in the three groups (Fig. 2C) while two proteins (RPL14 and SLC3A2) were commonly reduced by melatonin exposure (Fig. 2D).

3.2. Melatonin regulated proteins that are involved in critical pathways and cellular processes

Protein-protein interaction (PPI) networks were generated using the STRING database based on the differentially expressed proteins. Proteins that were upregulated by exposure to 0.8 mM melatonin enriched biological processes such as immune system, catalytic activity, and p53 checkpoint (Fig. 3A), while proteins functionally associated with cell differentiation, structural constituent of the cytoskeleton, and

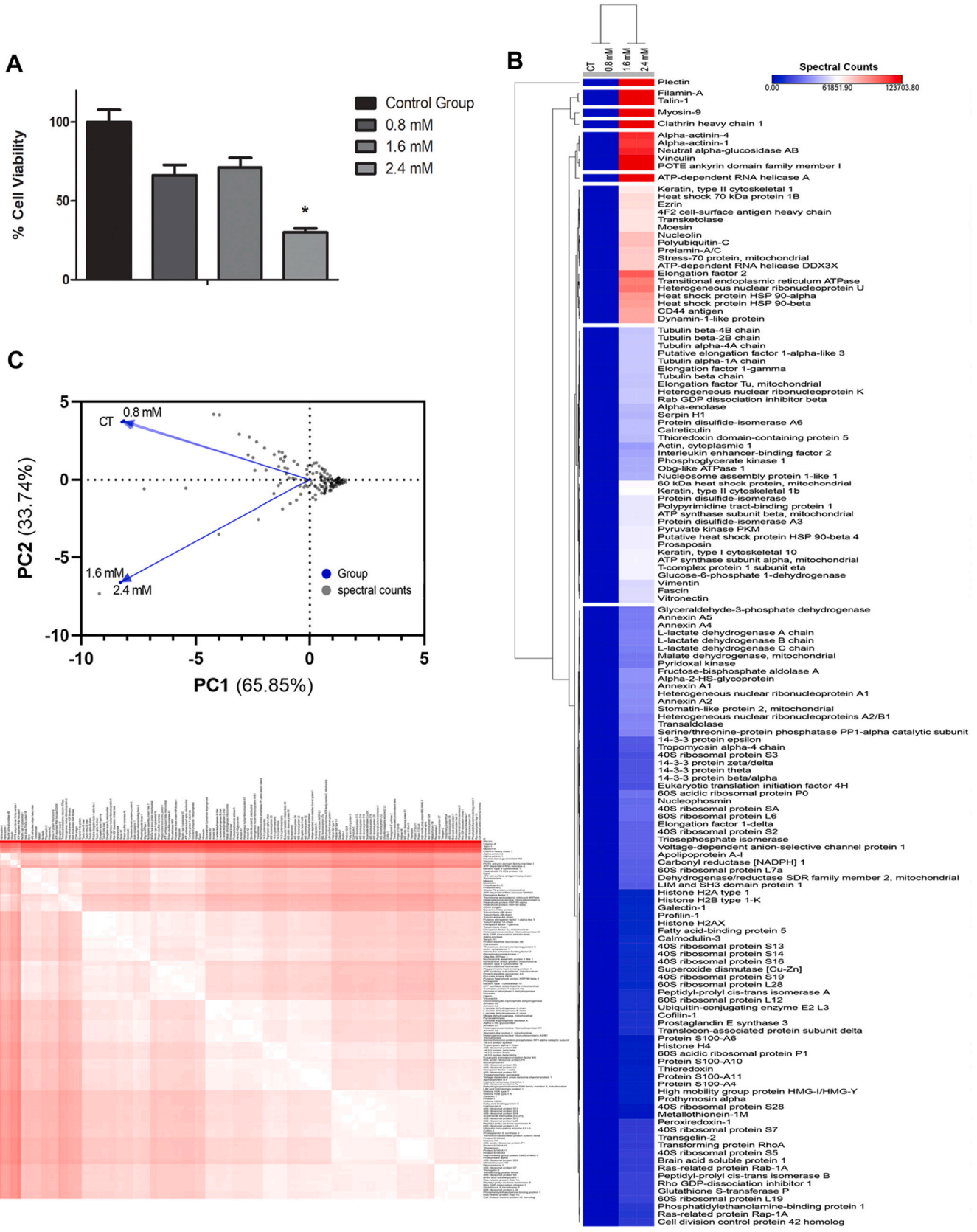

Fig. 1. Cell viability and spectral counts of proteins in ovarian cancer SKOV-3 cells after exposure to specific concentrations of melatonin (0.8, 1.6, and 2.4 mM) for 48 h. A) MTT assay after melatonin treatment. * $P < 0.01$ vs control group. Data are expressed as the mean ± standard error. One-way ANOVA, complemented by Tukey's test. B) Heat map depicting the spectral counts of proteins following the treatments. Rows and columns are clustered using Euclidean distance. C) Principal component analysis (PCA) of the protein spectra in the four experimental groups. D) Similarity matrix evidencing the correlation of spectra. CT: control group.

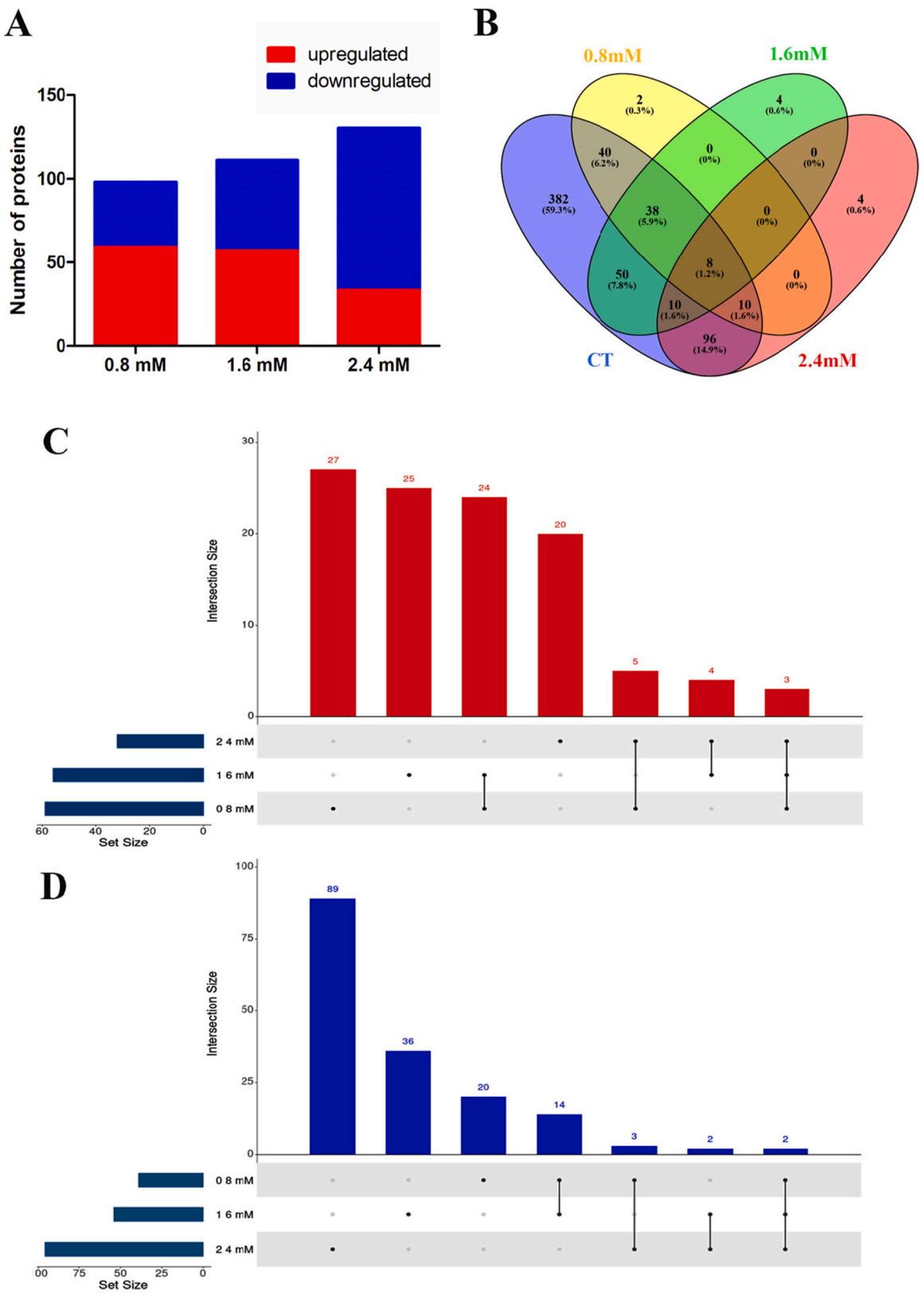

Fig. 2. The number of proteins identified across the experimental groups. A) Bar plot showing the number of increased and decreased proteins among the groups. B) Venn diagrams depicting common and exclusive proteins among the control group and melatonin-treated groups at the doses of 0.8 mM, 1.6 mM and 2.4 mM. The graph was generated using Venny 2.0 (https://bioinfogp.cnb.csic.es/tools/venny/). The intersections of proteins that were positively (C) and negatively (D) altered by melatonin shared among experimental groups. Graphics were generated using Intervene UpSet modules (https://intervene.shinyapps.io/intervene/). CT: control group.

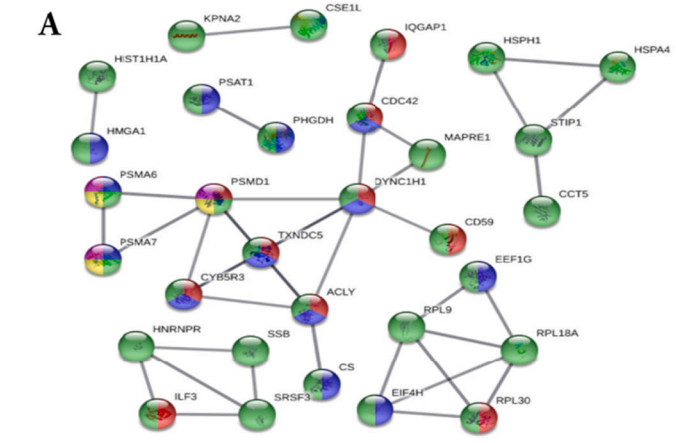

Immune system
Catalytic activity
Intracellular part
Proteossome
p53 checkpoint

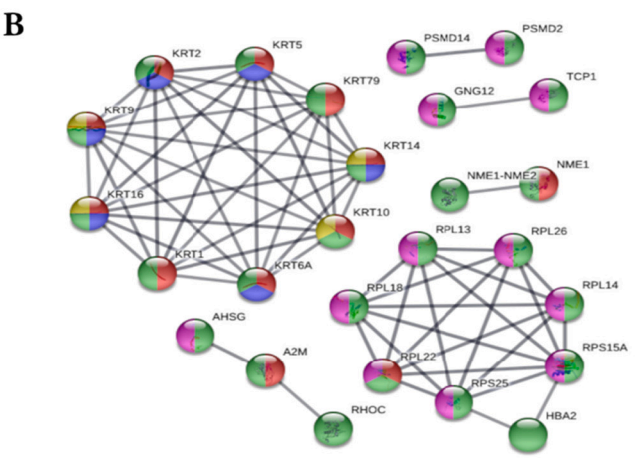

Cell differentiation
Structural constituent of cytoskeleton
Intracellular part
Estrogen signaling pathway
Metabolism of proteins

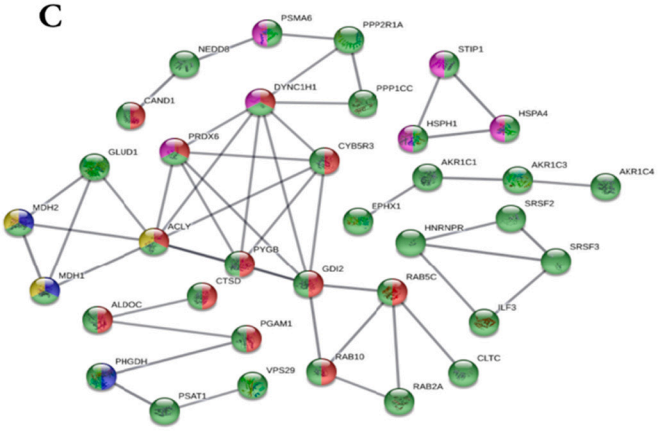

Immune response
L-malate dehydrogenase activity
Cytoplasm
Citrate cycle (TCA cycle)
Cellular responses to stress

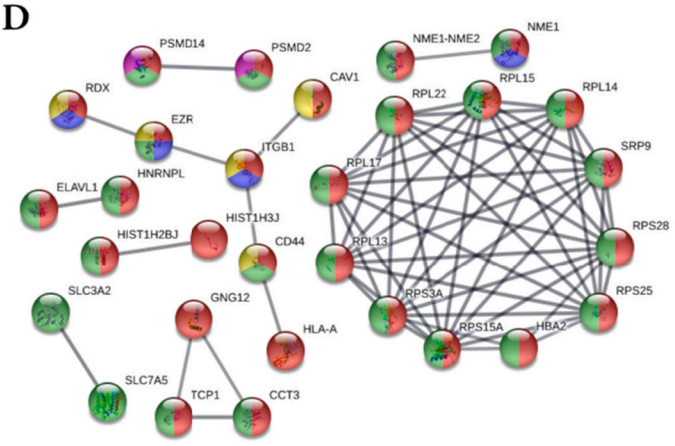

Regulation of biological process
Cytoskeletal protein binding
Cytosol
Proteoglycans in cancer
S fase

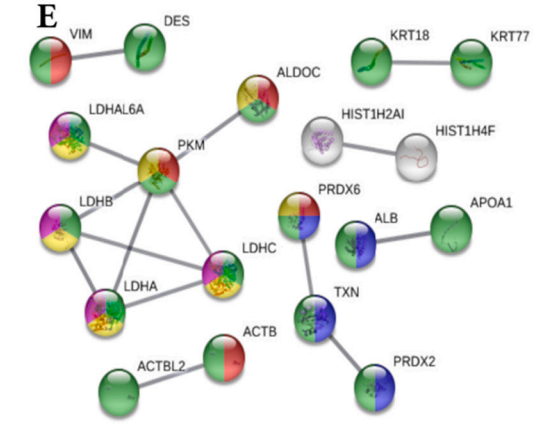

Immune system process
Antioxidant activity
Cytoplasm
Metabolic pathways
TCA and respiratory electron transport

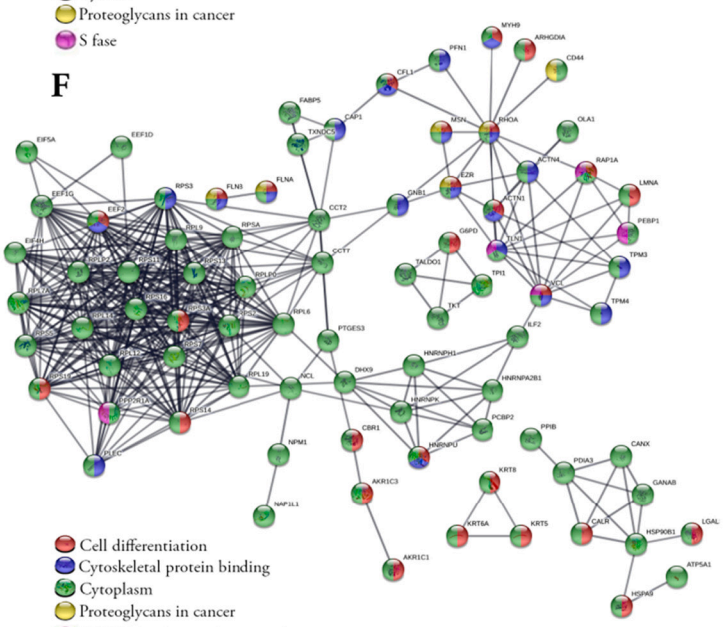

Cell differentiation
Cytoskeletal protein binding
Cytoplasm
Proteoglycans in cancer
MAPK Family signaling cascades

(caption on next page)

Fig. 3. Differentially altered proteins were associated with the protein-protein interaction (PPI) networks and the top five functional enrichments were based on GO terms, KEGG and Reactome pathways. PPI generated with proteins that were positively (A) and negatively (B) altered by the melatonin at the dose of 0.8 mM. PPI generated with proteins that were positively (C) and negatively (D) altered by the exposure to 1.6 mM melatonin. PPI generated with proteins that were positively (E) and negatively (F) altered by the exposure to 2.4 mM melatonin. Functional interaction analysis was performed using STRING 11.0 (PPI enrichment p-value < 0.001; minimum confidence score: 0.9). TCA: tricarboxylic acid cycle, MAPK: mitogen-activated protein kinase.

metabolism of proteins were enriched by decreased proteins (Fig. 3B). In addition, exposure to 1.6 mM of melatonin increased proteins involved in the immune response, L-malate dehydrogenase activity, and cellular responses to stress (Fig. 3C), and decreased proteins related to biological process regulation and S phase of the cell cycle (Fig. 3D). Regarding the concentration of 2.4 mM of melatonin, the increased proteins were mainly associated with tricarboxylic acid cycle, respiratory electron transport and other metabolic pathways (Fig. 3E). In contrast, decreased proteins were involved with cytoskeletal protein binding and MAPK signaling (Fig. 3F).

For a further correlation of the differentially altered proteins, we evaluated their interactions using KEGG and Reactome databases. Of note, functional enrichment analysis revealed signaling pathways related to the immune system and tricarboxylic acid metabolism as significantly increased in the three groups treated with melatonin (Fig. 4). Furthermore, treatment with 0.8 mM of melatonin promoted greater expression of proteins involved in the apoptotic pathway. Increased proteins also enriched pathways such as cellular stress response and tumor necrosis factor after treatments with 1.6 mM or 2.4 mM melatonin, respectively. Notably, cellular metabolism, estrogen signaling pathway, as well as the interleukin-1-related signaling was negatively altered in the group exposed to 0.8 mM of melatonin (Fig. 4A). Regarding the concentrations of 1.6 mM and 2.4 mM of melatonin, they negatively altered proteoglycans in cancer; while ERK1/ERK2 cascade were related to decreased proteins induced by 1.6 mM of melatonin (Fig. 4B), the signaling of the MAPK pathway and BRAF were predicted to be reduced after 2.4 mM melatonin (Fig. 4C).

The source of the differentially altered proteins by melatonin were also examined and they were classified according to the databases available in The Human Protein Atlas (the categories included molecules secreted by MDSEC, combined transmembrane protein topology and signal peptide predictor (Phobius), Signal IP, predicted membrane proteins (SPOCTOPUS), and tricarboxylic acid cycle. A set of 48 targets were selected based on the presence of at least one database (Fig. S1). To characterize the connectivity of these targets with important OC-related signaling pathways, we used the PINA 3.0 tool which was connected with data from The Cancer Genome Atlas Program (TCGA) considering ovarian cancer interactions (Fig. S2); a total of 17 secreted proteins were reported with high specificity in patients with OC, as shown in Fig. 5A. Six co-existing targets were shared by all databases. More specifically,

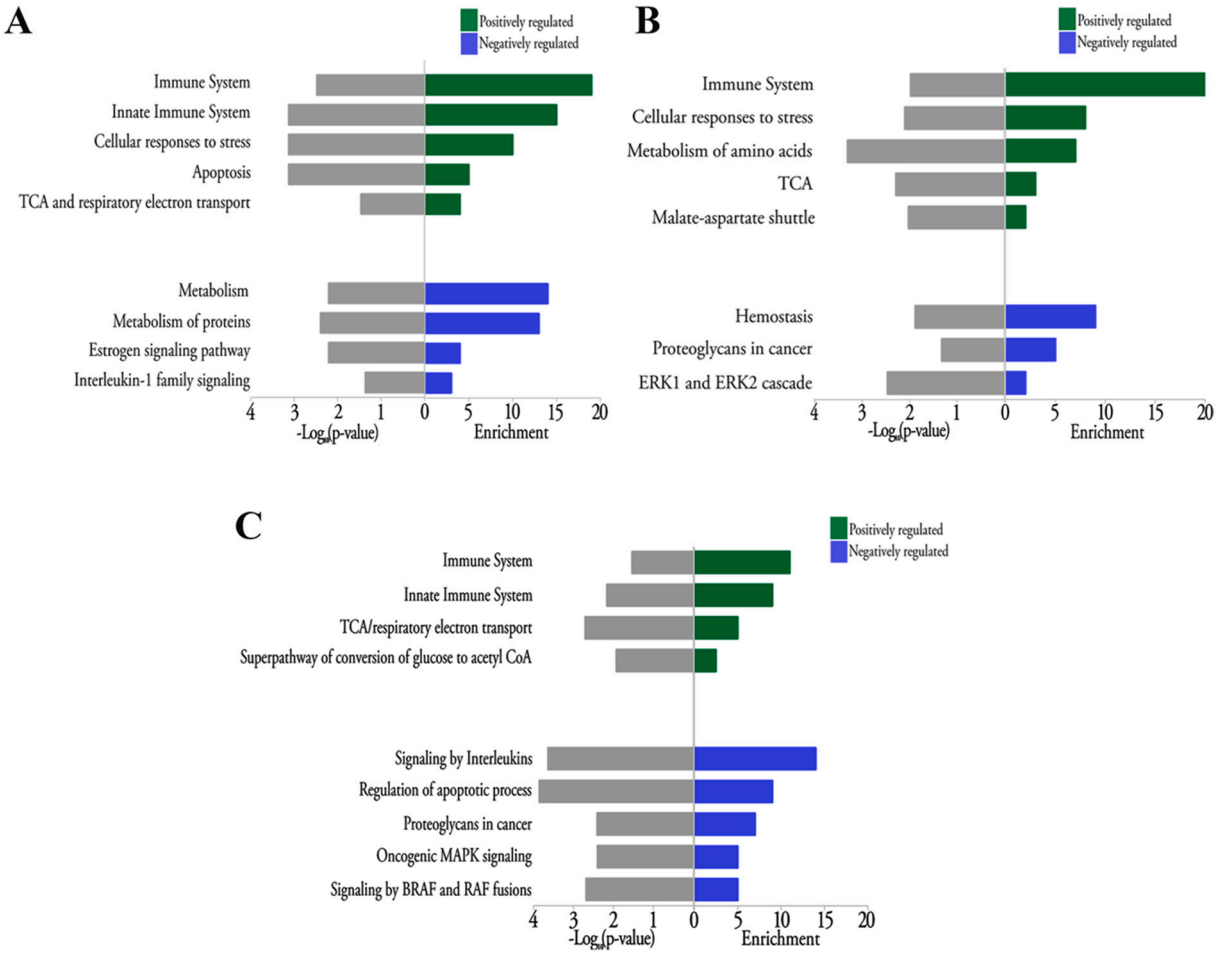

Fig. 4. Functional enrichment analysis using differentially expressed proteins after treatment with melatonin. Proteins that were positively (horizontal green bars) or negatively (horizontal blue bars) altered by melatonin at 0.8 mM (A), 1.6 mM (B), and 2.4 mM (C) enriched important functional pathways associated with OC cells (SKOV-3 cell line). Adjusted -Log_{10} P-value ≤ 0.05 (left bars) and number of enriched terms (right bars). Graphics were generated using GraphPad Prism 9.2. (For interpretation of the references to colour in this figure legend, the reader is referred to the web version of this article.)

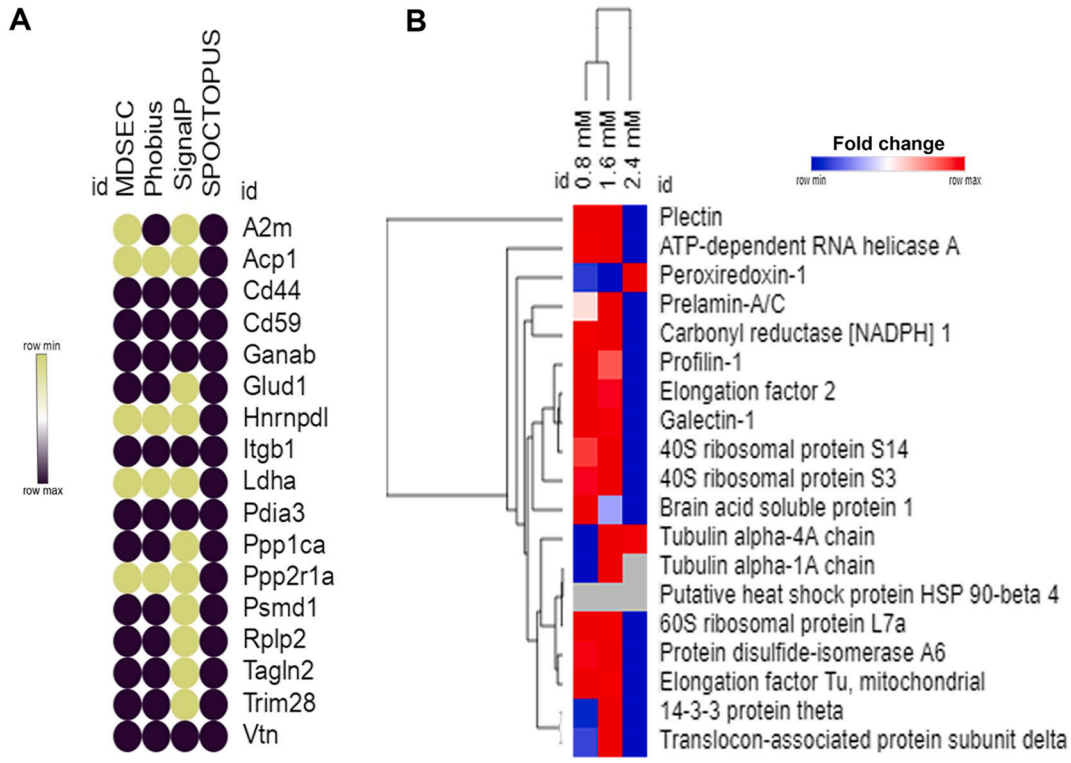

Fig. 5. Representative proteins altered by melatonin that interacted with important signaling pathways in OC. A) Graph showing 17 main proteins in the following databases (MDSEC, Phobius, Signal IP and SPOCTOPUS) available in the The Human Protein Atlas (HPA). Dark circles indicate the presence of the protein and beige indicates the absence of proteins. B) Heat map illustrating 19 proteins which are derived from exosomes of the SKOV-3 cells. Data were based on the fold-change value of each experimental group. Rows and columns were clustered using Euclidean distance. Access in September 2021. (For interpretation of the references to colour in this figure legend, the reader is referred to the web version of this article.)

Cd59 and Vtn were increased by melatonin at concentrations of 1.6 mM and 2.4 mM, respectively. The Cd44 and Itgb1 were decreased by melatonin at 1.6 mM, as well as Pdia3, Ganab, and Cd44 were reduced after exposure to 2.4 mM of melatonin. We further examined the proteins altered by melatonin that are secreted by the SKOV-3-derived exosomes according to a previous study by Cheng and colleagues [31]. After matching these molecules with our data, we identified 19 proteins varying along melatonin-treated groups. The proteins associated with SKOV-3 cells treated with 2.4 mM of melatonin showed a unique clustering profile and plectin, ATP-dependent RNA helicase A, prelamin A/C, carbonyl reductase [NADPH] 1, profilin-1, elongation factor-2, galectin-1, elongation factor Tu, mitochondrial, 40S ribosomal proteins, brain acid soluble protein 1, protein disulfide-isomerase A6, 14-3-3 protein theta, and translocon-associated protein subunit delta were all underrepresented (Fig. 5B).

3.3. Protein-coding genes altered by melatonin predict greater overall patient survival

Considering the genes encoding proteins that were altered by melatonin treatment over the doses, we investigated the relationship of these targets with overall patient survival. We exploited the cBioPortal platform to correlate OC patient's samples with differentially expressed genes (DEGs). Then, we identified and stratified patients who presented alterations/mutations in this gene set (red line) or no alterations (blue line) based on the targets potentially regulated by melatonin.

Importantly, OC samples of patients who showed altered target genes were associated with longer survival, as shown in the treatment groups of 0.8 (log-rank p-value = 0.04), 1.6 (log-rank p-value = 7.63e−3), and 2.4 mM (log-rank p-value = 0.01) (Fig. 6A). Based on the same criteria of the gene set encoding proteins that are melatonin-regulated, we further analyzed the top 10 genes with the highest mutation frequency comparing the altered and unaltered groups. Although not significant, the majority of genes of the altered group (melatonin-regulated) showed a reduced frequency of mutation (Fig. 6B).

3.4. Identification of shared targets between healthy ovarian tissue and melatonin-treated OC

To investigate genes shared between normal ovarian tissue and ovarian cancer (control group), we used publicly available gene expression data from the Genotype-Tissue Expression (GTEx). The 100 most-commonly expressed genes present in normal ovarian tissue were compared to DEGs in the control group and in the three groups exposed to melatonin. Among all genes, we detected 28 genes shared among the GTEx sample data and in at least one of our experimental groups (Fig. 7A). These targets were analyzed using a clusterization method where the treatment with melatonin showed a distinct gene expression profile of the OC cells exposed to 2.4 mM of melatonin, especially in the genes encoding ribosomal proteins. Furthermore, treatment with the lowest concentrations revealed a more similar pattern of expression of these ovarian regulatory targets (Fig. 7B). These results were confirmed by the principal component analysis (PCA), reinforcing the fact that the results of the lower concentrations of melatonin (0.8 mM and 1.6 mM) significantly differed from those of the higher dosage (2.4 mM) (Fig. 7C).

4. Discussion

In this series of studies, we evaluated the effects of melatonin on human ovarian carcinoma cells. Although there have been significant advances uncovering novel OC treatments, no decisive therapeutic option exists to date. Tumor cells develop metabolic changes that allow unrestrained pathological cell growth; thus, the identification of these changes may provide treatment benefits for patients [38]. Our results

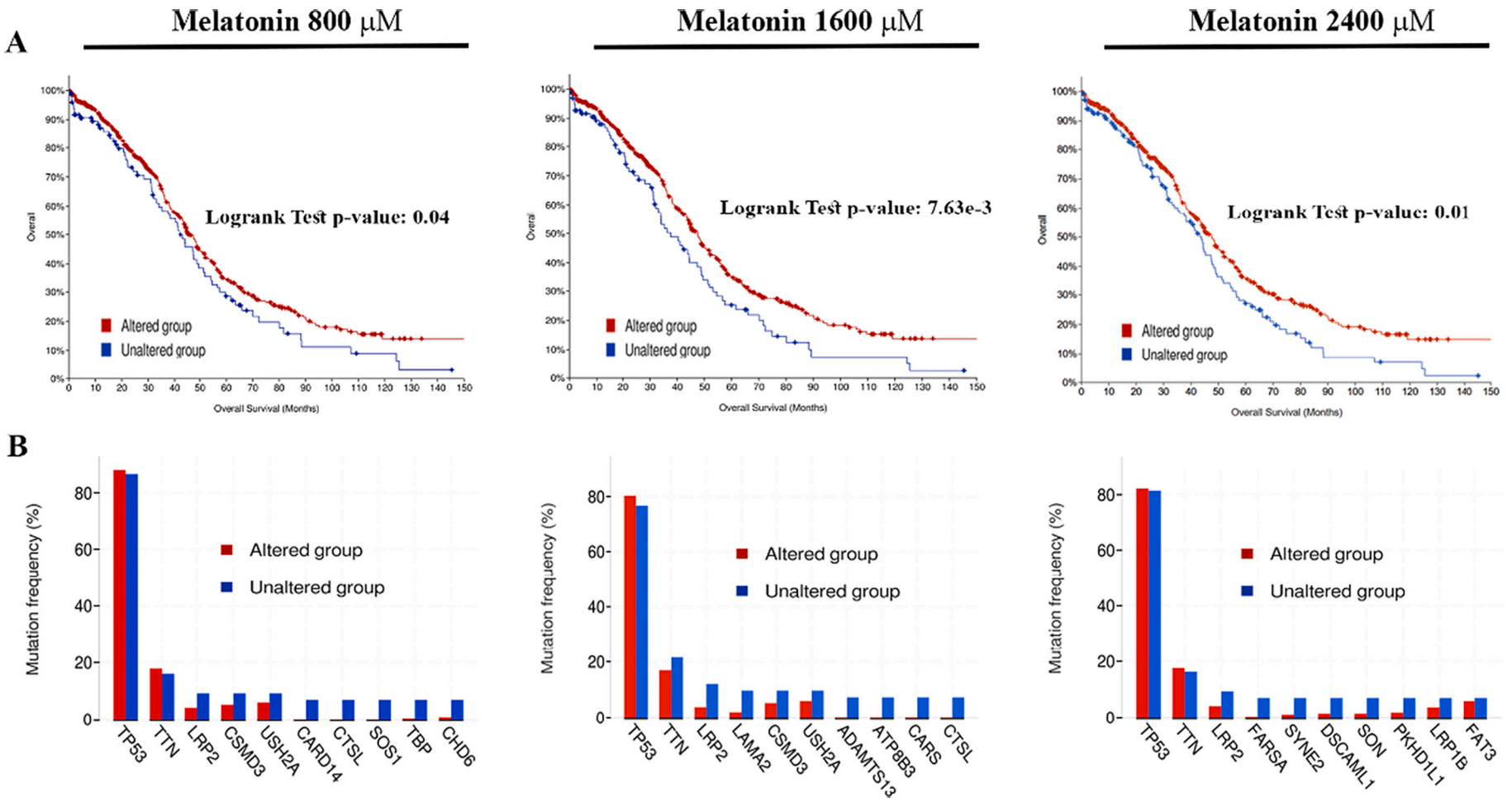

Fig. 6. Correlation of DEGs with prognosis in patients with OC. A) Overall survival curves comparing patients with altered (red line) and non-altered (blue line) targets that were affected by melatonin treatment in OC cells. Adjusted risk ratio with the respective 95% confidence intervals, and log-rank test p-value were determined by univariate Cox regression analyzes, and demonstrated as the Kaplan-Meier analysis. B) Correlation of the 10 most frequent mutated genes between altered (red bar) and unaltered (blue bar) groups. (For interpretation of the references to colour in this figure legend, the reader is referred to the web version of this article.)

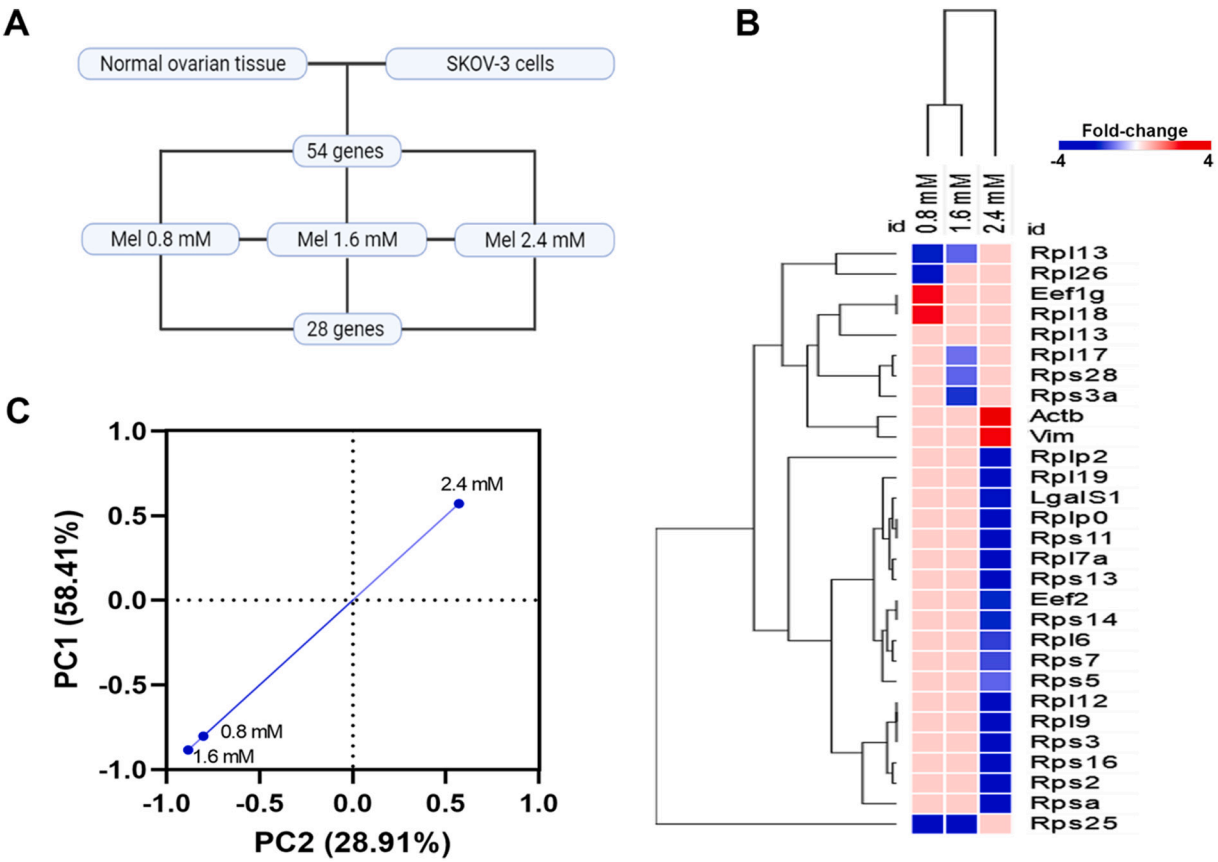

Fig. 7. Differentially altered targets after melatonin treatment in SKOV-3 cells. A) Diagram showing the number of common targets among all experimental groups and the 100 most expressed genes in normal ovarian tissue obtained from the GTEx biobank (https://gtexportal.org/home/). B) Heat map showing the expression levels (fold-change) of common targets in all dosing groups (positive and negative regulation) relatively to the control group and normal ovarian tissue. The rows (proteins) and columns (melatonin concentrations) were clustered using Euclidean distance. C) Principal component analysis (PCA) showing the individually determined points according to the doses of 0.8 mM, 1.6 mM, and 2.4 mM of melatonin.

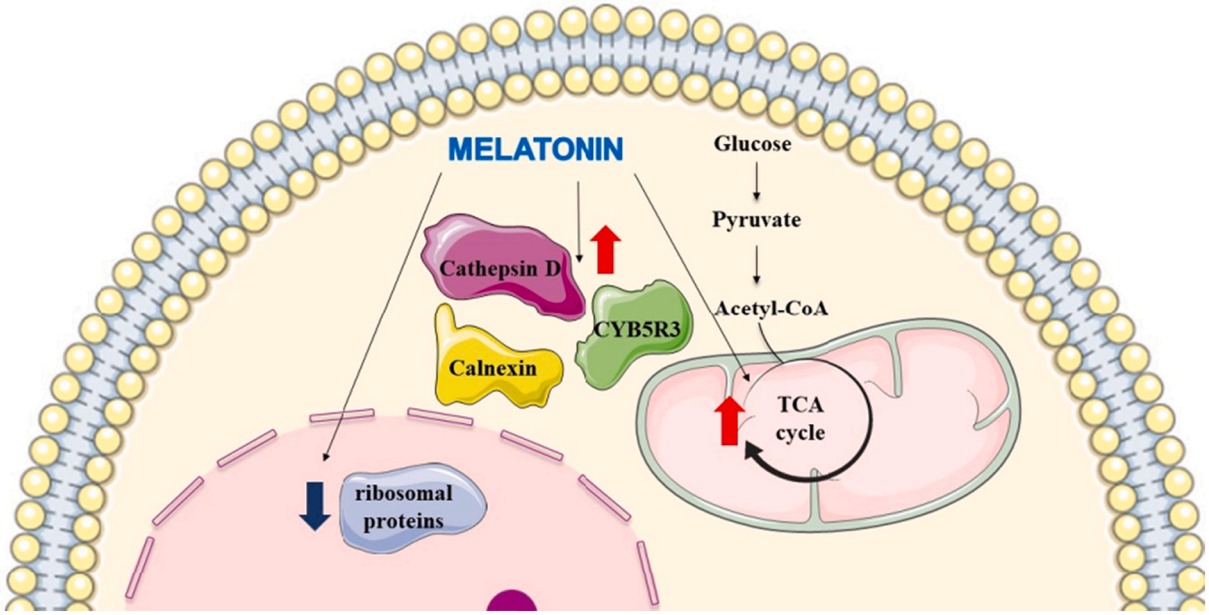

Fig. 8. Schematic illustration of the main proteome-based actions of melatonin in the OC cell. Treatment with melatonin was effective in increasing proteins associated with the immune response and TCA cycle while reducing the availability of ribosomal proteins. Red up arrow: increased proteins; blue down arrow: reduced proteins. TCA: tricarboxylic acid, CYB5R3: cytochrome *b*5 reductase 3. (For interpretation of the references to colour in this figure legend, the reader is referred to the web version of this article.)

demonstrated that melatonin promoted significant changes for the partial reestablishment of the OC cell functions, corroborating the findings of others who showed that melatonin is an effective adjuvant therapy to treat a variety of other cancers [39].

The pharmacological concentrations of melatonin used in this study are easily within the safety range of this molecule because of its very low toxicity [40–43]. Although the doses of 0.8 mM and 1.6 mM did not significantly reduce cell viability, these experimental groups showed a particular protein signature compared to the control group. Treatment with melatonin in ovarian carcinoma OVCAR-429 and PA-1 cells at doses of 0.4, 0.6 and 0.8 mM showed satisfactory results in limiting cell growth [44]. Since tumor cell types respond differently to the melatonin's effects, there are diverse treatment strategies regarding its proper concentration. Of note, breast cancer MCF-7/6 and MCF-7/Her2.1 strains were exposed to 1×10^{-6}mM of melatonin while the prostate cancer cells (LNCaP and 22Rv1 lineages) received 10^{-5} mM of melatonin and liver cancer cells (HepG2 cell line) were treated with 1 and 2.5 mM of melatonin [45–48]. In addition, melatonin can reach different levels in each subcellular compartment, so that it is essentially administered in amounts that exceed levels typically identified as physiological in the blood, thereby emphasizing that the high amount of exogenous melatonin may not reflect pharmacological levels for every cell compartment [20].

Notably, treatment of OC cells with different concentrations of melatonin influenced critical pathways associated with the immune system and mitochondrial metabolism (Fig. 8). The effects of melatonin on the immune system are well known, as it influences the viability of immune cells and contributes to the activation of the immune responses in the tumor microenvironment [49]. T lymphocytes have melatonin receptors (MT1 and MT2) on their surface and melatonin can induce the release of interleukin-2, interleukin-10, and interferon-γ, which consequently increases the number of effector T cells. This mechanism is explained by the fact that melatonin reduces the number of regulatory T cells during immunosuppression, such as in cancer, potentially stimulating the action of effector T lymphocytes, which are crucial for the immune defense against cancers cells [50].

The majority of proteins involved with the immune system did not document their decisive role in the OC cell. Of note, calnexin, a transmembrane chaperone responsible for quality control of glycoprotein in the endoplasmic reticulum, which was positively altered by melatonin, did not exhibit immunostaining in exosomes extracted from the plasma of patients with OC [51]. After analyzing the protein profile, high-grade serous OC cell lines had suppressed levels of CYB5R3 when compared to non-serous ovarian cancer, thereby increasing the anoikis resistance of these cells, which is an essential feature for the metastatic process [52].

Although the protease cathepsin D, involved in the degradation of intracellular proteins, is overexpressed in several types of cancer, including in OC [53], Chai et al. [54] compared the expression of cathepsin D by immunohistochemistry in benign tumors and in serous ovarian carcinoma. They found that high levels of cathepsin D provided longer survival time for patients, when compared to those with low expression.

Other melatonin-altered proteins that participated in the immune system, encoded by the *DYNC1H1*, *CAND1*, and *PSMA6* genes, have not yet demonstrated their potential role in OC. Thus, the identification of melatonin's action on these target molecules might be helpful in understanding its immunostimulatory effect. Many cancer cells, including OC cells, have their glycolytic metabolism reprogrammed, prioritizing energy production (ATP synthesis) in the cytosol through aerobic glycolysis, thus decreasing oxidative phosphorylation (this mechanism is referred to Warburg-type metabolism) [55]. The current results document the ability of melatonin to change some features related to the glycolytic metabolism of tumor cells, positively regulating proteins that participate in mitochondrial pathways such as the tricarboxylic acid cycle (TCA cycle) and the electron transport chain (ETC). Recently, it has been suggested that in cancer cells that exhibit Warburg-type metabolism, melatonin redirects glucose to mitochondrial oxidation via the reduction of PDK, thereby disinhibiting PDH which allows for the production of acetyl-CoA from pyruvate in the mitochondrial matrix [15]. Acetyl-CoA, which is an indispensable molecule for the TCA cycle, also serves as a required cofactor for AANAT, the rate-limiting enzyme responsible for the melatonin synthesis and is present in mitochondria [19]. The current findings are consistent with the data indicating that melatonin reprograms cancer cells from Warburg-type metabolism to mitochondrial glucose oxidation [13,16,18].

Mitochondrial ATP synthase is a crucial complex of the electron transport chain which is responsible for ATP production through the driving force of proton generation [41]; this enzyme was also increased by melatonin at the concentration of 2.4 mM. The inhibitory factor ATPase1 (IF1), whose expression is increased in ovarian adenocarcinoma [56], binds and inhibits the activity of ATP synthase by triggering a cascade of reactions. The synthesis of ATP is impaired by the enzyme inhibition and contributes to the metabolic reprogramming of the tumor cells finally activating MAPK and NF-κB pathways, while increasing cell proliferation and differentiation [57]. These signaling pathways were inhibited by melatonin in our previous studies with OC [58].

Melatonin significantly increased CD59 and VTN levels while reducing cell membrane proteins encoded by CD44, ITGB1, PDIA3 and GANAB in SKOV-3 cells. While studying cancer samples from patients diagnosed with advanced OC, Gao et al. [59] detected high expression of CD44, indicating an elevated likelihood of developing therapeutic resistance, metastasis, and disease recurrence. The same study reported that the CD44 knockdown re-established the sensitivity to the chemotherapy with paclitaxel in the OVCAR8 cell line. Furthermore, the cell surface receptor ITGB1 is significantly altered in OC, and its overexpression is related to cellular invasion [60]. Also, the downregulation of PDIA3 was associated with the reduction of SKOV-3 cell proliferation [61], and the inhibition of α-glucosidase encoded by GANAB showed antitumor activity in MCF-7 breast cancer cells and MDA-MB-231 [62]. Importantly, ovarian cancer stem cells isolated from the SKOV-3 cells are known to be influenced by melatonin which exhibited inhibitory effects on cell proliferation, invasion, and migration [63], corroborating the current findings.

Through the analysis of proteins secreted by exosomes derived from SKOV-3 cells, we found a distinct clustering profile of negatively altered proteins in cells exposed to 2.4 mM melatonin. Among them, we identified three connected proteins that are related to tumor progression (e.g., plectin, elongation factor 2, and ribosomal protein S14). Plectin is an over-expressed protein in several types of cancer, including OC; it is related to the cell-cell junction, migration, and cell differentiation. The increase in plectin levels was associated with chemoresistance and OC recurrence, being potentially considered a candidate biomarker [64].

Another protein decreased by melatonin was elongation factor 2 (EEF2), which is crucial for protein synthesis. Shi et al. [65] demonstrated that EEF2 was highly expressed in OC lineages, including SKOV-3 cells. This same study analyzed the expression of this target in samples from 119 patients with OC and observed higher survival rates in patients with lower EEF2 expression. Furthermore, targeting the elongation factor-2 kinase has been shown to inhibit cell proliferation and metastasis in OC [66]. The ribosomal protein S14 (RPS14) was also decreased by melatonin. The expression of this protein was evaluated in estrogen receptor-positive breast cancer cells where high levels of RPS14 were detected. Thus, decrease of RPS14 attenuates cell proliferation and metastasis while inducing apoptosis [67].

To strengthen the clinical implications of the findings, we performed a comparative study using data from patients with OC available from TCGA. We observed that genes encoding melatonin-altered proteins predicted higher survival rates in patients with OC given this set of analyzed molecules. Of importance, a decreased mutation frequency was also detected in some genes encoding melatonin-regulated proteins. More recently, a clinical study carried out with 955 patients displaying a poor prognosis with prostate cancer revealed that melatonin, as an

adjuvant therapy, improved their overall survival by an average of 13 months compared to the group that received radiation therapy only [68].

We also performed a comparative analysis of the proteins expressed in normal ovaries vs. ovarian cancers using the TCGA database and found a clear distinction among the experimental groups; treatment with lower doses of melatonin (0.8 mM and 1.6 mM) showed a different pattern of expression compared to OC cells to exposed to 2.4 mM melatonin. The highest dose of melatonin negatively altered ribosomal proteins, thus indicating the capacity of melatonin to impair the assembly of the ribosomal complex and, consequently, affecting protein synthesis. The ribosome, which is essential for protein translation, is comprised of ribosomal proteins (RPs) that are typically increased in the cellular machinery of different cancer types [69]. Thus, the inhibition of ribosome biogenesis leads to cell cycle arrest via the p53 and subsequent apoptosis [70].

Galectin-1 is highly expressed in OC, which results in increased migration and invasion of tumor cells, since it activates the MAPK and JNK/P38 signaling [71], a signaling pathway already reported to be inhibited by melatonin. Another study reported that the protein encoded by the eEF2 gene is overexpressed in OC, including in SKOV-3 cells; silencing this gene is linked to reduced cell proliferation, since it participates in the PI3K/Akt pathway which is directly related to cancer development and progression [72]. Akt participates in the activation of mTOR signaling, and we previously showed that melatonin significantly attenuated PI3K/Akt/mTOR pathway in an in vivo model of OC. Thus, melatonin may be a promising agent for controlling cell proliferation, survival, and differentiation [58].

Collectively, we documented that melatonin is capable of changing important proteins in OC cells. By stimulating proteins associated with mitochondrial metabolism, melatonin converts OC cells to a healthier phenotype which potentially hinders OC cell proliferation. Importantly, protein synthesis can be impaired in OC cells, especially in the cells treated with the highest melatonin concentration. Finally, melatonin represents a good option for the treatment of OC, because of its very high safety profile and since it is an efficient anti-cancer agent when used in combination with other therapeutics.

5. Conclusions

In summary, we demonstrate that melatonin modulates the proteome of SKOV-3 cells, mainly by changing proteins involved with the immune system and mitochondrial metabolism. Furthermore, melatonin treatment promoted significant alterations in proteins related to cancer aggressiveness, suggesting its use would be an effective therapeutic strategy to fight OC.

Data availability statement

The mass spectrometry data of this manuscript have been uploaded to the MassIVE Repository from Computer Science and Engineering University of California, San Diego (ftp://MSV000088681@massive.ucsd.edu/, accessed on 14 Jan 2022) with the dataset identifier MSV000088681.

CRediT authorship contribution statement

LGAC, RCC: conceived the hypothesis of the study, collected and analyzed the data, and drafted the manuscript. LBG, MSC, HSS, LDS, FRFS, DAPCZ: participated in the design, intellectual conception of the study, and in the acquisition of data. RJR: participated in critical revision of the manuscript. All authors have read and agreed to the version of the manuscript.

Declaration of competing interest

Authors declare no conflict of interest.

Data availability

Data will be made available on request.

Acknowledgments

We are grateful to Fundação de Amparo à Pesquisa do Estado de São Paulo, FAPESP (Grant number 2019/00906-6), CAPES (88887.482368/2020-00), and the National Council for Scientific and Technological Development, CNPq (Process 304108/2020-0) for providing financial support. We are thankful to the Institute of Biotechnology (IBTEC-UNESP) and to Luiz Antonio Lupi for the proteomics analyses of this study.

Appendix A. Supplementary data

Supplementary data to this article can be found online at https://doi.org/10.1016/j.lfs.2022.120352.

References

[1] R.L. Siegel, K.D. Miller, H.E. Fuchs, A. Jemal, Cancer statistics, 2021, ACS J. 71 (2021) 7–33, https://doi.org/10.3322/caac.21654.
[2] B.M. Reid, J.B. Permuth, T.A. Sellers, Epidemiology of ovarian cancer: a review, CancerBiol. Med. 14 (2017) 9–32, https://doi.org/10.20892/j.issn.2095-3941.2016.0084.
[3] C. La Vecchia, Ovarian cancer: epidemiology and risk factors, Eur. J. Cancer Prev. 26 (2017) 55–62, https://doi.org/10.1097/CEJ.0000000000000217.
[4] B.J. Winterhoff, M. Maile, A.K. Mitra, A. Sabe, M. Bazzaro, M.A. Geller, J. E. Abrahante, M. Klein, R. Hellweg, S.A. Mullany, K. Bechman, J. Daniel, T.K. Starr, Single cell sequencing reveals heterogeneity within ovarian cancer epithelium and cancer associated stromal cells, Gynecol. Oncol. 144 (2017) 598–606, https://doi.org/10.1016/j.ygyno.2017.01.015.
[5] R. Cornelison, D.C. Llaneza, C.N. Landen, Emerging therapeutics to overcome chemoresistance in epithelial ovarian cancer: a mini review, Int. J. Mol. Sci. 18 (2017) 2–20, https://doi.org/10.3390/ijms18102171.
[6] D. Acuña-Catroviejo, G. Escames, C. Venegas, M. Díaz-Csado, E. Lima-Cabello, L. C. López, S. Rosales-Corral, D.-X. Tan, R.J. Reiter, Extrapineal melatonina: sources, regulation, and potential functions, Cell. Mol. Life Sci. 71 (2014) 2997–3025, https://doi.org/10.1007/s00018-014-1579-2.
[7] W. Hu, Z. Ma, S. Di, S. Jiang, Y. Li, C. Fan, Y. Yang, D. Wang, Snapshot: implications for melatonin in endoplasmic reticulum homeostasis, Br J Pharmacol. 173 (206) 3431–3442. doi:10.1111/bph.13651.
[8] R.J. Reiter, J.C. Mayo, D.-X. Tan, R.M. Sainz, M. Alatorre-Jimenez, L. Qin, Melatonin as an antioxidant: under promises but over delivers, J. Pineal Res. 61 (2016) 253–278, https://doi.org/10.1111/jpi.12360.
[9] L.G.A. Chuffa, B.A. Fioruci-Fontinelli, L.O. Mendes, F.R.F. Seiva, M. Martinez, W. J. Fávaro, R.F. Domeniconi, P.F.F. Pinheiro, L.D. dos Santos, F.E. Martinez, Melatonin attenuates the TLR4-mediated inflammatory response through MyD88- and TRIF-dependent signaling pathways in an in vivo model of ovarian cancer, BMC Cancer 15 (2015) 34, https://doi.org/10.1186/s12885-015-1032-4.
[10] L.G.A. Chuffa, M.S. Alves, M. Martinez, I.C.C. Camargo, P.F.F. Pinheiro, R. F. Domeniconi, L.A. Lupi, F.E. Martinez, Apoptosis is triggered by melatonin in an in vivo model of ovarian carcinoma, Endocr. Relat. Cancer 23 (2016) 65–76, https://doi.org/10.1530/ERC-15-0463.
[11] L.G.A. Chuffa, F.R.F. Seiva, M.S. Cucielo, H.S. Silveira, R.J. Reiter, L.A. Lupi, Mitochondrial functions and melatonin: a tour of the reproductive cancers, Cel Mol Life Sci. 76 (2019) 837–863, https://doi.org/10.1007/s00018-018-2963-0.
[12] Y.R. Zonta, M. Martinez, I.C.C. Camargo, R.F. Domeniconi, L.A. Lupi, P.F. F. Pinheiro, R.J. Reiter, F.E. Martinez, L.G.A. Chuffa, Melatonin reduces angiogenesis in serous papillary ovarian carcinoma of ethanol-preferring rats, Int. J. Mol. Sci. 18 (2017) (2017) 763, https://doi.org/10.3390/ijms18040763.
[13] R.J. Reiter, R. Sharma, Q. Ma, S. Rosales-Corral, D. Acuna-Castroviejo, G. Escames, Inhibition of mitochondrial pyruvate dehydrogenase kinase: a proposed mechanism by which melatonin causes cancer cells to overcome cytosolic glycolysis, reduce tumor biomass and reverse insensitivity to chemotherapy, Melatonin Res. 2 (2019) 105–119, https://doi.org/10.32794/mr11250033.
[14] K. Tyagi, S. Mandal, A. Roy, Recent advancements in therapeutic targeting of the Warburg effect in refractory ovarian cancer: a promise towards disease remission, Biochim. Biophys. Acta Rev. Cancer 1876 (2021), 188563, https://doi.org/10.1016/j.bbcan.2021.188563.
[15] R.J. Reiter, R. Sharma, C. Rodriguez, V. Martin, S. Rosales-Corral, D.A.P.C. Zuccari, L.G.A. Chuffa, Part-time cancers and role of melatonin in determining their

metabolic phenotype, Life Sci. 278 (2021), 119597, https://doi.org/10.1016/j.lfs.2021.119597.
[16] X. Chen, B. Hao, D. Li, R.J. Reiter, Y. Bai, B. Abay, G. Chen, S. Lin, T. Zheng, Y. Ren, X. Xu, M. Li, L. Fan, Melatonin inhibits lung cancer development by reversing the Warburg effect via stimulating the SIRT3/PDH axis, J. Pineal Res. 2 (2021), e12755, https://doi.org/10.1111/jpi.12755.
[17] M. Li, B. Hao, M. Zhang, R.J. Reiter, S. Lin, T. Zheng, X. Chen, Y. Ren, L. Yue, B. Abay, G. Chen, X. Xu, Y. Shi, L. Fan, Melatonin enhances radiofrequency-induced NK antitumor immunity, causing cancer metabolism reprogramming and inhibition of multiple pulmonary tumor development, Signal Transduct. Target Ther. 6 (2021) 1–14, https://doi.org/10.1038/s41392-021-00745-7.
[18] R.J. Reiter, R. Sharma, Q. Ma, S. Rosales-Corral, L.G.A. Chuffa, Melatonin inhibits Warburg-dependent cancer by redirecting glucose oxidation to the mitochondria: a mechanistic hypothesis, Cell. Mol. Life Sci. 77 (2020) 2527–2542, https://doi.org/10.1007/s00018-019-03438-1.
[19] Y. Suofu, W. Li, F.G. Jean-Alphonse, J. Jia, N.K. Khattar, J. Li, S.V. Baranov, et al., Dual role of mitochondria in producing melatonin and driving GPCR signaling to block cytochrome c release, Proc. Natl. Acad. Sci. U. S. A. 114 (2017) E7997–E8006, https://doi.org/10.1073/pnas.1705768114.
[20] R.J. Reiter, R. Sharma, S. Rosales-Corral, Anti-Warburg effect of melatonin: a proposed mechanism to explain its inhibition of multiple diseases, Int. J. Mol. Sci. 22 (2021) 1–24, https://doi.org/10.3390/ijms22020764.
[21] F. Coscia, E. Lemgyel, J. Duraiswamy, B. Ashcrof, M. Bassani-Sternberg, M. Wierer, A. Johnson, K. Wroblewski, A. Montag, S.D. Yamada, B. López-Méndes, J. Nilsson, A. Mund, M. Mann, M. Curtis, Multi-level proteomics identifies CT45 as a chemosensitivity mediator and immunotherapy target in ovarian cancer, Cell 175 (2018) 159–170, https://doi.org/10.1016/j.cell.2018.08.065.
[22] A. Toss, E.D. Matteis, E. Rossi, L.D. Casa, A. Iannone, M. Federico, L. Cortesi, Ovarian cancer: can proteomics give new insights for therapy and diagnosis? Int. J. Mol. Sci. 14 (2013) 8271–8290, https://doi.org/10.3390/ijms14048271.
[23] Z. Huang, L. Ma, C. Huang, Q. Li, E.C. Nice, Proteomic profiling of human plasma for cancer biomarker discovery, Proteomics 17 (2017) 1–13, https://doi.org/10.1002/pmic.201600240.
[24] N. Li, H. Li, L. Cao, X. Zhan, Quantitative analysis of the mitochondrial proteome in human ovarian carcinomas, Endocr. Relat. Cancer 3 (2018) 1–66, https://doi.org/10.1530/ERC-18-0243.
[25] L.A. Lupi, F.K. Delella, M.S. Cucielo, G.G. Romagnoli, R. Kaneno, I.D.S. Nunes, R. F. Domeniconi, M. Martinez, F.E. Martinez, W.J. Fávaro, L.G.A. Chuffa, P-MAPA and Interleukin-12 reduce cell Migration/Invasion and attenuate the toll-like receptor-mediated inflammatory response in ovarian cancer SKOV-3 cells: a preliminary study, Molecules 25 (2019) 5, https://doi.org/10.3390/molecules25010005.
[26] L.A. Júnior, M.S. Cucielo, R.F. Domeniconi, L.D. dos Santos, H.S. Silveira, I. da Silva Nunes, M. Martinez, F.E. Martinez, W.J. Fávaro, L.G.A. Chuffa, P-MAPA and IL-12 differentially regulate proteins associated with ovarian cancer progression: a proteomic study, ACS Omega 4 (2019) 21761–21777, https://doi.org/10.1021/acsoega.9b02512.
[27] B.M. Barnes, L. Nelson, A. Tighe, G.J. Burghel, S. Desai, J.C. McGrail, R.D. Morgan, S.S. Taylor, I.-Hsuan Lin, Distinct transcriptional programs stratify ovarian cancer cell lines into the five major histological subtypes, Genome Med. 13 (2021) 1–19, https://doi.org/10.1186/s13073-021-00952-5.
[28] S. Gurunathan, M. Qasim, M.-H. Kang, J.-H. Kim, Role and therapeutic potential of melatonin in various type of cancers, Onco Targets Ther. 14 (2021) 2019–2052, https://doi.org/10.2147/OTT.S298512.
[29] D. Bu, H. Luo, P. Hou, Z. Wang, S. Zhang, Z. He, Y. Wu, L. Zhao, J. Liu, J. Guo, S. Fang, W. Cao, L. Yi, Y. Zhao, L. Kong, KOBAS-i: intelligent prioritization and exploratory visualization of biological functions for gene enrichment analysis, Nucleic Acids Res. 49 (2021) 317–325, https://doi.org/10.1093/nar/gkab447.
[30] A. Khan, A. Mathelier, Intervene: a tool for intersection and visualization of multiple gene or genomic region sets, BMC Bioinformatics 18 (2017) 1–8, https://doi.org/10.1186/s12859-017-1708-7.
[31] D. Szklarczyk, A.L. Gable, D. Lyon, A. Junge, S. Wyder, J. Huerta-Cepas, M. Simonovic, N.T. Doncheva, J.H. Morris, P. Bork, L.J. Jensen, C.V. Mering, STRING v11: protein-protein association networks with increased coverage, supporting functional discovery in genome-wide experimental datasets, Nucleic Acids Res. 8 (2019) 607–613, https://doi.org/10.1093/nar/gky1131.
[32] J. Gao, B.A. Aksoy, U. Dogrusoz, G. Dresdner, B. Gross, S.O. Sumer, Y. Sun, A. Jacobsen, R. Sinha, E. Larsson, E. Cerami, C. Sander, N. Schults, Integrative analysis of complex cancer genomics and clinical profiles using the cBioPortal, Sci. Signal. 2 (2013), https://doi.org/10.1126/scisignal.2004088.
[33] M. Uhlen, C. Zhang, S. Lee, E. Sjöstedt, L. Fagerberg, G. Bidkhori, R. Benfeitas, M. Arif, Z. Liu, F. Edfors, K. Sanli, K. von Feilitzen, P. Oksvold, E. Lundberg, S. Hober, P. Nilsson, J. Mattsson, J.M. Schwenk, H. Brunnström, B. Glimelius, T. Sjöblom, P.H. Edqvist, D. Djureinovic, P. Micke, C. Lindskog, A. Mardinoglu, F. Ponten, A pathology atlas of the human cancer transcriptome, Science 357 (2017), eaan2507, https://doi.org/10.1126/science.aan2507.
[34] L. Cheng, K. Zhang, Y. Qing, D. Li, M. Cui, P. Jin, T. Xu, Proteomic and lipidomic analysis of exosomes derived from ovarian cancer cells and ovarian surface epithelial cells, J. Ovarian Res. 22 (2020) 1–13, https://doi.org/10.1186/s13048-020-0609-y.
[35] K.G. Ardelie, E.T. Dermitzakis, The genotype-tissue expression (GTEx) pilot analysis: multitissue gene regulation, Science 8 (2015) 648–660, https://doi.org/10.1126/science.1262110.
[36] J. Lonsdale, J. Thomas, H.F. Moore, The genotype-tissue expression (GTEx) project, Nature 45 (2013) 580–585, https://doi.org/10.1038/ng.2653.
[37] J. Starruß, W. de Back, L. Brusch, A. Deutsch, Morpheus: a user-friendly modeling environment for multiscale and multicellular systems biology, Bioinformatics 30 (2014) 1331–1332, https://doi.org/10.1093/bioinformatics/btt772.
[38] R.J. Deberardinis, N.S. Chandel, Fundamentals of cancer metabolism, Sci. Adv. 2 (2016) 1–18, https://doi.org/10.1126/sciadv.1600200.
[39] R.J. Reiter, S.A. Rosales-Corral, D.-X. Tan, D. Acuna-Castroviejo, L. Qin, S.F. Yang, K. Xu, Melatonin, a full service anti-cancer agent: inhibition of initiation, progression and metastasis, Int. J. Mol. Sci. 18 (2017) 1–47, https://doi.org/10.3390/ijms18040843.
[40] R.S. Barberino, V.G. Menezes, A.E.A.S. Ribeiro, R.C. Palheta, X. Jiang, J.E.J. Smitz, M.H.T. Matos, Melatonin protects against cisplatin-induced ovarian damage in mice via the MT1 receptor and antioxidant activity, Biol. Reprod. 96 (2017) 1244–1255, https://doi.org/10.1093/biolre/iox053.
[41] S. Proietti, A. Cucina, M. Minini, M. Bizzarri, Melatonin, mitochondria, and the cancer cell, Cell. Mol. Life Sci. 74 (2017) 4015–4025, https://doi.org/10.1007/s00018-017-2612-z.
[42] S. Tordjman, S. Chokron, R. Delorme, A. Charrier, E. Bellissant, N. Jaafari, C. Fougerou, Melatonin: pharmacology, functions and therapeutic benefits, Curr. Neuropharmacol. 15 (2017) 434–443, https://doi.org/10.2174/1570159X14666161228122115.
[43] H. Zare, R. Shafabakhsh, R.J. Reiter, Z. Asemi, Melatonin is a potential inhibitor of ovarian cancer: molecular aspects, J. Ovarian Res. 12 (2019) 1–8, https://doi.org/10.1186/s13048-019-0502-8.
[44] C.J. Shen, C.C. Chang, Y.T. Chen, C.S. Lai, Y.C. Hsu, Melatonin suppresses the growth of ovarian cancer cell lines (OVCAR-429 and PA-1) and potentiates the effect of G1 arrest by targeting CDKs, Int. J. Mol. Sci. 17 (2016) 1–11, https://doi.org/10.3390/ijms17020176.
[45] S. Carbajo-Pescador, A. Garcia-Palimo, J. Martin-Renedo, M. Piva, J. González-Gallego, J.L. Mauriz, Melatonin modulation of intracellular signaling pathways in hepatocarcinoma HepG2 cell line: role of the MT1 receptor, J. Pineal Res. 51 (2011) 463–471, https://doi.org/10.1111/j.1600-079X.2011.00910.x.
[46] Y. Li, S. Li, Y. Zhou, X. Meng, J.J. Zhang, D.P. Xu, H.B. Li, Melatonin for the prevention and treatment of cancer, Oncotarget 8 (2017) 39896–39921, https://doi.org/10.18632/oncotarget.16379.
[47] L. Mao, L. Yuan, L.M. Slakey, F.E. Jones, M.E. Burow, S.M. Hill, Inhibition of breast cancer cell invasion by melatonin is mediated through regulation of the p38 mitogen-activated protein kinase signaling pathway, Breast Cancer Res. 12 (2010) 1–14, https://doi.org/10.1186/bcr2794.
[48] C.W. Tam, S.Y.W. Shiu, Functional interplay between melatonin receptor-mediated antiproliferative signaling and androgen receptor signaling in human prostate epithelial cells: potential implications for therapeutic strategies against prostate cancer, J. Pineal Res. 51 (2011) 297–312, https://doi.org/10.1111/j.1600-079X.2011.00890.x.
[49] F. Moradkkhani, M. Moloudizargari, M. Fallah, N. Asghari, H.H. Khoei, M. H. Asghari, Immunoregulatory role of melatonin on cancer, J. Cell. Physiol. 235 (2020) 745–757, https://doi.org/10.1002/jcp.29036.
[50] W. Ren, G. Liu, S. Chen, J. Yin, J. Wang, B. Tan, G. Wu, F.W. Bazer, Y. Peng, T. Li, R.J. Reiter, Y. Yin, Melatonin signaling in T cells: functions and applications, J. Pineal Res. 62 (2017) 1–15, https://doi.org/10.1111/jpi.12394.
[51] W. Zhang, X. Ou, X. Wu, Proteomics profiling of plasma exosomes in epithelial ovarian cancer: a potential role in the coagulation cascade, diagnosis and prognosis, Int. J. Oncol. 54 (2019) 1719–1733, https://doi.org/10.3892/ijo.2019.4742.
[52] K. Yamanoi, N. Matsumura, S.K. Murphy, T. Baba, K. Abiko, J. Hamanishi, K. Yamaguchi, M. Koshiyama, I. Konishi, M. Mandai, Suppression of ABHD2, identified through a functional genomics screen, causes anoikis resistance, chemoresistance and poor prognosis in ovarian cancer, Oncotarget 7 (2016) 47620–47636, https://doi.org/10.18632/oncotarget.9951.
[53] M.Z.I. Pranjol, N. Gutowski, M. Hannemann, J. Whatmore, The potential role of the proteases cathepsin D and cathepsin L in the progression and metastasis of epithelial ovarian cancer, Biomolecules 5 (2015) 3260–3279, https://doi.org/10.3390/biom5043260.
[54] Y. Chai, W. Wu, C. Zhou, J. Zhou, The potential prognostic value of cathepsin D protein in serous ovarian cancer, Arch. Gynecol. Obstet. 286 (2012) 465–471, https://doi.org/10.1007/s00404-012-2318-2.
[55] R.M. Pascale, D.F. Calvisi, M.M. Simile, C.F. Feo, F. Feo, The Warburg effect 97 years after its discovery, Cancers 12 (2020) 1–33, https://doi.org/10.3390/cancers12102819.
[56] J. Zhao, X. Liu, Y.L. Li, Expression of ATPase inhibitory factor 1 in normal and pathological tissues of female reproductive system, Nan Fang Yi Ke Da Xue Xue Bao 36 (2016) 1626–1631.
[57] P.B. Esparza-Moltó, J.M. Cuezva, The role of mitochondrial H+-ATP synthase in cancer, FrontOncol. 8 (2018) 1–8, https://doi.org/10.3389/fonc.2018.00053.
[58] L.G.A. Chuffa, R.J. Reiter, L.A. Lupi, Melatonin as a promising agent to treat ovarian cancer: molecular mechanisms, Carcinogenesis 38 (2017) 945–952, https://doi.org/10.1093/carcin/bgx054.
[59] Y. Gao, R. Foster, X. Yang, Y. Feng, J.K. Shen, H.J. Mankin, F.J. Hornicek, M. M. Amiji, Z. Duan, Up-regulation of CD44 in the development of metastasis, recurrence and drug resistance of ovarian cancer, Oncotarget 6 (2015) 9313–9326, https://doi.org/10.18632/oncotarget.3220.
[60] T. Zhu, R. Chen, J. Wang, H. Yue, X. Lu, J. Li, The prognostic value of ITGA and ITGB superfamily members in patients with high grade serous ovarian cancer, Cancel Cell Int. 20 (2020) 1–9, https://doi.org/10.1186/s12935-020-01344-2.
[61] Y. Zhu, L. Cai, J. Guo, N. Chen, X. Yi, Y. Zhao, J. Cai, Z. Wang, Depletion of dicer promotes epithelial ovarian cancer progression by elevating PDIA3 expression,

Tumor Biol. 37 (2016) 14009–14023, https://doi.org/10.1007/s13277-016-5218-4.
[62] N. Gueder, G. Allan, M.S. Telliez, F. Hague, J.M. Fernandez, E.M. Sanchez-Fernandez, C. Ortiz-Mellet, A. Ahidouch, H. Ouadid-Ahidouch, sp2-iminosugar α-glucosidase inhibitor 1-C-octyl-2-oxa-3-oxocastanospermine specifically affected breast cancer cell migration through Stim1, β1-integrin, and FAK signaling pathways, J. Cell. Physiol. 232 (2017) 3631–3640, https://doi.org/10.1002/jcp.25832.
[63] M. Akbarzadeh, A.A. Movassaghpour, H. Ghanbari, M. Kheirandish, N.F. Maroufi, R. Rahbarghazi, M. Nouri, N. Samadi, The potential therapeutic effect of melatonin on human ovarian cancer by inhibition of invasion and migration of cancer stem cells, Sci. Rep. 7 (2017) 1–11, https://doi.org/10.1038/s41598-017-16940-y.
[64] T. Wesley, S. Berzins, G. Kannourakis, N. Ahmed, The attributes of plakins in cancer and disease: perspectives on ovarian cancer progression, chemoresistance and recurrence, Cell Commun. Signal. 19 (2021) 1–21, https://doi.org/10.1186/s12964-021-00726-x.
[65] N. Shi, X. Chen, R. Liu, D. Wang, M. Su, Q. Wang, A. He, H. Gu, Eukaryotic elongation factors 2 promotes tumor cell proliferation and correlates with poor prognosis in ovarian cancer, Tissue Cell 53 (2018) 53–60, https://doi.org/10.1016/j.tice.2018.05.014.
[66] M.A. Erdogan, A. Ashour, E. Yuca, K. Gorgulu, B. Ozpolat, Targeting eukaryotic elongation factor-2 kinase suppresses the growth and peritoneal metastasis of ovarian cancer, Cell. Signal. 81 (2021), 109938, https://doi.org/10.1016/j.cellsig.2021.109938.
[67] X. Wang, S. Yao, G. Luo, Y. Zhou, Q. Fang, Downregulation of RPS14 inhibits the proliferation and metastasis of estrogen receptor-positive breast cancer cells, Anti-Cancer Drugs 32 (2021) 1019–1028, https://doi.org/10.1097/CAD.0000000000001112.
[68] G.M. Zharinov, O.A. Bogomolov, I.V. Chepurnaya, N.Y. Neklasova, V.N. Anisimov, Melatonin increases overall survival of prostate cancer patients with poor prognosis after combined hormone radiation treatment, Oncotarget 11 (2020) 3723–3729, https://doi.org/10.18632/oncotarget.27757.
[69] J.C. Guimarães, M. Zavolan, Patterns of ribossomal protein expression specify normal and malignant human cells, Genome Biol. 17 (2016) 1–13, https://doi.org/10.1186/s13059-016-1104-z.
[70] Z. Turi, M. Lacey, M. Mistrikk, P. Moudry, Impaired ribosome biogenesis: mechanisms and relevance to cancer and aging, Aging 11 (2019) 2515–2540, https://doi.org/10.18632/aging.101922.
[71] L. Zhu, Y. Zheng, H. Zhang, Y. Liu, H. Sun, P. Zhang, Galectin-1 induces metastasis and epithelial-mesenchymal transition (EMT) in human ovarian cancer cells via activation of MAPK JNK/p38 signalling pathway, Am. J. Transl. Res. 11 (2019) 3862–3878.
[72] N. Shi, X. Chen, R. Liu, D. Wang, M. Su, Q. Wang, A. He, H. Gu, Eukaryotic elongation factors 2 promotes tumor cell proliferation and correlates with poor prognosis in ovarian cancer, Tissue Cell 53 (2018) 53–60, https://doi.org/10.1016/j.tice.2018.05.014.

Supplementary Information and Supplementary Figure Legends

The proteomic landscape of ovarian cancer cells in response to melatonin

Roberta Carvalho Cesário[1]*, Leticia Barbosa Gaiotte[1], Maira Smaniotto Cucielo[1], Henrique Spaulonci Silveira[1], Lucilene Delazari dos Santos[2], Debora Aparecida Pires de Campos Zuccari[3], Russel J. Reiter[4], Luiz Gustavo de Almeida Chuffa[1].

[1] Department of Structural and Functional Biology, Institute of Biosciences, UNESP - Sao Paulo State University, Botucatu, Brazil.
[2] Center for the Study of Venoms and Venomous Animals (CEVAP), São Paulo State University (UNESP), Botucatu, SP, Brazil.
[3] Faculty of Medicine of São José do Rio Preto, São José do Rio Preto, São Paulo, 15090-000, Brazil.
[4] Departament of Cell Systems and Anatomy, UT Health, San Antonio, TX 782229, USA.

Running-title: Melatonin alters ovarian cancer proteome

***Corresponding author:**
Luiz Gustavo de Almeida Chuffa, Department of Structural and Functional Biology, Institute of Biosciences of Botucatu, UNESP - São Paulo State University, Botucatu, São Paulo, Brazil, Zip Code: 510; P.O Box: 18618-689, Rubião Júnior, s/n, Botucatu, SP – Brazil, Phone: +55 (14) 3880-0027, Fax: +55 (14) 3811-6361. Email: luiz-gustavo.chuffa@unesp.br

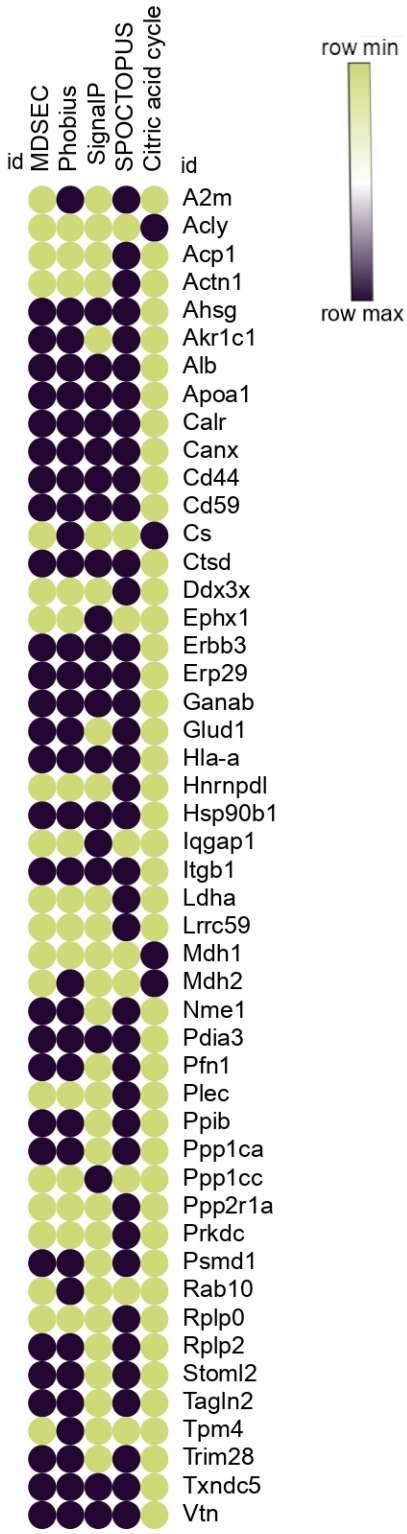

Figure S1. Heatmap illustrating 48 different proteins presented in at least one database based on the human protein atlas. Dark circles indicate the presence of the protein and beige indicates the absence of proteins in the following databases (MDSEC, Phobius, Signal IP and SPOCTOPUS) and citric acid cycle. Accessed in August 2021.

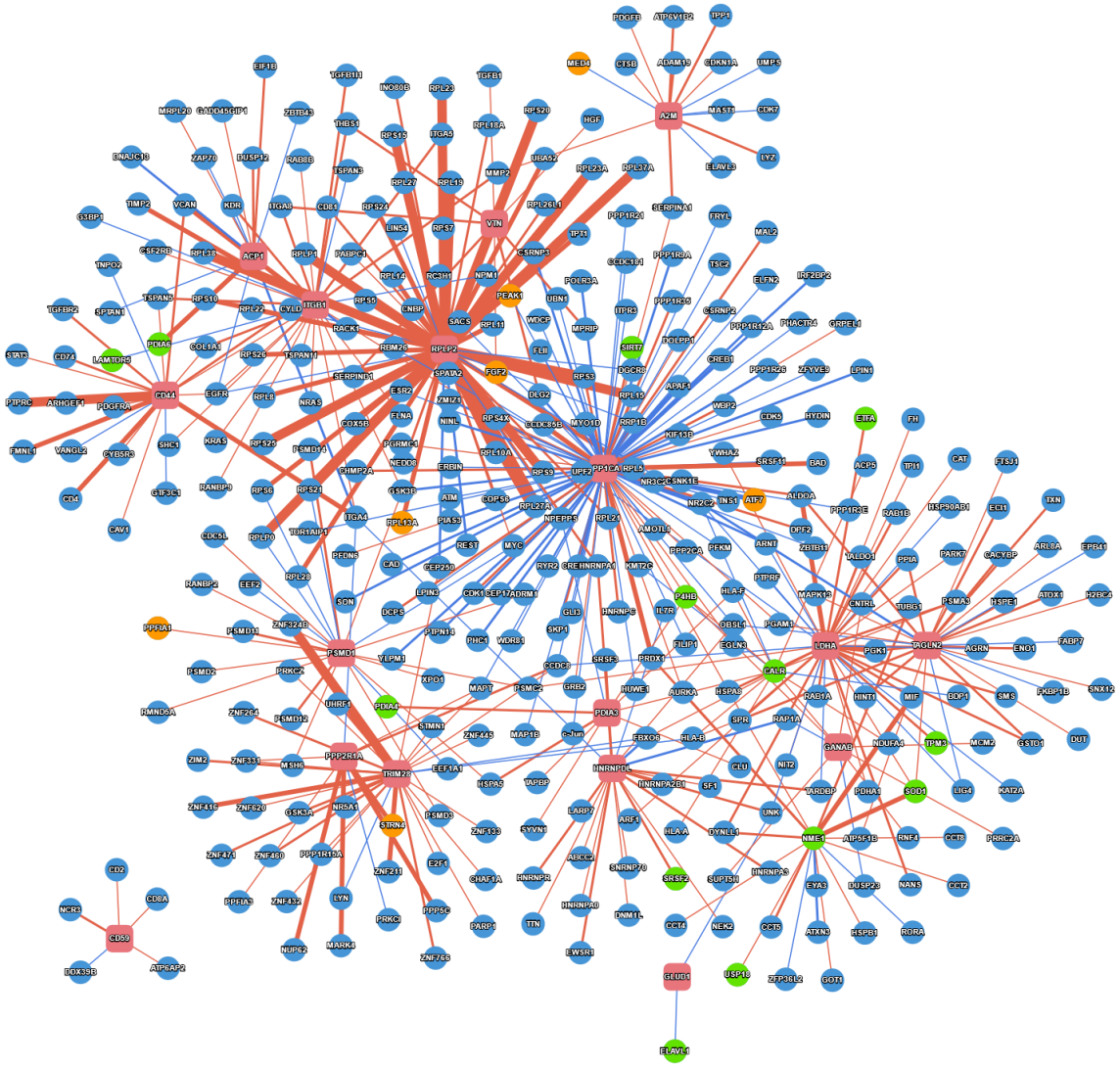

Figure S2. Protein network of the 48 selected targets modified by melatonin and associated with signaling pathways in OC. PINA 3.0 tool connected with data from The Cancer Genome Atlas Program (TCGA). Orange and green circles indicate targets related to patients at worse and good prognosis, respectively. Blue and red circles reflect high and low OC specificity, respectively (Spearman's correlation = 0.2; Tumor specificity score = 5). FDR < 0.05.

Table S1. Proteome of the SKOV-3 cells treated with vehicle only (control group)

Protein ID	Description	% Coverage	Protein Score
P06733	Alpha-enolase	0.5806	649.6363
P08670	Vimentin	0.6459	587.9025
P14618	Pyruvate kinase PKM	0.6234	469.0203
Q5VTE0	Putative elongation factor 1-alpha-like 3	0.368	468.9963
P68104	Elongation factor 1-alpha 1	0.368	468.9963
P21333	Filamin-A	0.2592	436.0844
P35579	Myosin-9	0.2633	388.3636
P07437	Tubulin beta chain	0.5068	386.3573
P68363	Tubulin alpha-1B chain	0.4235	375.8335
Q9BQE3	Tubulin alpha-1C chain	0.3875	365.8344
Q71U36	Tubulin alpha-1A chain	0.3925	344.7929
P07900	Heat shock protein HSP 90-alpha	0.2691	326.1379
Q09666	Neuroblast differentiation-associated protein AHNAK	0.1404	320.9325
P07355	Annexin A2	0.4808	314.8017
P08238	Heat shock protein HSP 90-beta	0.2873	307.8752
P04406	Glyceraldehyde-3-phosphate dehydrogenase	0.5254	297.1653
P68371	Tubulin beta-4B chain	0.4449	294.3569
Q05639	Elongation factor 1-alpha 2	0.203	275.7687
P04350	Tubulin beta-4A chain	0.3604	268.9128
P60709	Actin, cytoplasmic 1	0.408	264.9452
P63261	Actin, cytoplasmic 2	0.408	264.9452
P11142	Heat shock cognate 71 kDa protein	0.3545	264.0971
P04075	Fructose-bisphosphate aldolase A	0.5824	263.0258
Q9BVA1	Tubulin beta-2B chain	0.3371	261.1526
Q13885	Tubulin beta-2A chain	0.3371	259.5681
P13645	Keratin, type I cytoskeletal 10	0.4384	257.2587
O43707	Alpha-actinin-4	0.3085	256.2328
P04264	Keratin, type II cytoskeletal 1	0.2842	254.4582
P0DPH8	Tubulin alpha-3D chain	0.3222	241.6769
P0DPH7	Tubulin alpha-3C chain	0.3222	241.6769
P35908	Keratin, type II cytoskeletal 2 epidermal	0.3521	231.2938
P00338	L-lactate dehydrogenase A chain	0.3645	228.1515
Q6PEY2	Tubulin alpha-3E chain	0.2867	227.0076
P10809	60 kDa heat shock protein, mitochondrial	0.3717	223.3278
P04083	Annexin A1	0.4277	222.35
A6NMY6	Putative annexin A2-like protein	0.3599	219.8815
P68366	Tubulin alpha-4A chain	0.3393	211.053
P55072	Transitional endoplasmic reticulum ATPase	0.3896	201.9292
Q3ZCM7	Tubulin beta-8 chain	0.1509	190.4345
Q58FF7	Putative heat shock protein HSP 90-beta-3	0.1625	181.3669
A6NNZ2	Tubulin beta 8B	0.1171	179.43

P16104	Histone H2AX	0.2727	174.5576
Q96QV6	Histone H2A type 1-A	0.2977	174.5576
P13929	Beta-enolase	0.1544	169.481
P09104	Gamma-enolase	0.1406	168.3495
P62805	Histone H4	0.5146	163.5016
P0DMV9	Heat shock 70 kDa protein 1B	0.2418	159.6933
Q15149	Plectin	0.1065	158.7304
P0DMV8	Heat shock 70 kDa protein 1A	0.2418	156.5262
P63104	14-3-3 protein zeta/delta	0.4286	153.3469
P08758	Annexin A5	0.3844	153.2145
Q7L7L0	Histone H2A type 3	0.2692	153.1449
Q96KK5	Histone H2A type 1-H	0.2734	153.1449
Q99878	Histone H2A type 1-J	0.2734	153.1449
P04908	Histone H2A type 1-B/E	0.2692	153.1449
Q6FI13	Histone H2A type 2-A	0.2692	153.1449
P20671	Histone H2A type 1-D	0.2692	153.1449
P0C0S8	Histone H2A type 1	0.2692	153.1449
Q9BTM1	Histone H2A.J	0.2713	153.1449
Q93077	Histone H2A type 1-C	0.2692	153.1449
Q16777	Histone H2A type 2-C	0.2713	153.1449
Q14568	Heat shock protein HSP 90-alpha A2	0.2216	152.1821
Q06830	Peroxiredoxin-1	0.6884	152.0842
P62736	Actin, aortic smooth muscle	0.1565	149.6893
P63267	Actin, gamma-enteric smooth muscle	0.1569	149.6893
P68133	Actin, alpha skeletal muscle	0.1565	149.6893
P68032	Actin, alpha cardiac muscle 1	0.1565	149.6893
P00558	Phosphoglycerate kinase 1	0.307	149.0048
Q13509	Tubulin beta-3 chain	0.2111	145.9513
Q9NY65	Tubulin alpha-8 chain	0.2361	142.1327
P12814	Alpha-actinin-1	0.1939	141.6262
P02545	Prelamin-A/C	0.2801	137.7904
P11021	Endoplasmic reticulum chaperone BiP	0.2309	135.2256
P15311	Ezrin	0.2082	132.7197
Q8IUE6	Histone H2A type 2-B	0.2462	131.4819
P13639	Elongation factor 2	0.2179	131.3774
Q9BUF5	Tubulin beta-6 chain	0.1099	130.324
P25705	ATP synthase subunit alpha, mitochondrial	0.2061	127.662
P29401	Transketolase	0.2793	124.7607
Q6S8J3	POTE ankyrin domain family member E	0.0679	124.2537
P54652	Heat shock-related 70 kDa protein 2	0.1268	121.4145
O75369	Filamin-B	0.1341	115.9216
A5A3E0	POTE ankyrin domain family member F	0.0465	113.9255
P07737	Profilin-1	0.4714	113.3057
Q9Y490	Talin-1	0.1291	112.7514
P09525	Annexin A4	0.3009	110.9915

P18206	Vinculin	0.2002	108.0374
P35527	Keratin, type I cytoskeletal 9	0.26	106.1004
P09382	Galectin-1	0.7778	101.7611
P17066	Heat shock 70 kDa protein 6	0.1104	99.156
P08865	40S ribosomal protein SA	0.3085	96.8213
P19338	Nucleolin	0.1845	96.65
Q9H4B7	Tubulin beta-1 chain	0.0643	96.5386
P08195	4F2 cell-surface antigen heavy chain	0.1778	96.1624
Q9BYX7	Putative beta-actin-like protein 3	0.1067	95.0108
P62258	14-3-3 protein epsilon	0.4078	92.9657
P61978	Heterogeneous nuclear ribonucleoprotein K	0.2484	91.8398
P57053	Histone H2B type F-S	0.4127	91.3621
Q99880	Histone H2B type 1-L	0.4127	91.3621
Q99879	Histone H2B type 1-M	0.4127	91.3621
Q93079	Histone H2B type 1-H	0.4127	91.3621
Q5QNW6	Histone H2B type 2-F	0.4127	91.3621
P62807	Histone H2B type 1-C/E/F/G/I	0.4127	91.3621
P58876	Histone H2B type 1-D	0.4127	91.3621
O60814	Histone H2B type 1-K	0.4127	91.3621
Q99877	Histone H2B type 1-N	0.4127	91.3621
P06748	Nucleophosmin	0.1973	90.9625
P67936	Tropomyosin alpha-4 chain	0.2944	89.4259
P07237	Protein disulfide-isomerase	0.2362	89.2699
P23528	Cofilin-1	0.4759	89.1347
P23396	40S ribosomal protein S3	0.3909	87.9251
P60174	Triosephosphate isomerase	0.5175	87.6918
P23527	Histone H2B type 1-O	0.3333	87.2679
Q16778	Histone H2B type 2-E	0.3333	87.2679
P33778	Histone H2B type 1-B	0.3333	87.2679
P06899	Histone H2B type 1-J	0.3333	87.2679
P35580	Myosin-10	0.0415	86.4233
Q8N257	Histone H2B type 3-B	0.2778	82.0809
P34931	Heat shock 70 kDa protein 1-like	0.092	80.2001
Q00610	Clathrin heavy chain 1	0.0812	77.5519
P22626	Heterogeneous nuclear ribonucleoproteins A2/B1	0.17	76.8089
P26038	Moesin	0.1248	73.4806
Q71UI9	Histone H2A.V	0.2031	72.057
P0C0S5	Histone H2A.Z	0.2031	72.057
P08727	Keratin, type I cytoskeletal 19	0.1625	71.6339
P38646	Stress-70 protein, mitochondrial	0.1517	71.3462
P0CG38	POTE ankyrin domain family member I	0.0316	69.5709
P04259	Keratin, type II cytoskeletal 6B	0.0745	68.962
P07195	L-lactate dehydrogenase B chain	0.2455	68.6056
Q58FF8	Putative heat shock protein HSP 90-beta 2	0.1575	67.4798
P26599	Polypyrimidine tract-binding protein 1	0.1695	65.1859

P06576	ATP synthase subunit beta, mitochondrial	0.2854	65.1546
P16402	Histone H1.3	0.1493	64.92
P16403	Histone H1.2	0.1549	64.92
P10412	Histone H1.4	0.1507	64.92
P21796	Voltage-dependent anion-selective channel protein 1	0.3251	64.7162
P05787	Keratin, type II cytoskeletal 8	0.1884	63.7284
P31946	14-3-3 protein beta/alpha	0.3293	62.2328
P05388	60S acidic ribosomal protein P0	0.3123	61.9601
P30050	60S ribosomal protein L12	0.4303	61.7237
P22314	Ubiquitin-like modifier-activating enzyme 1	0.1342	61.5567
P32119	Peroxiredoxin-2	0.2424	60.9376
Q08211	ATP-dependent RNA helicase A	0.074	59.5529
P62979	Ubiquitin-40S ribosomal protein S27a	0.3013	58.8372
P0CG47	Polyubiquitin-B	0.2052	58.8372
P62987	Ubiquitin-60S ribosomal protein L40	0.3672	58.8372
P0CG48	Polyubiquitin-C	0.0686	58.8372
P61981	14-3-3 protein gamma	0.17	58.4764
P12956	X-ray repair cross-complementing protein 6	0.1346	58.27
Q00839	Heterogeneous nuclear ribonucleoprotein U	0.0848	58.0796
Q58FG1	Putative heat shock protein HSP 90-alpha A4	0.0574	57.3948
P02765	Alpha-2-HS-glycoprotein	0.0545	56.7023
P48741	Putative heat shock 70 kDa protein 7	0.1063	56.571
Q14315	Filamin-C	0.0272	56.2029
P17661	Desmin	0.0468	55.8666
P09211	Glutathione S-transferase P	0.381	55.3847
P62826	GTP-binding nuclear protein Ran	0.3287	54.8477
P14625	Endoplasmin	0.1432	54.656
P16949	Stathmin	0.349	53.9514
P27348	14-3-3 protein theta	0.1755	53.6182
P62937	Peptidyl-prolyl cis-trans isomerase A	0.1879	52.9556
P35241	Radixin	0.0738	52.4997
P31943	Heterogeneous nuclear ribonucleoprotein H	0.2027	52.4971
P61604	10 kDa heat shock protein, mitochondrial	0.5196	51.7033
P05387	60S acidic ribosomal protein P2	0.6957	51.1182
P04792	Heat shock protein beta-1	0.3024	50.9969
Q15084	Protein disulfide-isomerase A6	0.1886	50.8772
P37837	Transaldolase	0.2136	50.854
P35609	Alpha-actinin-2	0.0638	50.7229
Q562R1	Beta-actin-like protein 2	0.0904	50.2445
P26641	Elongation factor 1-gamma	0.1579	49.4581
P08729	Keratin, type II cytoskeletal 7	0.1748	49.0457
Q9H853	Putative tubulin-like protein alpha-4B	0.1162	48.6072
P48668	Keratin, type II cytoskeletal 6C	0.0727	48.5506
P02538	Keratin, type II cytoskeletal 6A	0.0727	48.5506
Q08043	Alpha-actinin-3	0.0388	48.1735

P09972	Fructose-bisphosphate aldolase C	0.1593	48.0713
Q01518	Adenylyl cyclase-associated protein 1	0.1832	48.0519
P09651	Heterogeneous nuclear ribonucleoprotein A1	0.1237	47.8596
Q96A08	Histone H2B type 1-A	0.2126	47.4144
P15531	Nucleoside diphosphate kinase A	0.3947	46.7067
P30101	Protein disulfide-isomerase A3	0.2198	46.6054
P0DP24	Calmodulin-2	0.1745	46.3498
Q15365	Poly(rC)-binding protein 1	0.2051	45.5511
P13647	Keratin, type II cytoskeletal 5	0.0542	45.5339
P50990	T-complex protein 1 subunit theta	0.2318	45.502
P62241	40S ribosomal protein S8	0.2885	45.0635
Q04917	14-3-3 protein eta	0.1707	44.8981
Q99497	Protein/nucleic acid deglycase DJ-1	0.3862	44.6857
P0DP23	Calmodulin-1	0.1745	44.2716
P0DP25	Calmodulin-3	0.1745	44.2716
Q5XKE5	Keratin, type II cytoskeletal 79	0.043	43.9068
P60660	Myosin light polypeptide 6	0.1987	43.7953
O94925	Glutaminase kidney isoform, mitochondrial	0.0792	43.7726
O95678	Keratin, type II cytoskeletal 75	0.0417	42.7825
P62081	40S ribosomal protein S7	0.2629	42.5616
P10599	Thioredoxin	0.3524	42.3226
P31947	14-3-3 protein sigma	0.1089	42.2625
P63244	Receptor of activated protein C kinase 1	0.2366	42.2214
P22392	Nucleoside diphosphate kinase B	0.3026	42.0273
Q8NHW5	60S acidic ribosomal protein P0-like	0.2145	41.5808
P68431	Histone H3.1	0.2059	41.1103
P84243	Histone H3.3	0.2059	41.1103
Q6NXT2	Histone H3.3C	0.2074	41.1103
Q16695	Histone H3.1t	0.2059	41.1103
Q71DI3	Histone H3.2	0.2059	41.1103
P29692	Elongation factor 1-delta	0.1957	40.7977
P84077	ADP-ribosylation factor 1	0.3536	40.5702
P61204	ADP-ribosylation factor 3	0.3536	40.5702
Q58FF6	Putative heat shock protein HSP 90-beta 4	0.0752	40.3214
P05556	Integrin beta-1	0.0852	39.8474
P23284	Peptidyl-prolyl cis-trans isomerase B	0.1898	39.6287
Q14697	Neutral alpha-glucosidase AB	0.0794	38.8219
P41219	Peripherin	0.0447	38.5829
Q58FG0	Putative heat shock protein HSP 90-alpha A5	0.0808	38.2439
P07205	Phosphoglycerate kinase 2	0.0983	38.1109
P55795	Heterogeneous nuclear ribonucleoprotein H2	0.1225	38.1068
P35749	Myosin-11	0.0218	37.4774
P84085	ADP-ribosylation factor 5	0.2333	37.3639
P09429	High mobility group protein B1	0.1721	37.1529
P06753	Tropomyosin alpha-3 chain	0.1439	36.4935

P08779	Keratin, type I cytoskeletal 16	0.0677	36.4686
P02533	Keratin, type I cytoskeletal 14	0.0678	36.4686
Q99832	T-complex protein 1 subunit eta	0.1197	36.4366
O00299	Chloride intracellular channel protein 1	0.1743	36.4229
P06703	Protein S100-A6	0.1667	36.0877
P50991	T-complex protein 1 subunit delta	0.0835	35.6734
P07910	Heterogeneous nuclear ribonucleoproteins C1/C2	0.2222	35.6071
P19012	Keratin, type I cytoskeletal 15	0.0504	35.2026
Q04695	Keratin, type I cytoskeletal 17	0.0532	35.2026
P00441	Superoxide dismutase [Cu-Zn]	0.3247	35.0786
P62263	40S ribosomal protein S14	0.1589	35.0646
P45880	Voltage-dependent anion-selective channel protein 2	0.2347	34.8336
P62269	40S ribosomal protein S18	0.2632	34.7847
P62424	60S ribosomal protein L7a	0.2143	34.46
P62753	40S ribosomal protein S6	0.1285	34.375
Q15366	Poly(rC)-binding protein 2	0.1562	34.2296
P78371	T-complex protein 1 subunit beta	0.1402	33.8397
P37802	Transgelin-2	0.2211	33.3966
P18085	ADP-ribosylation factor 4	0.3333	33.3733
P30086	Phosphatidylethanolamine-binding protein 1	0.246	33.3003
P31949	Protein S100-A11	0.2571	32.7442
P32969	60S ribosomal protein L9	0.349	31.9999
P52565	Rho GDP-dissociation inhibitor 1	0.1569	31.7903
Q32P51	Heterogeneous nuclear ribonucleoprotein A1-like 2	0.1094	31.7483
P60842	Eukaryotic initiation factor 4A-I	0.1552	30.9256
P62906	60S ribosomal protein L10a	0.2627	30.1493
P62701	40S ribosomal protein S4, X isoform	0.1559	30.0364
P07951	Tropomyosin beta chain	0.1056	29.764
Q13268	Dehydrogenase/reductase SDR family member 2, mitochondrial	0.225	29.7481
P26447	Protein S100-A4	0.2772	29.4581
P15880	40S ribosomal protein S2	0.1775	28.9096
P52209	6-phosphogluconate dehydrogenase, decarboxylating	0.1408	28.7697
P0CG39	POTE ankyrin domain family member J	0.0222	28.2029
P11940	Polyadenylate-binding protein 1	0.1101	28.0317
P46782	40S ribosomal protein S5	0.0735	28.0116
P05141	ADP/ATP translocase 2	0.1745	27.5136
P69905	Hemoglobin subunit alpha	0.2183	27.3579
P62829	60S ribosomal protein L23	0.2	27.2754
Q13838	Spliceosome RNA helicase DDX39B	0.1028	27.2612
P62249	40S ribosomal protein S16	0.1918	27.0075
P51149	Ras-related protein Rab-7a	0.2319	26.6442
Q12905	Interleukin enhancer-binding factor 2	0.1487	26.3783
P61247	40S ribosomal protein S3a	0.1591	26.3735
Q9H361	Polyadenylate-binding protein 3	0.0919	26.3721

P12236	ADP/ATP translocase 3	0.1409	26.2039
P39019	40S ribosomal protein S19	0.1931	26.0976
P27797	Calreticulin	0.1295	26.083
Q7Z794	Keratin, type II cytoskeletal 1b	0.0208	25.9346
P04080	Cystatin-B	0.2449	25.6881
Q14240	Eukaryotic initiation factor 4A-II	0.1057	25.172
P16401	Histone H1.5	0.1062	25.1182
Q6ZMR3	L-lactate dehydrogenase A-like 6A	0.0361	24.8022
P07864	L-lactate dehydrogenase C chain	0.0361	24.8022
Q6NZI2	Caveolae-associated protein 1	0.0846	24.7542
P16152	Carbonyl reductase [NADPH] 1	0.2058	24.4558
Q07020	60S ribosomal protein L18	0.25	24.4169
P46776	60S ribosomal protein L27a	0.223	24.3579
P50395	Rab GDP dissociation inhibitor beta	0.0742	24.3462
O00571	ATP-dependent RNA helicase DDX3X	0.0816	24.255
P62857	40S ribosomal protein S28	0.1739	23.8636
P60953	Cell division control protein 42 homolog	0.1571	23.8207
O15523	ATP-dependent RNA helicase DDX3Y	0.0636	23.7688
P51991	Heterogeneous nuclear ribonucleoprotein A3	0.1323	23.5635
P27824	Calnexin	0.0726	23.3809
Q96AG4	Leucine-rich repeat-containing protein 59	0.2345	23.334
P62280	40S ribosomal protein S11	0.2278	23.2808
Q15185	Prostaglandin E synthase 3	0.2375	23.2656
P30613	Pyruvate kinase PKLR	0.0296	23.061
P50914	60S ribosomal protein L14	0.107	22.8085
P36578	60S ribosomal protein L4	0.1077	22.7602
P06454	Prothymosin alpha	0.2252	22.6248
P49368	T-complex protein 1 subunit gamma	0.1009	22.4641
P61586	Transforming protein RhoA	0.1036	22.2947
Q01546	Keratin, type II cytoskeletal 2 oral	0.0313	22.11
P00505	Aspartate aminotransferase, mitochondrial	0.0953	21.5627
P50454	Serpin H1	0.1483	21.4685
P49411	Elongation factor Tu, mitochondrial	0.073	21.0018
P38159	RNA-binding motif protein, X chromosome	0.0895	20.9389
P57721	Poly(rC)-binding protein 3	0.0889	20.7074
Q7Z3Y7	Keratin, type I cytoskeletal 28	0.0539	20.6487
O60361	Putative nucleoside diphosphate kinase	0.1898	20.5806
P09493	Tropomyosin alpha-1 chain	0.0352	20.2987
P30153	Serine/threonine-protein phosphatase 2A 65 kDa regulatory subunit A alpha isoform O	0.0764	20.2436
P22492	Histone H1t	0.0531	20.2059
P04843	Dolichyl-diphosphooligosaccharide--protein glycosyltransferase subunit 1	0.1219	20.0846
P06744	Glucose-6-phosphate isomerase	0.1237	19.9874
Q14847	LIM and SH3 domain protein 1	0.1226	19.771

B7ZW38	Heterogeneous nuclear ribonucleoprotein C-like 3	0.1092	19.7332
B2RXH8	Heterogeneous nuclear ribonucleoprotein C-like 2	0.1092	19.7332
O60812	Heterogeneous nuclear ribonucleoprotein C-like 1	0.1092	19.7332
P0DMR1	Heterogeneous nuclear ribonucleoprotein C-like 4	0.1092	19.7332
Q13813	Spectrin alpha chain, non-erythrocytic 1	0.0218	19.6439
P23526	Adenosylhomocysteinase	0.0764	19.5546
Q14103	Heterogeneous nuclear ribonucleoprotein D0	0.062	19.5174
P59998	Actin-related protein 2/3 complex subunit 4	0.1607	19.4217
P62913	60S ribosomal protein L11	0.1292	19.347
P53999	Activated RNA polymerase II transcriptional coactivator p15	0.189	19.3371
Q9NQC3	Reticulon-4	0.0109	19.1556
P12035	Keratin, type II cytoskeletal 3	0.0175	19.0933
P18124	60S ribosomal protein L7	0.121	18.6453
Q02539	Histone H1.1	0.0512	18.6278
Q9H0C2	ADP/ATP translocase 4	0.0635	18.5628
P12235	ADP/ATP translocase 1	0.0671	18.5628
Q9H254	Spectrin beta chain, non-erythrocytic 4	0.0043	18.3424
P11216	Glycogen phosphorylase, brain form	0.0498	18.1976
P08134	Rho-related GTP-binding protein RhoC	0.1036	18.1674
Q7Z406	Myosin-14	0.013	18.0718
P05386	60S acidic ribosomal protein P1	0.5175	17.8785
P40926	Malate dehydrogenase, mitochondrial	0.1686	17.8204
P14136	Glial fibrillary acidic protein	0.0394	17.7615
O60701	UDP-glucose 6-dehydrogenase	0.1498	17.5944
Q9Y281	Cofilin-2	0.1024	17.5441
P50502	Hsc70-interacting protein	0.0976	17.4609
Q8IZP2	Putative protein FAM10A4	0.15	17.4609
P40925	Malate dehydrogenase, cytoplasmic	0.1407	17.417
P60866	40S ribosomal protein S20	0.2521	17.3176
B2RPK0	Putative high mobility group protein B1-like 1	0.109	16.9144
P40261	Nicotinamide N-methyltransferase	0.0606	16.9048
P17987	T-complex protein 1 subunit alpha	0.1169	16.8444
P62277	40S ribosomal protein S13	0.351	16.8191
P45877	Peptidyl-prolyl cis-trans isomerase C	0.0283	16.7205
O43447	Peptidyl-prolyl cis-trans isomerase H	0.0339	16.7205
Q16658	Fascin	0.1521	16.7193
P05783	Keratin, type I cytoskeletal 18	0.0442	16.6549
P55854	Small ubiquitin-related modifier 3	0.1165	16.5527
Q6EEV6	Small ubiquitin-related modifier 4	0.1263	16.5527
P61956	Small ubiquitin-related modifier 2	0.1263	16.5527
P26373	60S ribosomal protein L13	0.1327	16.4463
P07197	Neurofilament medium polypeptide	0.0098	16.3865
P12036	Neurofilament heavy polypeptide	0.0088	16.3865
P07196	Neurofilament light polypeptide	0.0166	16.3865

Q16352	Alpha-internexin	0.018	16.3865
P04004	Vitronectin	0.0314	16.3682
P62834	Ras-related protein Rap-1A	0.0598	16.2027
P62851	40S ribosomal protein S25	0.16	16.1742
P63241	Eukaryotic translation initiation factor 5A-1	0.1299	16.135
Q6IS14	Eukaryotic translation initiation factor 5A-1-like	0.1299	16.135
P25398	40S ribosomal protein S12	0.2576	15.9163
P52907	F-actin-capping protein subunit alpha-1	0.1678	15.6281
P46781	40S ribosomal protein S9	0.1443	15.4817
Q01105	Protein SET	0.1414	15.0849
O00764	Pyridoxal kinase	0.0994	14.9873
P14649	Myosin light chain 6B	0.0625	14.9291
Q9GZV4	Eukaryotic translation initiation factor 5A-2	0.0784	14.8639
P23246	Splicing factor, proline- and glutamine-rich	0.0863	14.6417
P30048	Thioredoxin-dependent peroxide reductase, mitochondrial	0.1758	14.5782
P12004	Proliferating cell nuclear antigen	0.0996	14.3536
Q13263	Transcription intermediary factor 1-beta	0.0311	14.2461
P67809	Y-box-binding protein 1	0.1111	14.2399
P51148	Ras-related protein Rab-5C	0.1065	14.1433
P17844	Probable ATP-dependent RNA helicase DDX5	0.0814	14.0766
P60981	Destrin	0.1758	14.0655
O00148	ATP-dependent RNA helicase DDX39A	0.0749	13.8679
P61224	Ras-related protein Rap-1b	0.0598	13.8543
P80723	Brain acid soluble protein 1	0.1233	13.6882
P60903	Protein S100-A10	0.1753	13.6362
P0DME0	Protein SETSIP	0.1358	13.6002
Q9UJZ1	Stomatin-like protein 2, mitochondrial	0.0702	13.5877
E9PAV3	Nascent polypeptide-associated complex subunit alpha, muscle-specific form	0.0202	13.4476
Q13765	Nascent polypeptide-associated complex subunit alpha	0.1953	13.4476
Q01650	Large neutral amino acids transporter small subunit 1	0.0493	13.3759
Q15056	Eukaryotic translation initiation factor 4H	0.0806	13.3717
P68036	Ubiquitin-conjugating enzyme E2 L3	0.1429	13.3504
P15121	Aldo-keto reductase family 1 member B1	0.0854	13.3209
Q7Z3Y8	Keratin, type I cytoskeletal 27	0.0632	13.31
Q96E39	RNA binding motif protein, X-linked-like-1	0.0692	13.0653
P02795	Metallothionein-2	0.1967	13.0598
P80297	Metallothionein-1X	0.1967	13.0598
P04732	Metallothionein-1E	0.1967	13.0598
Q8N339	Metallothionein-1M	0.1967	13.0598
P13640	Metallothionein-1G	0.1935	13.0598
Q8NC51	Plasminogen activator inhibitor 1 RNA-binding protein	0.0882	12.7243
Q9Y277	Voltage-dependent anion-selective channel protein 3	0.0671	12.6593
Q92945	Far upstream element-binding protein 2	0.0774	12.5757

Q02878	60S ribosomal protein L6	0.125	12.5566
P14866	Heterogeneous nuclear ribonucleoprotein L	0.0509	12.4832
O14950	Myosin regulatory light chain 12B	0.1279	12.4161
P19105	Myosin regulatory light chain 12A	0.1287	12.4161
P16070	CD44 antigen	0.031	12.3519
O00429	Dynamin-1-like protein	0.0856	12.35
P04626	Receptor tyrosine-protein kinase erbB-2	0.0279	12.3256
P39023	60S ribosomal protein L3	0.0471	12.1008
P30040	Endoplasmic reticulum resident protein 29	0.0843	11.9844
P13646	Keratin, type I cytoskeletal 13	0.0393	11.8879
Q2M2I5	Keratin, type I cytoskeletal 24	0.0343	11.8879
A0A1B0GUS4	Ubiquitin-conjugating enzyme E2 L5	0.1429	11.828
P11413	Glucose-6-phosphate 1-dehydrogenase	0.0505	11.8236
P62873	Guanine nucleotide-binding protein G(I)/G(S)/G(T) subunit beta-1	0.0941	11.79
Q4VXU2	Polyadenylate-binding protein 1-like	0.0423	11.7047
P62316	Small nuclear ribonucleoprotein Sm D2	0.161	11.701
P30041	Peroxiredoxin-6	0.1027	11.656
P52597	Heterogeneous nuclear ribonucleoprotein F	0.1398	11.4263
P12277	Creatine kinase B-type	0.0709	11.2934
P13010	X-ray repair cross-complementing protein 5	0.0751	11.0753
Q7Z3Z0	Keratin, type I cytoskeletal 25	0.04	11.0354
Q9UQ80	Proliferation-associated protein 2G4	0.0964	10.9768
P07602	Prosaposin	0.0305	10.9578
P62244	40S ribosomal protein S15a	0.1308	10.8596
P18621	60S ribosomal protein L17	0.1304	10.8362
Q02543	60S ribosomal protein L18a	0.1989	10.7923
P30044	Peroxiredoxin-5, mitochondrial	0.0654	10.7828
P52272	Heterogeneous nuclear ribonucleoprotein M	0.0123	10.777
O43399	Tumor protein D54	0.1602	10.7123
P15559	NAD(P)H dehydrogenase [quinone] 1	0.0474	10.5881
O60664	Perilipin-3	0.0714	10.529
P05023	Sodium/potassium-transporting ATPase subunit alpha-1	0.0323	10.4884
P62847	40S ribosomal protein S24	0.0902	10.4066
Q5JQF8	Polyadenylate-binding protein 1-like 2	0.055	10.2938
Q07955	Serine/arginine-rich splicing factor 1	0.0403	10.2656
P60763	Ras-related C3 botulinum toxin substrate 3	0.0938	10.1962
P15153	Ras-related C3 botulinum toxin substrate 2	0.0938	10.1962
P63000	Ras-related C3 botulinum toxin substrate 1	0.0938	10.1962
Q9HAV0	Guanine nucleotide-binding protein subunit beta-4	0.0588	10.1919
P62879	Guanine nucleotide-binding protein G(I)/G(S)/G(T) subunit beta-2	0.0588	10.1919
P28066	Proteasome subunit alpha type-5	0.0415	10.1243
P13693	Translationally-controlled tumor protein	0.0756	10.1148
P46783	40S ribosomal protein S10	0.1273	9.811

Q15907	Ras-related protein Rab-11B	0.0963	9.7553
P62491	Ras-related protein Rab-11A	0.0972	9.7553
Q9Y696	Chloride intracellular channel protein 4	0.1976	9.747
P62820	Ras-related protein Rab-1A	0.1122	9.6198
Q92928	Putative Ras-related protein Rab-1C	0.1144	9.6198
Q9H0U4	Ras-related protein Rab-1B	0.1144	9.6198
Q01813	ATP-dependent 6-phosphofructokinase, platelet type	0.037	9.6151
Q15323	Keratin, type I cuticular Ha1	0.0168	9.6133
O76013	Keratin, type I cuticular Ha6	0.015	9.6133
Q14525	Keratin, type I cuticular Ha3-II	0.0173	9.6133
Q14532	Keratin, type I cuticular Ha2	0.0156	9.6133
O76014	Keratin, type I cuticular Ha7	0.0156	9.6133
O76015	Keratin, type I cuticular Ha8	0.0154	9.6133
Q92764	Keratin, type I cuticular Ha5	0.0154	9.6133
Q8TAA3	Proteasome subunit alpha-type 8	0.043	9.57
O14818	Proteasome subunit alpha type-7	0.0444	9.57
Q9UBI6	Guanine nucleotide-binding protein G(I)/G(S)/G(O) subunit gamma-12	0.375	9.567
O75828	Carbonyl reductase [NADPH] 3	0.0578	9.5234
P42330	Aldo-keto reductase family 1 member C3	0.0557	9.5091
P52895	Aldo-keto reductase family 1 member C2	0.0557	9.5091
Q04828	Aldo-keto reductase family 1 member C1	0.0557	9.5091
Q9P0L0	Vesicle-associated membrane protein-associated protein A	0.0884	9.4382
P35268	60S ribosomal protein L22	0.1016	9.2616
Q9ULV4	Coronin-1C	0.0211	9.2211
Q5JXB2	Putative ubiquitin-conjugating enzyme E2 N-like	0.0719	9.186
P61088	Ubiquitin-conjugating enzyme E2 N	0.0724	9.186
P78417	Glutathione S-transferase omega-1	0.0913	9.1263
Q9Y266	Nuclear migration protein nudC	0.0967	9.0648
P55209	Nucleosome assembly protein 1-like 1	0.0435	9.0637
P01023	Alpha-2-macroglobulin	0.0075	9.0597
Q9NTK5	Obg-like ATPase 1	0.0657	8.99
Q14019	Coactosin-like protein	0.1127	8.8899
P25789	Proteasome subunit alpha type-4	0.069	8.8455
Q9NQ39	Putative 40S ribosomal protein S10-like	0.1193	8.8223
P49458	Signal recognition particle 9 kDa protein	0.2326	8.7632
Q01469	Fatty acid-binding protein 5	0.1481	8.7004
P30419	Glycylpeptide N-tetradecanoyltransferase 1	0.0645	8.671
P53675	Clathrin heavy chain 2	0.0073	8.6688
O00487	26S proteasome non-ATPase regulatory subunit 14	0.0419	8.5566
Q58FF3	Putative endoplasmin-like protein	0.0426	8.5508
Q16881	Thioredoxin reductase 1, cytoplasmic	0.0524	8.5152
P02008	Hemoglobin subunit zeta	0.0493	8.4901
P35237	Serpin B6	0.0399	8.4586

P26583	High mobility group protein B2	0.1292	8.4417
P61313	60S ribosomal protein L15	0.0882	8.4235
P05455	Lupus La protein	0.0882	8.4059
Q14764	Major vault protein	0.0605	8.3906
P02647	Apolipoprotein A-I	0.0599	8.3892
Q14204	Cytoplasmic dynein 1 heavy chain 1	0.0071	8.3612
P00387	NADH-cytochrome b5 reductase 3	0.1096	8.3069
P68402	Platelet-activating factor acetylhydrolase IB subunit beta	0.0393	8.2895
P20073	Annexin A7	0.0738	8.2487
P63208	S-phase kinase-associated protein 1	0.0736	8.1807
P16520	Guanine nucleotide-binding protein G(I)/G(S)/G(T) subunit beta-3	0.0294	8.0192
Q16555	Dihydropyrimidinase-related protein 2	0.0664	7.99
P05198	Eukaryotic translation initiation factor 2 subunit 1	0.0381	7.8186
P23497	Nuclear autoantigen Sp-100	0.0091	7.8153
P14314	Glucosidase 2 subunit beta	0.0246	7.7756
P31153	S-adenosylmethionine synthase isoform type-2	0.038	7.6449
P26006	Integrin alpha-3	0.0285	7.533
O43809	Cleavage and polyadenylation specificity factor subunit 5	0.0793	7.5144
P35080	Profilin-2	0.1	7.5032
Q8IVF2	Protein AHNAK2	0.0062	7.4752
O43491	Band 4.1-like protein 2	0.0418	7.4338
P40429	60S ribosomal protein L13a	0.0542	7.348
Q6NVV1	Putative 60S ribosomal protein L13a protein RPL13AP3	0.1078	7.348
P51571	Translocon-associated protein subunit delta	0.1098	7.2636
P24844	Myosin regulatory light polypeptide 9	0.064	7.2618
P53396	ATP-citrate synthase	0.0209	7.1952
Q14974	Importin subunit beta-1	0.0308	7.1865
P84098	60S ribosomal protein L19	0.0459	7.1856
P58107	Epiplakin	0.0112	7.1659
P61020	Ras-related protein Rab-5B	0.0512	7.1476
P48643	T-complex protein 1 subunit epsilon	0.0665	6.9918
Q92688	Acidic leucine-rich nuclear phosphoprotein 32 family member B	0.0837	6.9735
P43487	Ran-specific GTPase-activating protein	0.0896	6.9388
P61254	60S ribosomal protein L26	0.1241	6.8823
P04632	Calpain small subunit 1	0.0373	6.6931
Q9Y617	Phosphoserine aminotransferase	0.0595	6.6166
Q03135	Caveolin-1	0.0449	6.6013
P49207	60S ribosomal protein L34	0.0684	6.5016
A6NHL2	Tubulin alpha chain-like 3	0.0202	6.4771
Q99714	3-hydroxyacyl-CoA dehydrogenase type-2	0.0766	6.4337
Q1KMD3	Heterogeneous nuclear ribonucleoprotein U-like protein 2	0.0134	6.4258
P12429	Annexin A3	0.0557	6.3808

P04439	HLA class I histocompatibility antigen, A alpha chain	0.0438	6.3
P36873	Serine/threonine-protein phosphatase PP1-gamma catalytic subunit group: P62136, P62140	0.0526	6.1896
Q13200	26S proteasome non-ATPase regulatory subunit 2	0.0463	6.0629
P38919	Eukaryotic initiation factor 4A-III	0.0268	6.0257
P35637	RNA-binding protein FUS	0.0475	6.0239
P20339	Ras-related protein Rab-5A	0.0512	5.9825
P24666	Low molecular weight phosphotyrosine protein phosphatase	0.057	5.9417
P22234	Multifunctional protein ADE2	0.0424	5.9396
P46940	Ras GTPase-activating-like protein IQGAP1	0.0169	5.9354
P55060	Exportin-2	0.0309	5.9207
Q92841	Probable ATP-dependent RNA helicase DDX17	0.0453	5.8422
P40227	T-complex protein 1 subunit zeta	0.0433	5.8268
P54727	UV excision repair protein RAD23 homolog B	0.0416	5.7483
P61026	Ras-related protein Rab-10	0.055	5.7309
P49591	Serine--tRNA ligase, cytoplasmic	0.0525	5.6479
Q99460	26S proteasome non-ATPase regulatory subunit 1	0.0199	5.5969
Q9UHD8	Septin-9	0.058	5.5851
P18669	Phosphoglycerate mutase 1	0.1378	5.5345
Q9Y265	RuvB-like 1	0.0307	5.5333
Q9UHQ1	Nuclear prelamin A recognition factor	0.0351	5.4892
P00367	Glutamate dehydrogenase 1, mitochondrial	0.0287	5.4203
P20042	Eukaryotic translation initiation factor 2 subunit 2	0.0601	5.3952
O43175	D-3-phosphoglycerate dehydrogenase	0.0507	5.332
P00492	Hypoxanthine-guanine phosphoribosyltransferase	0.1789	5.3045
P52943	Cysteine-rich protein 2	0.0769	5.2583
Q03252	Lamin-B2	0.0323	5.2564
P31942	Heterogeneous nuclear ribonucleoprotein H3	0.0491	5.2258
Q6DD88	Atlastin-3	0.0222	5.208
P34932	Heat shock 70 kDa protein 4	0.0321	5.2055
P27816	Microtubule-associated protein 4	0.0234	5.1194
Q8NFI4	Putative protein FAM10A5	0.0352	5.0753
Q9UKM9	RNA-binding protein Raly	0.0556	5.0644
P24534	Elongation factor 1-beta	0.0311	5.0384
P30085	UMP-CMP kinase	0.0612	4.9778
Q00688	Peptidyl-prolyl cis-trans isomerase FKBP3	0.0491	4.9687
P30154	Serine/threonine-protein phosphatase 2A 65 kDa regulatory subunit A beta isoform	0.0283	4.9145
Q96KP4	Cytosolic non-specific dipeptidase	0.0442	4.9134
Q15843	NEDD8	0.1728	4.9126
P84103	Serine/arginine-rich splicing factor 3	0.1341	4.8945
P62136	Serine/threonine-protein phosphatase PP1-alpha catalytic subunit	0.0515	4.8686
P62140	Serine/threonine-protein phosphatase PP1-beta catalytic subunit	0.052	4.8686

Q7L1Q6	Basic leucine zipper and W2 domain-containing protein 1	0.0501	4.7863
P13987	CD59 glycoprotein	0.0938	4.7735
P50995	Annexin A11	0.0178	4.7555
Q9Y4G6	Talin-2	0.009	4.73
Q8NBS9	Thioredoxin domain-containing protein 5	0.1065	4.7275
P63220	40S ribosomal protein S21	0.2289	4.6729
O14556	Glyceraldehyde-3-phosphate dehydrogenase, testis-specific	0.0172	4.6111
P62888	60S ribosomal protein L30	0.0696	4.5943
P07099	Epoxide hydrolase 1	0.0593	4.5773
P26368	Splicing factor U2AF 65 kDa subunit	0.0821	4.5528
B5ME19	Eukaryotic translation initiation factor 3 subunit C-like protein	0.0263	4.551
Q99613	Eukaryotic translation initiation factor 3 subunit C	0.0263	4.551
O75390	Citrate synthase, mitochondrial	0.0236	4.5338
O43390	Heterogeneous nuclear ribonucleoprotein R	0.0205	4.5145
Q00325	Phosphate carrier protein, mitochondrial	0.0331	4.4782
P62310	U6 snRNA-associated Sm-like protein LSm3	0.1176	4.4745
Q9NR31	GTP-binding protein SAR1a	0.1162	4.4617
O75821	Eukaryotic translation initiation factor 3 subunit G	0.0406	4.4324
Q15181	Inorganic pyrophosphatase	0.0657	4.2947
Q86VP6	Cullin-associated NEDD8-dissociated protein 1	0.022	4.2004
P17516	Aldo-keto reductase family 1 member C4	0.0279	4.0977
P46779	60S ribosomal protein L28	0.0803	4.0878
Q9NQA5	Transient receptor potential cation channel subfamily V member 5	0.0082	4.0488
Q13310	Polyadenylate-binding protein 4	0.0404	3.9745
Q92804	TATA-binding protein-associated factor 2N	0.0389	3.9301
Q15691	Microtubule-associated protein RP/EB family member 1	0.0709	3.796
P31948	Stress-induced-phosphoprotein 1	0.035	3.7912
P39748	Flap endonuclease 1	0.0526	3.7563
Q12906	Interleukin enhancer-binding factor 3	0.0235	3.5567
P60900	Proteasome subunit alpha type-6	0.0488	3.5501
Q13435	Splicing factor 3B subunit 2	0.0134	3.5372
Q9H299	SH3 domain-binding glutamic acid-rich-like protein 3	0.1075	3.5052
P05062	Fructose-bisphosphate aldolase B	0.0192	3.4803
P26639	Threonine--tRNA ligase 1, cytoplasmic	0.0166	3.3885
P42166	Lamina-associated polypeptide 2, isoform alpha	0.0187	3.2304
P42167	Lamina-associated polypeptide 2, isoforms beta/gamma	0.0286	3.2304
Q13247	Serine/arginine-rich splicing factor 6	0.0523	3.1766
P16989	Y-box-binding protein 3	0.0457	3.1015
Q9Y2T7	Y-box-binding protein 2	0.0467	3.1015
P17096	High mobility group protein HMG-I/HMG-Y	0.0841	3.0958
P30049	ATP synthase subunit delta, mitochondrial	0.0833	3.092
P49915	GMP synthase [glutamine-hydrolyzing]	0.0159	3.0869

P29034	Protein S100-A2 OS=Homo sapiens	0.0918	3.0803
P08754	Guanine nucleotide-binding protein G(i) subunit alpha	0.0508	3.0692
Q9UNX3	60S ribosomal protein L26-like 1	0.0621	3.0666
P07339	Cathepsin D	0.0243	3.047
Q01130	Serine/arginine-rich splicing factor 2	0.0317	3.0367
Q9BRL6	Serine/arginine-rich splicing factor 8	0.0248	3.0367
P78527	DNA-dependent protein kinase catalytic subunit	0.0046	2.9852
Q15717	ELAV-like protein 1	0.0399	2.9515
P19367	Hexokinase-1	0.0185	2.9445
P52292	Importin subunit alpha-1	0.0284	2.9426
O15347	High mobility group protein B3	0.065	2.9226
Q01082	Spectrin beta chain, non-erythrocytic 1	0.0102	2.8875
Q9UBQ7	Glyoxylate reductase/hydroxypyruvate reductase	0.0732	2.8865
Q8WUD1	Ras-related protein Rab-2B	0.0509	2.8664
P61019	Ras-related protein Rab-2A	0.0519	2.8664
P50453	Serpin B9	0.0399	2.8614
Q92598	Heat shock protein 105 kDa	0.0315	2.8218
Q9H910	Jupiter microtubule associated homolog 2	0.0737	2.7218
O76003	Glutaredoxin-3	0.0627	2.7201
P00403	Cytochrome c oxidase subunit 2	0.0441	2.6516
O14979	Heterogeneous nuclear ribonucleoprotein D-like	0.0571	2.6499
P35659	Protein DEK	0.0507	2.6454
P35606	Coatomer subunit beta'	0.0232	2.6135
Q16629	Serine/arginine-rich splicing factor 7	0.0588	2.4865
Q9UBQ0	Vacuolar protein sorting-associated protein 29	0.0549	2.2584
Q96FQ6	Protein S100-A16	0.1165	2.2124
P06493	Cyclin-dependent kinase 1	0.0337	2.2051
O00410	Importin-5	0.0182	2.0688
Q969H8	Myeloid-derived growth factor	0.0867	2.0247

Table S2. Differentially expressed proteins in SKOV-3 cells treated with melatonin at the dose of 0.8 mM *versus* Control group

Protein ID	Description	% Coverage	Protein Score	Fold-change
P60900	Proteasome subunit alpha type-6	0.1016	26.2909	3.58
P31948	Stress-induced-phosphoprotein 1	0.1381	23.5424	3.35
Q92598	Heat shock protein 105 kDa	0.0618	18.5898	3.19
P52292	Importin subunit alpha-1	0.0662	14.954	3.08
P78527	DNA-dependent protein kinase catalytic subunit	0.0097	13.9178	3.07
P17516	Aldo-keto reductase family 1 member C4	0.0526	35.7536	2.98
Q8NBS9	Thioredoxin domain-containing protein 5	0.1319	19.4689	2.90
Q86VP6	Cullin-associated NEDD8-dissociated protein 1	0.061	22.8593	2.85

Q14764	Major vault protein	0.1176	36.8226	2.78
Q12906	Interleukin enhancer-binding factor 3	0.0727	12.7105	2.58
P30049	ATP synthase subunit delta, mitochondrial	0.0833	11.6744	2.54
P07339	Cathepsin D	0.0243	10.727	2.54
P48643	T-complex protein 1 subunit epsilon	0.085	28.6673	2.46
Q15181	Inorganic pyrophosphatase	0.2007	17.7213	2.42
P07099	Epoxide hydrolase 1	0.0593	15.0005	2.42
P07864	L-lactate dehydrogenase C chain	0.0361	38.129	2.41
O43390	Heterogeneous nuclear ribonucleoprotein R	0.0332	14.8806	2.40
Q6ZMR3	L-lactate dehydrogenase A-like 6A	0.3554	300.4616	2.27
P19367	Hexokinase-1	0.0305	8.4966	2.17
Q15691	Microtubule-associated protein RP/EB family member 1	0.1455	10.6889	2.17
Q99460	26S proteasome non-ATPase regulatory subunit 1	0.0514	17.0454	2.17
Q8WUD1	Ras-related protein Rab-2B	0.0509	8.8383	2.17
P62136	Serine/threonine-protein phosphatase PP1-alpha catalytic subunit	0.1606	20.2447	2.15
Q8IVF2	Protein AHNAK2	0.0167	32.5168	2.15
O75390	Citrate synthase, mitochondrial	0.0579	16.7685	2.04
Q15056	Eukaryotic translation initiation factor 4H	0.0524	34.3514	2.01
O43175	D-3-phosphoglycerate dehydrogenase	0.0638	17.9309	1.99
P46940	Ras GTPase-activating-like protein IQGAP1	0.0428	26.1319	1.99
P53396	ATP-citrate synthase	0.0527	28.4553	1.98
P04626	Receptor tyrosine-protein kinase erbB-2	0.0622	36.3178	1.95
P84103	Serine/arginine-rich splicing factor 3	0.1341	15.1348	1.89
O14818	Proteasome subunit alpha type-7	0.1371	24.5759	1.86
O14979	Heterogeneous nuclear ribonucleoprotein D-like	0.0571	6.707	1.85
P62888	60S ribosomal protein L30	0.0696	10.4138	1.80
P23246	Splicing factor, proline- and glutamine-rich	0.0806	45.7282	1.79
P55060	Exportin-2	0.0412	16.522	1.78
Q14204	Cytoplasmic dynein 1 heavy chain 1	0.0211	33.2119	1.78
O43491	Band 4.1-like protein 2	0.0418	19.5213	1.77
P05455	Lupus La protein	0.1225	31.5994	1.74
Q9UJZ1	Stomatin-like protein 2, mitochondrial	0.1573	34.5919	1.73
O00429	Dynamin-1-like protein	0.1141	45.2959	1.72
Q02539	Histone H1.1	0.1131	73.6956	1.70
P34932	Heat shock 70 kDa protein 4	0.0321	11.7731	1.69
P17096	High mobility group protein HMG-I/HMG-Y	0.0841	7.7614	1.68
P12277	Creatine kinase B-type	0.1601	33.9924	1.67
P32969	60S ribosomal protein L9	0.3646	58.7288	1.63
P06703	Protein S100-A6	0.1667	41.8	1.61
Q9Y617	Phosphoserine aminotransferase	0.1486	17.6418	1.59
Q9Y265	RuvB-like 1	0.0899	19.2192	1.59
O00299	Chloride intracellular channel protein 1	0.4108	60.1509	1.58
Q96FQ6	Protein S100-A16	0.1165	12.5614	1.58
P60953	Cell division control protein 42 homolog	0.1571	40.6056	1.57

P13987	CD59 glycoprotein	0.0938	11.7415	1.56
Q13268	Dehydrogenase/reductase SDR family member 2, mitochondrial	0.4929	81.9277	1.55
P27824	Calnexin	0.1351	64.1756	1.55
P00387	NADH-cytochrome b5 reductase 3	0.1462	21.8648	1.53
Q02543	60S ribosomal protein L18a	0.1989	28.7432	1.52
P10599	Thioredoxin	0.3524	54.3371	1.52
P26641	Elongation factor 1-gamma	0.1076	56.8225	1.48
P37837	Transaldolase	0.184	46.6245	-1.50
P08134	Rho-related GTP-binding protein RhoC	0.1813	31.0384	-1.51
P59998	Actin-related protein 2/3 complex subunit 4	0.2262	21.3202	-1.51
P35908	Keratin, type II cytoskeletal 2	0.2981	290.6706	-1.51
Q13200	26S proteasome non-ATPase regulatory subunit 2	0.0132	6.6715	-1.52
Q5XKE5	Keratin, type II cytoskeletal 79	0.2981	290.6706	-1.54
P69905	Hemoglobin subunit alpha	0.2183	46.0319	-1.54
P19338	Nucleolin	0.1831	111.7485	-1.55
O00487	26S proteasome non-ATPase regulatory subunit 14	0.0419	9.3164	-1.56
P17987	T-complex protein 1 subunit alpha	0.0683	19.2608	-1.57
P04264	Keratin, type II cytoskeletal 1	0.2981	290.6706	-1.59
P27816	Microtubule-associated protein 4	0.0113	7.1045	-1.62
P35527	Keratin, type I cytoskeletal 9	0.4024	206.04	-1.66
P15531	Nucleoside diphosphate kinase A	0.2303	34.7017	-1.68
P09429	High mobility group protein B1	0.1721	33.3847	-1.74
Q96AG4	Leucine-rich repeat-containing protein 59	0.1075	20.3017	-1.74
P50914	60S ribosomal protein L14	0.107	19.5633	-1.76
P22392	Nucleoside diphosphate kinase B	0.1382	25.988	-1.79
P01023	Alpha-2-macroglobulin	0.0075	14.6726	-1.83
P13645	Keratin, type I cytoskeletal 10	0.4024	206.04	-1.84
P35241	Radixin	0.0789	58.5671	-1.86
Q9UBI6	Guanine nucleotide-binding protein G(I)/G(S)/G(O) subunit gamma-12	0.1528	7.5731	-1.90
P35268	60S ribosomal protein L22	0.1016	7.5446	-1.92
P13647	Keratin, type II cytoskeletal 5	0.0559	36.9608	-1.95
P08195	4F2 cell-surface antigen heavy chain	0.1603	70.4721	-2.02
O43399	Tumor protein D54	0.1699	9.3764	-2.02
P62244	40S ribosomal protein S15a	0.1308	7.2772	-2.04
P02538	Keratin, type II cytoskeletal 6A	0.2981	290.6706	-2.07
P08779	Keratin, type I cytoskeletal 16	0.4024	206.04	-2.12
P02765	Alpha-2-HS-glycoprotein	0.0545	71.8179	-2.13
P02533	Keratin, type I cytoskeletal 14	0.0953	38.3113	-2.16
P26373	60S ribosomal protein L13	0.09	14.2384	-2.17
Q07020	60S ribosomal protein L18	0.1862	11.6514	-2.18
P61254	60S ribosomal protein L26	0.1172	3.6552	-2.31
Q1KMD3	Heterogeneous nuclear ribonucleoprotein U-like protein 2	0.0134	3.3361	-2.38

P62851	40S ribosomal protein S25	0.224	8.3053	-2.64
Q5JXB2	Putative ubiquitin-conjugating enzyme E2 N-like	0.0719	2.6579	-3.06
Q15907	Ras-related protein Rab-11B	0.0505	3.1541	-3.26
P68402	Platelet-activating factor acetylhydrolase IB subunit beta	0.1223	2.9023	-4.12

Table S3. Differentially expressed proteins in SKOV-3cells treated with melatonin at the dose of 1.6 mM *versus* Control group

Protein ID	Description	% Coverage	Protein Score	Fold-change
Q16555	Dihydropyrimidinase-related protein 2	0.5017	299.4682	12.24
P12277	Creatine kinase B-type	0.3963	234.6669	7.07
P18669	Phosphoglycerate mutase 1	0.374	82.075	4.19
Q86VP6	Cullin-associated NEDD8-dissociated protein 1	0.052	23.0192	3.72
P00367	Glutamate dehydrogenase 1, mitochondrial	0.1667	41.7729	3.16
P05023	Sodium/potassium-transporting ATPase subunit alpha-1	0.0909	54.7136	3.07
P40926	Malate dehydrogenase, mitochondrial	0.3876	129.3402	2.99
P19367	Hexokinase-1	0.0305	12.3727	2.80
P78527	DNA-dependent protein kinase catalytic subunit	0.0121	8.5036	2.80
Q9UBQ0	Vacuolar protein sorting-associated protein 29	0.0549	7.32	2.64
P04626	Receptor tyrosine-protein kinase erbB-2	0.0781	53.3382	2.63
P07339	Cathepsin D	0.0558	11.0822	2.49
P61019	Ras-related protein Rab-2A	0.1179	12.3598	2.46
Q13268	Dehydrogenase/reductase SDR family member 2, mitochondrial	0.4964	130.8409	2.45
O00410	Importin-5	0.0182	6.1535	2.43
Q92598	Heat shock protein 105 kDa	0.0886	15.3478	2.42
O00429	Dynamin-1-like protein	0.1345	46.8261	2.41
P34932	Heat shock 70 kDa protein 4	0.0667	19.2811	2.31
Q04828	Aldo-keto reductase family 1 member C1	0.2105	33.021	2.29
Q14204	Cytoplasmic dynein 1 heavy chain 1	0.0306	28.449	2.28
P40925	Malate dehydrogenase, cytoplasmic	0.2455	83.4767	2.21
P31948	Stress-induced-phosphoprotein 1	0.0755	15.4149	2.18
Q15843	NEDD8 OS=Homo sapiens	0.3457	33.1573	2.13
P60900	Proteasome subunit alpha type-6	0.1016	14.0605	2.05
Q8IVF2	Protein AHNAK2	0.0147	26.2971	2.01
P50395	Rab GDP dissociation inhibitor beta	0.2225	82.8778	2.00
P07099	Epoxide hydrolase 1	0.0593	13.2115	1.95
Q12906	Interleukin enhancer-binding factor 3	0.0324	11.8228	1.95
P09972	Fructose-bisphosphate aldolase C	0.2033	117.0601	1.93
P00387	NADH-cytochrome b5 reductase 3	0.1096	22.3441	1.92
P02647	Apolipoprotein A-I	0.0599	19.6469	1.88
O43175	D-3-phosphoglycerate dehydrogenase	0.0638	12.1527	1.86

P17516	Aldo-keto reductase family 1 member C4	0.0526	20.7517	1.85
Q9Y617	Phosphoserine aminotransferase	0.1486	14.8634	1.83
P30049	ATP synthase subunit delta, mitochondrial	0.1369	8.7017	1.81
O43390	Heterogeneous nuclear ribonucleoprotein R	0.0205	6.9904	1.77
P30041	Peroxiredoxin-6	0.2188	24.3457	1.74
Q00610	Clathrin heavy chain 1	0.1839	238.0097	1.73
P17096	High mobility group protein HMG-I/HMG-Y	0.2336	12.3529	1.73
P11216	Glycogen phosphorylase, brain form OS=Homo sapiens	0.1305	43.6236	1.73
Q13263	Transcription intermediary factor 1-beta	0.0515	30.2406	1.70
P05455	Lupus La protein	0.1418	22.5871	1.70
P30040	Endoplasmic reticulum resident protein 29	0.0169	12.7073	1.68
P46940	Ras GTPase-activating-like protein IQGAP1	0.1503	62.6149	1.67
P27824	Calnexin	0.1854	34.0505	1.67
Q9UJZ1	Stomatin-like protein 2, mitochondrial	0.1393	26.1315	1.67
P42330	Aldo-keto reductase family 1 member C3	0.1574	20.9752	1.64
P42330	Aldo-keto reductase family 1 member C3	0.09	12.8358	1.64
P51148	Ras-related protein Rab-5C	0.1131	25.6446	1.63
P61026	Ras-related protein Rab-10	0.1307	27.2324	1.62
P15559	NAD(P)H dehydrogenase [quinone] 1	0.1341	12.0743	1.61
P30153	Serine/threonine-protein phosphatase 2A 65 kDa regulatory subunit A alpha isoform	0.0445	14.9868	1.57
P84103	Serine/arginine-rich splicing factor 3	0.1393	16.1908	1.57
P53396	ATP-citrate synthase	0.0759	12.9125	1.56
P36873	Serine/threonine-protein phosphatase PP1-gamma catalytic subunit	0.0633	3.8833	1.55
P49591	Serine--tRNA ligase, cytoplasmic	0.5778	453.9548	1.52
Q01130	Serine/arginine-rich splicing factor 2	0.147	47.9823	1.51
Q13509	Tubulin beta-3 chain	0.1629	3.4652	1.50
P05787	Keratin, type II cytoskeletal 8	0.2372	156.0825	-1.50
Q03135	Caveolin-1	0.2326	5.8586	-1.50
P15311	Ezrin	0.1667	39.5193	-1.51
P49458	Signal recognition particle 9 kDa protein	0.2571	31.8905	-1.53
P06703	Protein S100-A6	0.0543	4.5504	-1.54
P31949	Protein S100-A11	0.5879	130.0167	-1.54
P18621	60S ribosomal protein L17	0.2759	151.5018	-1.54
Q06830	Peroxiredoxin-1	0.0629	11.1287	-1.55
P68032	Actin, alpha cardiac muscle 1	0.0419	5.6106	-1.55
P52907	F-actin-capping protein subunit alpha-1	0.0509	15.4156	-1.55
O00487	26S proteasome non-ATPase regulatory subunit 14	0.063	7.0528	-1.56
P14866	Heterogeneous nuclear ribonucleoprotein L	0.2039	38.2229	-1.56
P04439	HLA class I histocompatibility antigen, A alpha chain	0.1739	13.8681	-1.58
P22392	Nucleoside diphosphate kinase B	0.09	13.5295	-1.59
P62857	40S ribosomal protein S28	0.3333	52.1011	-1.60
P26373	60S ribosomal protein L13	0.0545	72.3817	-1.61
P06899	Histone H2B type 1-J	0.0399	3.4223	-1.62

P02765	Alpha-2-HS-glycoprotein	0.2303	39.9361	-1.62
Q15717	ELAV-like protein 1	0.0361	21.4645	-1.64
P15531	Nucleoside diphosphate kinase A	0.0531	19.724	-1.65
Q6ZMR3	L-lactate dehydrogenase A-like 6ª	0.0491	3.6312	-1.65
P22492	Histone H1t OS=Homo sapiens	0.0606	8.5883	-1.66
Q00688	Peptidyl-prolyl cis-trans isomerase FKBP3	0.0726	125.0105	-1.68
P40261	Nicotinamide N-methyltransferase	0.0547	7.7375	-1.68
A5A3E0	POTE ankyrin domain family member F	0.0617	44.0982	-1.68
P43487	Ran-specific GTPase-activating protein	0.0318	6.6701	-1.69
P35241	Radixin	0.1016	8.5905	-1.72
O43491	Band 4.1-like protein 2	0.2143	64.0309	-1.74
P35268	60S ribosomal protein L22	0.057	3.2118	-1.77
P08195	4F2 cell-surface antigen heavy chain	0.2136	4.6785	-1.78
P24666	Low molecular weight phosphotyrosine protein phosphatase	0.245	23.4663	-1.79
O43399	Tumor protein D54	0.031	10.203	-1.81
P60660	Myosin light polypeptide 6	0.0739	30.5635	-1.89
P16070	CD44 antigen	0.0837	3.1749	-1.89
P05556	Integrin beta-1	0.0233	3.7879	-1.90
Q92688	Acidic leucine-rich nuclear phosphoprotein 32 family member B	0.1838	42.4295	-1.94
Q13310	Polyadenylate-binding protein 4	0.1591	22.3199	-1.95
P68431	Histone H3.1	0.0577	62.2629	-1.96
P61247	40S ribosomal protein S3a	0.1064	15.7872	-1.98
P0CG38	POTE ankyrin domain family member I	0.331	35.7561	-2.01
P49368	T-complex protein 1 subunit gamma	0.0899	13.5392	-2.01
P69905	Hemoglobin subunit alpha	0.1528	7.1041	-2.02
P17987	T-complex protein 1 subunit alpha	0.107	11.9234	-2.09
Q9UBI6	Guanine nucleotide-binding protein G(I)/G(S)/G(O) subunit gamma-12	0.0963	7.016	-2.11
P50914	60S ribosomal protein L14	0.022	3.0173	-2.16
Q15907	Ras-related protein Rab-11B	0.0355	9.7626	-2.21
Q13200	26S proteasome non-ATPase regulatory subunit 2	0.0263	3.174	-2.23
Q01650	Large neutral amino acids transporter small subunit 1	0.0881	15.4435	-2.24
B5ME19	Eukaryotic translation initiation factor 3 subunit C-like protein	0.0199	3.0525	-2.26
P12004	Proliferating cell nuclear antigen	0.0441	3.4804	-2.37
Q9NZR1	Tropomodulin-2	0.0692	2.7857	-2.47
P61313	60S ribosomal protein L15	0.072	4.1205	-2.52

Table S4. Differentially expressed proteins in SKOV-3 cells treated with melatonin at the dose of 2.4 mM versus Control group

Protein ID	Description	% Coverage	Protein Score	Fold-change
Q6ZMR3	L-lactate dehydrogenase A-like 6A	102	0.007883725	5.60
P07864	L-lactate dehydrogenase C chain	89	0.006878936	5.37
Q7Z794	Keratin, type II cytoskeletal 1b	71	0.003152099	3.46
P06703	Protein S100-A6	94	0.026801229	3.12
P02647	Apolipoprotein A-I	14	0.001345508	2.82
Q13268	Dehydrogenase/reductase SDR family member 2, mitochondrial	59	0.005407087	2.67
P17661	P17661	105	0.005732721	2.63
P10599	Thioredoxin OS=Homo sapiens	85	0.020772989	2.57
P07195	L-lactate dehydrogenase B chain	93	0.00714506	2.47
P05783	Keratin, type I cytoskeletal 18	456	0.019732382	2.29
P62805	Histone H4	267	0.066518647	2.27
P63267	Actin, gamma-enteric smooth muscle	227	0.015491996	2.26
Q562R1	Beta-actin-like protein 2	71	0.004845514	2.21
P02042	Hemoglobin subunit delta	71	0.004845514	2.15
P14618	Pyruvate kinase PKM	573	0.027690415	2.09
P60709	Actin, cytoplasmic 1	408	0.027918898	2.09
P17096	High mobility group protein HMG-I/HMG-Y	5	0.001199101	2.02
P04004	Vitronectin	21	0.001127355	1.88
P0DP25	Calmodulin-3	23	0.003961056	1.86
P00338	L-lactate dehydrogenase A chain	205	0.015844741	1.74
P40926	Malate dehydrogenase, mitochondrial	10	0.000759194	1.73
P32119	Peroxiredoxin-2	136	0.017536996	1.70
P0CG38	POTE ankyrin domain family member I	134	0.003198643	1.70
P0DMV9	Heat shock 70 kDa protein 1B	165	0.006605342	1.69
P09972	Fructose-bisphosphate aldolase C	109	0.007684126	1.67
P08670	Vimentin	726	0.039977909	1.59
P0CG48	Polyubiquitin-C	53	0.00198543	1.57
P68363	Tubulin alpha-1B chain	261	0.014850235	1.57
P0C0S8	Histone H2A type 1	190	0.037504175	1.55
P07737	Profilin-1	37	0.00678177	-1.53
P46782	40S ribosomal protein S5	10	0.00125788	-1.56
P62820	Ras-related protein Rab-1A	2	0.000250349	-1.56
P25705	ATP synthase subunit alpha, mitochondrial	29	0.001345681	-1.59
Q01469	Fatty acid-binding protein 5	4	0.000760319	-1.61
P29401	Transketolase	45	0.001853505	-1.62
P62873	Guanine nucleotide-binding protein G(I)/G(S)/G(T) subunit beta-1	3	0.000226418	-1.62
P11413	Glucose-6-phosphate 1-dehydrogenase	3	0.00014948	-1.64
P02538	Keratin, type II cytoskeletal 6A	726	0.039977909	-1.64
Q04828	Aldo-keto reductase family 1 member C1	6	0.00047667	-1.66
P61978	Heterogeneous nuclear ribonucleoprotein K	30	0.001662684	-1.67
P60174	Triosephosphate isomerase	30	0.001662684	-1.69
P13647	Keratin, type II cytoskeletal 5	726	0.039977909	-1.70

P23284	Peptidyl-prolyl cis-trans isomerase B	15	0.001781997	-1.75
P22626	Heterogeneous nuclear ribonucleoproteins A2/B1	14	0.001017707	-1.79
P62081	40S ribosomal protein S7	14	0.001851807	-1.81
P23528	Cofilin-1	20	0.003091657	-1.84
P06748	P06748	22	0.001920192	-1.87
Q02878	60S ribosomal protein L6	6	0.000534599	-1.92
P30086	Phosphatidylethanolamine-binding protein 1	3	0.00041167	-1.92
Q15185	Prostaglandin E synthase 3	7	0.001122658	-1.94
P52565	Rho GDP-dissociation inhibitor 1	3	0.000377364	-1.95
Q14315	Filamin-C	18	0.000169502	-1.96
P06454	Prothymosin alpha	9	0.002080601	-1.96
P30101	Protein disulfide-isomerase A3	14	0.000711387	-2.02
P62263	40S ribosomal protein S14	7	0.001189571	-2.13
P12814	Alpha-actinin-1	19	0.000546586	-2.13
P13639	Elongation factor 2	32	0.000957044	-2.14
P27797	Calreticulin	4	0.000246146	-2.17
P80723	Brain acid soluble protein 1	4	0.000452172	-2.19
P09382	Galectin-1	19	0.003611513	-2.28
O15523	ATP-dependent RNA helicase DDX3Y	5	0.000193812	-2.30
Q15056	Eukaryotic translation initiation factor 4H	2	0.000206942	-2.34
P62834	Ras-related protein Rap-1A	5	0.000697303	-2.36
Q99832	T-complex protein 1 subunit eta	9	0.000425316	-2.37
P05388	60S acidic ribosomal protein P0	12	0.000971385	-2.37
O00571	ATP-dependent RNA helicase DDX3X	5	0.000193812	-2.44
P62277	40S ribosomal protein S13	5	0.000849694	-2.52
Q14847	LIM and SH3 domain protein 1	3	0.000294951	-2.53
P06753	Tropomyosin alpha-3 chain	6	0.000620825	-2.55
P16403	Histone H1.2	10	0.00120473	-2.61
P62424	60S ribosomal protein L7a	7	0.000675283	-2.64
P38646	Stress-70 protein, mitochondrial	5	0.00018896	-2.70
Q12905	Interleukin enhancer-binding factor 2	6	0.000394781	-2.74
P84098	60S ribosomal protein L19	2	0.000261844	-2.81
Q16658	Fascin	4	0.000208201	-2.81
Q58FG0	Putative heat shock protein HSP 90-alpha A5	4	0.000307314	-2.82
O43707	Alpha-actinin-4	21	0.000591521	-2.83
P55209	Nucleosome assembly protein 1-like 1	2	0.000131257	-2.89
P37802	Transgelin-2	5	0.000644742	-3.09
P35579	Myosin-9	51	0.000667703	-3.11
P61586	Transforming protein RhoA	4	0.000531829	-3.18
Q9NTK5	Obg-like ATPase 1	2	0.0001296	-3.23
P39019	40S ribosomal protein S19	3	0.000530912	-3.61
P18206	Vinculin	13	0.000294171	-3.65
P23396	40S ribosomal protein S3	6	0.000633599	-3.67
P32969	60S ribosomal protein L9	2	0.000267299	-3.70
Q8NBS9	Thioredoxin domain-containing protein 5	1	5.93999E-05	-3.73

P30050	60S ribosomal protein L12	4	0.000622079	-3.75
P02545	Prelamin-A/C	14	0.00054104	-3.88
P62249	40S ribosomal protein S16	3	0.000527276	-3.92
P15880	40S ribosomal protein S2	5	0.000437897	-3.96
O75369	Filamin-B	39	0.000378077	-3.98
P29692	Elongation factor 1-delta	3	0.000273958	-4.26
P21333	Filamin-A	39	0.000378077	-4.26
P08195	4F2 cell-surface antigen heavy chain	12	0.000488776	-4.30
P16070	CD44 antigen	2	6.91664E-05	-4.35
P15311	Ezrin	14	0.000613055	-4.50
P26038	Moesin	7	0.000311309	-4.72
P26641	Elongation factor 1-gamma	5	0.000293601	-4.73
P08865	40S ribosomal protein SA	4	0.000347942	-4.74
Q00839	Heterogeneous nuclear ribonucleoprotein U	5	0.00015552	-4.77
P37837	Transaldolase	5	0.000380723	-4.88
P16152	Carbonyl reductase [NADPH] 1	2	0.000185276	-4.98
P67936	Tropomyosin alpha-4 chain	6	0.000620825	-5.06
Q14697	Neutral alpha-glucosidase AB	3	8.1549E-05	-5.60
Q08211	ATP-dependent RNA helicase A	3	6.06159E-05	-6.44
P19338	Nucleolin	4	0.000144568	-6.47
P63241	Eukaryotic translation initiation factor 5A-1	1	0.000166628	-6.79
Q9Y490	Talin-1	7	7.06908E-05	-6.84
P26447	Protein S100-A4	2	0.000508134	-8.18
Q15149	Plectin	4	2.19135E-05	-18.69